2019

Estimating Soil Organic Carbon in Cultivated Soils Using Soil Test Data, Remote Sensing Imagery from Satellites (Landsat 8 and PlantScope), and Web Soil Survey Data

Muhammed Halil Koparan
South Dakota State University

ESTIMATING SOIL ORGANIC CARBON IN CULTIVATED SOILS USING SOIL TEST DATA, REMOTE SENSING IMAGERY FROM SATELLITES (LANDSAT 8 AND PLANETSCOPE), AND WEB SOIL SURVEY DATA

BY

MUHAMMED HALIL KOPARAN

A thesis submitted in partial fulfillment of the requirements for the

Master of Science

Major in Plant Science

South Dakota State University

2019

ESTIMATING SOIL ORGANIC CARBON IN CULTIVATED SOILS USING SOIL TEST DATA, REMOTE SENSING IMAGERY FROM SATELLITES (LANDSAT 8 AND PLANETSCOPE), AND WEB SOIL SURVEY DATA

MUHAMMED HALIL KOPARAN

This thesis is approved as a creditable and independent investigation by a candidate for the Master of Science in Plant Science and is acceptable for meeting the thesis requirements for this degree. Acceptance of this does not imply that the conclusions reached by the candidate are necessarily the conclusions of the major department.

Douglas Malo, Ph.D.
Thesis Advisor — Date

David Wright, Ph.D.
Head, Department of Plant Science — Date

Kinchel C. Doerner Ph.D.
Dean, Graduate School — Date

ACKNOWLEDGEMENTS

First, I would like to thank the Republic of Turkey Ministry of Agriculture and Forestry, for providing this great opportunity and funding my thesis and educational training. Special thanks to my academic advisor, Dr. Douglas Malo, for his support, respect, kindness, and valuable academic knowledge. He guided me in the right the direction whenever he thought I needed it. Mary Malo was great grandmother and true friend of me and my family. You will be always with us. This research would not have been possible without their help and support.

I would also like to thank my committee members, Dr. David Clay, Dr. Cheryl Reese, and Dr. Lee Weidauer who were involved in the project. Without their guidance and passion, this research would not have been successfully conducted. I would also like to acknowledge Dr. Hossein Moradi Rekabdarkolaee with the South Dakota State University (SDSU) Mathematics and Statistics Department for the valuable hours spent helping me with the statistical data analysis. Without his support, this part of the research would have taken endless time. Also, many thanks to Shaina Westhoff for the hours spent soil sampling and analyzing. She is great person and very kind, and her sons are just cute, we love them. Honestly, I have learned how to make decisions from her (always and forever, ` we will get it done`). It will be great pleasure to host you in Turkey. A special thank you goes to Kunal Sood, a Geographic Information System (GIS) specialist in Himachal Paradesh (HP) State Agriculture University, Centre for Geoinformatics Research and Training, Palampur, India. Even though we had never met before, he is a key partner in this research. The GIS and remote sensing interpolation parts of this study would have been painful without his help and advice. I believe that we will continue this

friendship and keep contributing something good for humanity. I would also like to thank Christine Morris of the SDSU Soil Testing Lab and Janet M. Miller for providing me protocols and teaching me how to analyze soils. I would also thank to Mr. Wittnebel, Mr. Kleinjan, and Mr. Vanderweerd for providing their fields to use in this study.

Finally, I would like to thank my family. Thanks to my sisters and brother for their endless support. My biggest gratitude is to my dad and my mom who wanted me to follow the science and always help humanity. Dad, I know we will meet again. Thanks to you, for your advice and encouragement, I will always be helping people and I will be always carrying your love with me, till the end of my time. To my wife, who never made me think of giving up. She always encouraged me, sacrificed everything that she had for me. My love, you will be always my other half and thank you for our son. You two will be always my everything that I have ever asked from God. May God enlighten all our ways and make our hearts firm with trust and love for Him.

TABLE OF CONTENTS

ABBREVIATIONS

~ - Approximately

< - Less Than (e.g. <2mm = less than 2mm)

>- Greater Than (e.g. >10 = greater than 10)

°C – Degree(s) Celsius

µm – Micrometer or Micron

α – Confidence Level

AA – Atomic Adsorption

APEX - Airborne Prism Experiment

ArcMap® - Geospatial Processing Program (Software)

ASTER - Advanced Spaceborne Thermal Emission and Reflectance

$Band_L$ # - Landsat 8 Band #

$Band_P$ # - PlanetScope Band #

BI - Brightness Index

BI_L – Brightness Index for Landsat 8

BI_P – Brightness Index for PlanetScope

BMPs - Best Management Practices

BSI - Bare Soil Index

BSI_L – Bare Soil Index for Landsat 8

BSI_P – Bare Soil Index for PlanetScope

C – Carbon

Ca^{2+} - Calcium Cation

$CaCO_3$ – Calcium Carbonate

CEC - Cation Exchange Capacity

cm - Centimeters

$cmol_c\ kg^{-1}$ – Centimoles of Charge per Kilogram

CO_2 – Carbon Dioxide

CO_3^{2-} - Carbonate

CV – Cross Validation

DEM- Digital Elevation Model

DI - Deionized

DN – Digital Number

dS m^{-1} – DeciSiemens per Meter

EC - Electrical Conductivity

ESRI – Environmental Systems Research Institute

ESRI® - Environment for Visualizing Images software

Fe -Iron

Fe^{2+} - Ferrous Iron Cation

Fe^{3+} - Ferric Iron Cation

ft - Feet

g - Gram

g kg^{-1} – Grams per Kilogram

g L^{-1} – Grams per Liter

GIS - Geographic Information System

GPS - Global Positioning System

H_2O_2 – Hydrogen Peroxide

H_a – Alternative Hypothesis

ha - Hectare(s)

HCl - Hydrochloric Acid

H_o – Hypothesis Tested

HT – Heated Weight

IC - Inorganic Carbon

K^+ - Potassium Cation

km - Kilometers

L - Soil-brightness Correction Factor

LiDAR – Light Detection and Ranging

LTM - Landsat Thematic Mapper

LULC – Land Use and Land Cover

m – Meters

meq - Milliequivalent

mg kg^{-1} – Milligram per Kilogram

Mg^{2+} - Magnesium Cation

min – Minutes

mL - Milliliters

MLRA – Major Land Resource Area

mm – Millimeter

MN - Minnesota, USA

MSAVI1 - Modified Soil-adjusted Vegetation Index 1

MSAVI2 - Modified Soil-adjusted Vegetation Index 2

$MSAVI2_L$ - Modified Soil-adjusted Vegetation Index for Landsat 8

$MSAVI2_P$ - Modified Soil-adjusted Vegetation Index for PlanetScope

MSE – Mean Square Error

N – North or Nitrogen

n - Number of Samples or Observations

Na^+ - Sodium Cation

NASA - National Aeronautics and Space Administration

NDVI - Normalized Difference Vegetation Index

$NDVI_L$ - Normalized Difference Vegetation Index for Landsat 8

$NDVI_P$ - Normalized Difference Vegetation Index for PlanetScope

NE - Northeast

NH_4OA_c – Ammonium Acetate

NH_4^+- Ammonium Cation

NH_4F - Ammonium Fluoride

NIR - Near Infrared Radiation

nm - Nanometer

NO_3^- -Nitrate Anion

NRCS – Natural Resources Conservation Service

NW – Northwest

OC- Organic Carbon

OLI - Operational Land Imager

OLS – Ordinary Least Square

OM – Organic Matter

P – Phosphorous

P – Probability Level

PC – Principle Component

PCR – Principle Component Regression

PLSR - Partial Least Square Regression

PO_4^{3-} - Phosphate Anion

ppm – Parts per Million

prob > |t| - Probability of Value Greater than Absolute Value of t

PSR - Penalized-spline Signal Regression

r – Correlation Coefficient

R^2 - Coefficient of Determination

RBF – Radial Basis Functions

Red - Red Radiation

RMSE - Root Mean Square Error

RR – Ridge Regression

RS - Remote Sensing

S – South

SAR – Sodium Adsorption Ratio

SAVI – Soil-adjusted Vegetation Index

SD - South Dakota, USA

SE – Southeast

SMP – Lime Requirement Test

SOC - Soil Organic Carbon

SOEC- Sum of Extractable Cations

SOM - Soil Organic Matter

SSE – Sum of Square Error

STD – Soil Test Data

std – Standard

SVMR - Support Vector Machine Regression

SW – Southwest

SWA – SoilWeb Application

SWIR - Short-wave Infrared Radiation

t – t Statistic

TC - Total Carbon

TIRS – Thermal Infrared Sensor

TM - Thematic Map

TOA – Top of Atmosphere

UAV - Unmanned Aircraft Vehicle

USA - United States of America

USDA – United States Department of Agriculture

VIF – Variance Inflation Factor

W - West

WSS - Web Soil Survey

wt – Weight

LIST OF FIGURES

LIST OF TABLES

ABSTRACT

ESTIMATING SOIL ORGANIC CARBON IN CULTIVATED SOILS USING SOIL TEST DATA, REMOTE SENSING IMAGERY FROM SATELLITES (LANDSAT 8 AND PLANETSCOPE IMAGERY), AND WEB SOIL SURVEY DATA

MUHAMMED HALIL KOPARAN

2019

Soil organic carbon (SOC) is an important soil parameter of cultivated soils that needs to be monitored and mapped regularly to enhance soil health and productivity. SOC levels in cultivated areas is difficult to monitor for farmers and is costly to analyze using traditional methods. The objective of this study was to estimate surface SOC distribution in selected soils of Major Land Resource Areas (MLRA) 102A (Rolling Till Plain, Brookings County, SD) and 103 (Central Iowa and Minnesota Till Prairies, Lac qui Parle County, MN) using soil sample data, Web Soil Survey (WSS) data, and satellite imagery (Landsat 8 and PlanetScope). Different satellite imagery bands and band combinations were used to reach more accurate results. The dominant soils in the area are Haplustolls, Calciustolls, and Endoaquolls formed in silty sediments, local silty alluvium, and till. Sites were selected and soil samples were collected in May 2018 after planting. SOC and soil properties were measured at the 0-15 cm depth.

SOC was mainly affected by soil texture in the studied selected soils. Multiple-linear regression was used to build SOC prediction models from soil test data. The final SOC model (using stepwise regression) is SOC_p = 3.98 + (-0.210 pH) + (-0.220 Sand [g kg^{-1}]) + (0.040 Sum of Extractable Cation, SOEC [$cmol_c$ kg^{-1}]). The Ridge Regression (RR) (CV = 0.066, MSE = 0.063) and Principal Component Regression (PCR) (CV =

0.071, MSE = 0.068) were used to deal with multicollinearity and RR was determined to be as the best model, with 82.7% of variation in SOC explained by the RR model.

Landsat 8 and PlanetScope spectral bands and different indices were also used to develop SOC prediction models. The stepwise regression analyses revealed that the Landsat 8 prediction model had multicollinearity problem. Ridge regression and PCR were applied, and RR was chosen as the best model with SOC_p = -26.7 + (0.310 BSI_L) + (-23.2 Band 5_L) + (75.8 Band 2_L) + (-51.1 Band 3_L) + (-3.05 Band 7_L). The RR model (CV = 0.24, MSE = 0.22) explained 37.0% of the variation in SOC for Landsat 8. The reduced PlanetScope model was SOC_p = -25.1 + (2980 $Band4_P$) + (0.327 BSI_P). Approximately 60.0% of the variation in SOC was explanined by the Ordinary Least Square (OLS) (CV = 0.15, MSE = 0.14) model and was free of multicollinearity.

WSS data showed similar patterns as soil test data for SOC predictions. The best model for WSS data was a linear regression, SOC_p = 3.37 + (-0.0200 Sand WSS [g kg^{-1}]) and 49.0% of the variation in SOC was explained by this model. WSS data were then added as variables into the spatial (satellite) estimation models. The Landsat 8 and WSS data explained 53.3%, PlanetScope and WSS data explained 68.8% of the SOC variation.

Based on these results, deciding on the number of soil sampling points, and the use of specific variables in the model is very crucial for the model development. Estimating SOC by minimizing the number of needed soil sampling points, using satellite imagery, and public free sources provides an easy, efficient and cost-effective way to monitor SOC levels and identify the best management systems for producers and natural resource managers. This project produced accurate SOC prediction models using soil test data, satellite imagery and Web Soil Survey data. This SOC estimation model helps

farmers, resource managers, and researchers to monitor SOC concentration on the soil surface using remote sensing alone, or with WSS data, or with a minimal amount of soil test data.

CHAPTER 1: Introduction and Literature Review

Introduction

Throughout history, Earth has faced many changes in land use and the loss of soil organic matter (SOM) caused by climate change (Zribi et al., 2011). Soil organic matter is defined as a composite of plant and animal residue at different chemical and biological stages (Schnitzer, 1982). Organic carbon (OC) exists in the SOM components, while inorganic carbon (IC) is present in the carbonate (CO_3^{2-}) minerals like lime and dolomite (Nelson and Sommers, 1996). Soil organic carbon (SOC) is an important soil health property and a critical factor for soil management, crop production, and soil quality (Chen et al., 2000). Soil organic carbon determination is typically carried out with direct methods which consist of field sampling and applying laboratory analysis for results. However, as the technology has advanced and more low cost, time efficient scientific approaches have evolved. Indirect methods using Remote Sensing (RS) and Geographic Information Systems (GIS) have the potential to replace traditional SOC methods (Post et al., 2001).

Soil Organic Carbon (SOC) and Soil Organic Matter (SOM)

Soil organic matter has been defined as a key component for crop production for many years and research has shown that soil color and soil fertility are related to SOM (Zomer et al., 2017). Soil organic matter primarily is derived from plant residue (Allison, 1973). Soil can be considered as the most crucial, largest, and fragile carbon (C) reservoir in the world (Swift, 2001). Soil organic carbon is a valuable soil parameter, which impacts the agricultural productivity and contains roughly 75% of Total Carbon (TC) pool of terrestrial ecosystem. Soils store more C than vegetation and the atmosphere

combined (Elbasiouny et al., 2014). Higher SOC levels enhance essential ecosystem functions, soil structure, soil quality, nutrient and water holding capacity, and energy supplies for soil microbial fauna (Chung et al., 2008). Over decades, producers have applied fertilizers, and chemicals, employed different management systems, and added other inputs to increase plant production and crop yield. However, these improvements can cause detrimental problems (e.g., water pollution and degradation of SOM). Correspondingly, the use of sustainable management systems is needed to reduce harmful environmental effects of some agricultural chemical applications and conventional land use (Ludwig et al., 2010).

When soil health is considered and evaluated, the decisive role of SOC and SOM is obvious. This subject has been studied many times. Increasing SOC levels improves crop production by affecting three main crop yield factors; (1) enhanced plant available water holding capacity; (2) increased plant nutrient levels, storage, and availability; and (3) improved soil physical properties (Lal, 2006) Crop selection, management techniques, tillage, and fertilization are keys to improve SOC content. Soil C levels can be increased by applying nitrogen (N) fertilizers, using diverse crop rotation, reduced tillage, and limiting crop removal (Havlin et al., 1990). Management techniques impact the effect of N application, soil texture, and weather condition on plant growth (Alvarez, 2005). Moreover, a study conducted by Studdert (2000) showed that an appropriate crop rotation system and conservation tillage system could reduce SOC degradation.

On the other hand, conventional crop systems, excess fertilization, and conventional tillage systems often have adverse effects on SOC levels causing the deterioration of soil physical properties (Hati et al., 2008). Some crop rotation systems

like corn (*Zea mays L.*) – soybean (*Glycine max*) do not affect SOC concentration when compared to continuous corn cropping (Bronick and Lal, 2005). Tillage systems play a vital role in crop production and land use. Long-term conventional tillage system naturally decrease SOC content by breaking down aggregates, reducing aggregate stability, and increasing soil bulk density(Liu et al., 2014).

As a result, studies in environmental simulations, modeling, mapping, and predicting agriculture need better quality and cost-effective data. Accordingly, inexpensive and time efficient methods and applications are required for soil analysis in order to select appropriate management systems and best land use (Gomez et al., 2008).

Basic Remote Sensing Processes as Imagery

Soil health characteristics can be reduced due to the significant land use changes caused by changes in physical, biological, and chemical properties particularly, SOC. There are various major factors that cause SOC depletion due to frequent tillage, increased aeration, higher temperatures, etc. Many tools and techniques have been used to analyze the changes in soil characteristics. Geographic information systems (GIS) and remote sensing (RS) are constantly improving and becoming more useful for the management of agricultural areas, urban areas, and environmentally sensitive areas.

Remote sensing can be defined as the science of gaining information of data acquired by a device that does not touch any object, field, or phenomenon in the study areas (Lillesand et al., 2014). Remote sensing can also be described as Physical Object, Sensor Data, Extracted Information, and Applications (Campbell and Wynne, 2011). Remote sensing (Image capture) can be performed using satellite and unmanned aircraft vehicle (UAV) platforms. In many aspects, satellite and UAV sensors have similarities

and differences considering their altitude and stability which cause different image properties (Richards and Richards, 1999). Remote sensing data can be obtained in analog or digital formats. Data in analog format can be defined as airborne or satellite remote sensing platforms which are displayed in paper form. Digital image utilization and quality have increased significantly with the development of technology, high-resolution displays, and digital image processing software. Recent information extraction and digital change detection techniques have simplified image processing (Narumalani et al., 2002).

Remote Sensing of Soil Properties

The importance of soil cannot be overstated. Soil is a natural resource covering large areas of the Earth's surface. Soil has many different and vital roles in the ecosystems such as energy fluxes and plant and animal productivity to supply human needs. Considering and evaluating the importance of soil in our life, monitoring and choosing best management practices to protect soil is necessary and crucial for humanity survival. Over decades, researchers have been focusing on finding an easy, time-efficient, and inexpensive way to map, monitor, and estimate soil use and soil property changes by developing RS applications such as usage of the microwave, light detection and ranging (LiDAR), multispectral imagery, and spectrometry. LiDAR is a measuring method using light in the form of laser to calculate ranges (different distances) to the Earth (Detection, 2013).

Singh (2016) performed a study to review the use of the microwave, optical, LiDAR, and hyperspectral remote sensing data for soil mapping. Hyperspectral can be characterized as high spectral resolution that comes from hundreds of band channels (Melgani and Bruzzone, 2004). The hypothesis was that RS would enable the enhancing

of incomplete thematic and spatial coverage of the available soil databases. The approach is capable of measuring soil properties like texture, mineralogy, soil moisture, iron, salinity, and SOC. Airborne, space-borne, and original measurements utilizing active, passive, and optical microwave instruments have been successfully used in sparsely vegetated areas. Another study reviewing the utilization of satellite remote sensing for mapping of soils demonstrated how infrared, thermal, multispectral, as well as active and passive microwave space-borne sensors are effective in the delineation of soil units (Dewitte et al., 2012). The sensors are also helpful in the evaluation of key soil properties as well as risks to soil functions resulting from changes in soil moisture content, salinization, texture, and SOC.

Soil moisture at various depths is very beneficial for plant growth. Soil surface water content (water held in 0-10cm) is a key property for energy fluxes and hydrological process at the soil surface. Predicting soil moisture and the monitoring of soil moisture in unvisited areas would provide a cost-effective way to assist farmers in utilizing best management practices (BMPs) to protect soil health and enhance soil moisture content. Working in known areas and measuring soil moisture content in large areas encourage people to use a new methodology like RS. Remote sensing studies of soil moisture content started in the early 1980s (Alavipanah et al., 2016). Recently, microwave data was found to be the most suitable RS application to estimate soil moisture content. However, the accuracy of the microwave data is affected negatively by soil type, vegetation type, surface residue, and surface roughness (Cashion et al., 2005).

Soil salinity can be described as one of the most land degrading processes. Using conventional laboratory methods to measure soil salinity is both costly and time-

consuming. The potential of utilizing RS to monitor soil salinity using satellite imagery has been studied. Yong-Ling et al. (2010) found a strong correlation between observed soil salinity and estimated soil salinity based on RS. Also, they mentioned that monitoring soil salinity using RS in a cost-effective way is possible by using Hyperion reflectance data. However, there is a limitation for estimating soil salinity regarding multispectral satellite imagery. Low spectral and spatial resolution satellite imagery can cause misclassification of bare, course-textured soils as saline soils (Metternicht and Zinck, 2003). In another study to monitor soil salinity, Glowienka et al. (2016) used remote sensing and GIS techniques to analyze soil properties in southeast Poland. Specifically, the techniques were used to perform a temporal and spatial analysis of the soil salinity as well as soil pH. Thorough interpolation procedures were undertaken using specialist image analysis software like ArcMap® and ENVI® and these software packages allow one to visualize data in the form of raster and vector maps for the spatial distribution of the examined soil properties. For the purpose of the analysis of RS data, satellite images Landsat 5 Thematic Mapper (TM) was used. In a similar study, Wu et al. (1997) used GIS and RS to evaluate the soil properties in Finney County, Kansas. The land use and land cover (LULC) map was derived using seasonal Landsat (TM) images. Geographic information system techniques helped in the calculation of the soil erodibility index, and the accuracy was significantly better than manual calculation. Zhang et al. (2008) found that there are strong correlations between the measured soil erodibility values and those calculated from soil erodibility estimators. A study by Scudiero et al. (2014) demonstrated the usefulness of the multi-year (temporal) Landsat's surface reflectance data as a measure for the characterization of the soil salinity spatial

variability. Even more studies have exhibited the importance of RS data in the delineation of soil properties such as silt, sand, SOC, and clay content based on interrelationships among the reflectance spectra and soil properties (Barnes and Baker, 2000; Thomasson et al., 2001; Gomez et al., 2008).

Soil texture significantly impacts pedological and ecological process in soil such as infiltration, aggregate stability, and soil wind and water erosion. Quantitative soil texture maps based on RS tools are beneficial in terms of management, and prediction of the specific areas when compared to traditional maps (Scull et al., 2003). The study by Apan et al. (2002) concluded that using Bands 2 (visible red) and 8 (Shortwave Infrared,SWIR) of Advanced Spaceborne Thermal Emission and Reflectance (ASTER) image, and first principal component 1 (converting 9 ASTER bands into a new data set to identify the number of endmembers) were beneficial for discriminating soil features like soil texture. Moreover, there are some other options for mapping soil texture such as hyperspectral data. Hyperspectral remote sensing basically provides more detailed spectral data information for each pixel of an image (Ben-Dor et al., 2013). Zribi et al. (2012) used TERRASAR-X radar data to measure and predict soil surface texture in a semi-arid region and found that soil texture and was correlated to radar images. TERRASAR-X is German national synthetic-aperture radar (SAR)-satellite system. Basically, this system is able to combine high resolution images for more detailed summary analysis for synoptic application (Werninghaus, 2004).

By combining visuals from a digital elevation model (DEM) for landform classification and the ASTER sensor, Saadat et al. (2008) found that spectral RS data enhances the likelihood of differentiating topographically homogenous landforms

improving the classification. A study by Ehsani and Quiel (2009) also concluded the same after using Landsat and Shuttle Radar Topographic Mission DEM to analyze landscape elements. Dobos et al. (2001) observed the synthesis of coarse resolution Advanced Very High-Resolution Radiometer data and DEM obtained terrains were favorable data for the characterization of delineating soil patterns and soil forming environments. A digital elevation map is a raster file with elevation data for each pixel cell used to create aspects and slope maps of specified areas (Klingebiel et al., 1987).

Remote Sensing of Soil Organic Carbon

Geostatistical techniques have been used to map SOC content. The various satellite imagery band combinations are used to identify the digital signatures. The amount of SOC content in different slopes, soils, and land use categories can be analyzed using the GIS and RS techniques. Studies predicting SOC are primarily based on various methods, the accuracy of the results, and obtaining the necessary number of soil samples. Increasing farm input cost and crop production values, drive producers to seek modern technologies in order to enhance their crop yield and land management systems (Seelan et al., 2003). This research project focuses on estimating SOC using RS applications such as a spectrometer data, satellite imagery, and drone imagery.

Soil organic carbon, like many other soil properties, is highly influenced by soil type as well as distinct environmental variables. Over the years, the Earth's surface has experienced profound changes in land use and land cover. Activities such as continuous cultivation and intensive grazing have disturbed and diminished the SOC, thereby impacting global warming and climate change (Kumar, 2013). As such, it is important that conservation practices are evaluated for the sake of mitigating climate change

impacts as well as enhancing SOC sequestration. Conservation calls for environmental modeling, monitoring, and risk assessment. These all rely on accurate and detailed information on temporal and spatial variations in soil properties (Forkuor et al., 2017). The collection of this information is known as soil mapping, and while various ways of doing it exist, GIS and RS have proved to be less time consuming and more cost-effective than traditional methods, with comparable results.

Remote sensing and GIS techniques have proven extremely useful in the estimation of SOC. In most cases, remotely sensed data is used jointly with classification, kriging, and regression tree analyses to help in the prediction of soil properties of unvisited areas. Bhunia et al. (2017) used both spaceborne satellite data and ground verification in districts in India to estimate the SOC stock. A multivariate regression model was applied to estimate the spatial distribution of SOC using the satellite data derived indices. The regression analysis uncovered the relationship between SOC and the bare soil index as well as the normalized difference vegetation index (NDVI). A significant correlation between the SOC estimated from satellite data and those observed through ground verification was found. Ben-Dor and Levin (2000) also demonstrated how regression modeling could be used to map SOC. Understanding the need for an accurate estimation of SOC, Sarmadian et al. (2014) suggested the Radial Basis Functions (RBF) method as an appropriate way of exploring SOC spatial patterns. In a similar study Fidencio et al. (2002) concluded that diffuse reflectance spectroscopy in the Near-Infrared radiation (NIR) region with data treated by RBF is quick, confidential, and clear.

Castaldi et al. (2018) demonstrated a method to estimate SOC from RS data that did not require any chemical or physical laboratory analysis. Known as `bottom-up`, the method employed both the Airborne Prism Experiment (APEX) hyperspectral airborne data and the pan-European topsoil database from the Land Use/Cover Area frame statistical survey to develop bare cropland fields' SOC maps. The SOC content was estimated using partial least squares regression models and it was found to be satisfactorily accurate. In a similar study, Stevens et al. (2010) used airborne imaging spectroscopy to map SOC at a regional level. Specifically, they used hyperspectral images that were captured with an AHS-160 sensor. Penalized-spline signal regression (PSR), partial least square regression (PLSR), and support vector machine regression (SVMR) were three distinct multivariate calibration techniques used to show the relationship of reflectance data to surface SOC. PSR was effective in dealing with some noisy spectral features. The study took advantage of the ability of spectroscopy to use Short-wave Infrared radiation (SWIR) and reflectance in the visible and near-infrared.

A study by Gomez et al. (2008) compared the predictions of SOC using RS data and visible and near-infrared reflectance hyperspectral proximal data. Partial least squares regression helped in predicting SOC contents using RS and proximal spectra. The study found that the accuracy of the prediction was unaffected by the spectral resolution of the RS and proximal data. However, the accuracy of the SOC predictions utilizing the Hyperion spectra was lower than the Agrispec data. Agrispec is a commercial sensor that measures NIR and SWIR spectra for agricultural RS application and analysis. Hyperion spectra can be defined as a high resolution sensor which has 220 spectral bands (from 0.4 to 2.5 micrometer, µm, or micron) and the spatial resolution is 30m (Griffin et al., 2005).

In essence, the study demonstrated a significant potential for the use of hyperspectral remote sensing predicting SOC. Bartholomeus et al. (2008) demonstrated how the mapping of SOC over large areas could be achieved using spectrally-based indices. Regarding the reflectance spectroscopy, the detection of the SOC content was rooted in the components of SOC (starch, lignin, and cellulose). In another study, McCarty et al. (2010) explored how imaging spectroscopy used to derive a soil C map.

Effects of Soil Properties on Soil Spectral Feature

Soil reflectance is a cumulative feature which comes from the different spectral signatures of the inharmonious combination of mineral and organic substances of mineral soil surfaces (Stoner and Baumgardner, 1981). There are several studies that have demonstrated the dependent contribution of soil parameters such as organic matter (OM), organic carbon (OC), moisture content, soil texture, structure, and iron concentration on spectral reflectance taking place soils Mathews et al., 1973; Karmanov., 1970).

Soil color becomes darker (higher C values, lower Munsell color values, and lower Munsell color chromas) when the soil moisture content changes from dry to moist. The reason for becoming darker is explained by changing the environment from air to water around the soil particles (Twomey et al., 1986). In this regard, soil reflectance is substantially affected by moisture content. Lobell and Asner (2002) mentioned that reflected radiance from soil surface represents strong passive signal suitable to satellite. In addition, they compared the spectral signature of wet soil and dry soil under SWIR radiation, and demonstrated that there is a difference between wet and dry soil reflectance, soil reflectance declined while soil moisture increased. Moreover, soil moisture content strongly depends on soil texture. Lillesand et al. (2014) mentioned that

soils which consist of coarse textures, like sand, are often called “well-drained soil” and they do not have ability to hold water in their structural units. Poorly drained soils are often fine-textured soils (soils with clay and silt in the name) and are able to hold more water. As a consequence, low moisture content results in high reflectance while high moisture content results in low reflectance.

More than 30% of tilled USA cropland is considered as erodible land (Takiff Smith, 1991). In order to decrease erosion, farmers started to use no-tillage systems and cover crops. Crop residue is an effective way to prevent movement of soil particles by water erosion (Daughtry, 2001). Crop residues on the soil surface impact soil reflectance. Nagler et al. (2000) mentioned that RS techniques have partial success in estimating plant residue cover. The reason for this is that plant residue and soil have a similar patterns in terms of spectral signatures in the visible and near-infrared wavelength ranges. Wiegand and Richardson (1992) demonstrated that there are limited spectral signature differences between soil and plant residue, resulting in great difficulty to distinguish soil and plant residue.

The impact of landscape position on soil reflectance have been acknowledged for decades (Stohr and West, 1985). Teillet et al. (1982) mentioned that slopes facing the sunlight (eg. SE, S, and SW) collect more sunlight and become brighter than slopes facing away from the sunlight (eg.NW, NE, and N). Piekarczyk et al. (2016) concluded that high clay and silt contents contribute to creating a rougher soil surface, while high sand contents greatly decrease soil surface roughness. Moreover, they found that surface roughness reduced spectral reflectance, a measure of tortuosity. The relationship between soil surface roughness and spectral features of the soil surface should be developed and

calculated in terms of a correction factor in order to use for RS applications for precision agriculture.

The Earth has a stock of elemental iron (Fe), and Fe is the fourth most abundant element in the Earth's crust. The average Fe concentration is 5.1% of the mass, and the average ferric (Fe^{+3}) and ferrous (Fe^{+2}) is recorded as 5.3×10^{23}g (Ronov and Yaroshevsky, 1969). Because of the indirect role Fe has on the spectral signature of soils, it is also important to monitor and estimate Fe concentration. Soileau and McCracken (1967) pointed out that free Fe oxides have a strong relationship with soil texture and structure. Free Fe oxides have ability of absorbing, high surface energy, and helping soil structural cementation due to its electrochemical feature (Zhang et al., 2016). Moreover, free Fe oxides can have a cementation effect on soil particles by causing flocculation of soil particles. Formless free Fe can coat soil particles with clay films that affect the interaction of clay minerals and natural sunlight radiation. As a result, Fe has a strong correlation with soil color and soil clay content. In order to discriminate the Fe effect or to estimate Fe concentration in the soil, high spectral resolution RS data should be used (Ben-Dor et al., 1999).

There are many important factors that impact soils, soil C levels, and soil health. However, the influence of these factors makes this system complicated. For example, changes in yield can be the result of changes in soil electrical conductivity, EC (Lund et al., 1999). In this regard, RS is a time efficient and cost-effective method to gather data, monitor, map, and predict soil properties in a given area. Furthermore, using proper data for the aim of the given studies is very crucial in terms of different characteristic of soil elements. For instance, some soil properties like soil salinity could require use of

hyperspectral and laboratory data (Yong-Ling et al., 2010). Being aware of constraints and limitations of RS data and applications (such as vegetation interference and spectral confusion) and how they influence image processing, interpreting data, and analysis should be considered (Alavipanah et al., 2016).

Web Soil Survey (WSS)

Web Soil Survey (WSS) is the web site that provides soil data and land use information managed by the United States Department of Agriculture (USDA) Natural Resources Conservation Service (NRCS) in collaboration with National Cooperative Soil Survey. Basically, WSS has soil maps and available data for the farmers, producers, researches, and land managers (Malo, 2008). The WSS website provides tremendous natural resources information for almost all of the United States and its territories. Moreover, WSS can provide traditional hardcopy document and spatial data. Web Soil Survey is a comprehensive database. Depending on the purpose of use, it can be used to create different maps demonstrating the spatial visualization of different soil properties or thematic map classes. For instance, soil salinity, taxonomic classification, and surface SOM maps, can be created easily using GIS (Beaudette and O'Geen, 2009). Web Soil Survey is not only for agricultural activities, it is also very useful for road or engineering purposes, land managers, and policymakers. Furthermore, WSS provides an opportunity to monitor soil changes for years. In this regard, WSS provides important soil data to consider how production, soil quality, sustainability, land management, and the environment interact (Tugel et al., 2005). The SoilWeb app (SWA) is newly designed website to gather digital soil information. The program can be accessed online using the following link: casoilresource.lawr.ucdavis.edu. The use of this application is available

on computers, tablets, iPads, or smartphones. The SWA provides opportunity to obtain soil data for a specific area. The soil data that can be obtained from the application includes the official soil series description, % sand, % silt, % clay, bulk density, % total carbon, % organic carbon, % organic matter, pH, base saturation, CEC, % gypsum, % $CaCO_3$ (lime), SAR (sodium adsorption ratio), and so on. Basically, the SWA is a great tool to gather soil data and land information in order to select appropriate management practices and land-use (Malo, 2016).

Research Objectives

The objectives of my research are;

1. To measure SOC and other selected soil properties in five selected fields and develop a model to estimate SOC using selected soil properties.
2. To develop models to estimate SOC using Landsat 8 Operational Land Imager (OLI) and PlanetScope Satellite Imagery.
3. To develop models to estimate SOC using WSS data and compare to measured and model predicted SOC levels.
4. To develop models that use soil properties, RS, and WSS data to estimate SOC levels

REFERENCES

Alavipanah, S. K., Damavandi, A. A., Mirzaei, S., Rezaei, A., Hamzeh, S., Matinfar, H. R., Teimouri, H., and Javadzarrin, I. (2016). Remote sensing application in evaluation of soil characteristics in desert areas. *Natural Environment Change* **2**, 1-24.

Allison, F. E. (1973). "Soil organic matter and its role in crop production," Elsevier.

Alvarez, R. (2005). A review of nitrogen fertilizer and conservation tillage effects on soil organic carbon storage. *Soil Use and Management* **21**, 38-52.

Apan, A., Kelly, R., Jensen, T., Butler, D., Strong, W., and Basnet, B. (2002). Spectral discrimination and separability analysis of agricultural crops and soil attributes using ASTER imagery. *In* "11th Australasian Remote Sensing and Photogrammetry Conference", pp. 396-411.

Barnes, E., and Baker, M. (2000). Multispectral data for mapping soil texture: possibilities and limitations. *Applied Engineering in Agriculture* **16**, 731.

Bartholomeus, H., Schaepman, M., Kooistra, L., Stevens, A., Hoogmoed, W., and Spaargaren, O. (2008). Spectral reflectance based indices for soil organic carbon quantification. *Geoderma* **145**, 28-36.

Beaudette, D., and O'Geen, A. (2009). Soil-Web: an online soil survey for California, Arizona, and Nevada. *Computers & Geosciences* **35**, 2119-2128.

Ben-Dor, E., Irons, J., and Epema, G. (1999). Soil reflectante. *Manual of Remote Sensing: Remote Sensing for Earth Science; Rencz, AN, Ryerson, RA, Eds*, 111-187.

Ben-Dor, E., and Levin, N. (2000). Determination of surface reflectance from raw hyperspectral data without simultaneous ground data measurements: a case study of the GER 63-channel sensor data acquired over Naan, Israel. *International Journal of Remote Sensing* **21**, 2053-2074.

Ben-Dor, E., Schläpfer, D., Plaza, A. J., Malthus, T. J. A. M. f. E. R. M., Instruments, W.-V. V., and Co. KGaA, W. (2013). Hyperspectral remote sensing. **413**, 456.

Bhunia, G. S., Kumar Shit, P., and Pourghasemi, H. R. (2017). Soil organic carbon mapping using remote sensing techniques and multivariate regression model. *Geocarto International*, 1-12.

Bronick, C. J., and Lal, R. (2005). Manuring and rotation effects on soil organic carbon concentration for different aggregate size fractions on two soils in northeastern Ohio, USA. *Soil and Tillage Research* **81**, 239-252.

Campbell, J. B., and Wynne, R. H. (2011). "Introduction to remote sensing," Guilford Press.

Cashion, J., Lakshmi, V., Bosch, D., and Jackson, T. J. (2005). Microwave remote sensing of soil moisture: evaluation of the TRMM microwave imager (TMI) satellite for the Little River Watershed Tifton, Georgia. *Journal of hydrology* **307**, 242-253.

Castaldi, F., Chabrillat, S., Jones, A., Vreys, K., Bomans, B., and van Wesemael, B. (2018). Soil Organic Carbon Estimation in Croplands by Hyperspectral Remote APEX Data Using the LUCAS Topsoil Database. *Remote Sensing* **10**, 153.

Chen, F., Kissel, D. E., West, L. T., and Adkins, W. (2000). Field-scale mapping of surface soil organic carbon using remotely sensed imagery. *Soil Science Society of America Journal* **64**, 746-753.

Chung, H., Grove, J. H., and Six, J. (2008). Indications for soil carbon saturation in a temperate agroecosystem. *Soil Science Society of America Journal* **72**, 1132-1139.

Daughtry, C. S. (2001). Discriminating crop residues from soil by shortwave infrared reflectance. *Agronomy Journal* **93**, 125-131.

Detection, L. L. (2013). Ranging—is a remote sensing method used to examine the surface of the Earth. *NOAA. Archived from the original on* **4**.

Dewitte, O., Jones, A., Elbelrhiti, H., Horion, S., and Montanarella, L. (2012). Satellite remote sensing for soil mapping in Africa: An overview. *Progress in physical geography* **36**, 514-538.

Dobos, E., Montanarella, L., Nègre, T., and Micheli, E. (2001). A regional scale soil mapping approach using integrated AVHRR and DEM data. *International Journal of Applied Earth Observation and Geoinformation* **3**, 30-42.

Ehsani, A. H., and Quiel, F. (2009). A semi-automatic method for analysis of landscape elements using Shuttle Radar Topography Mission and Landsat ETM+ data. *Computers & Geosciences* **35**, 373-389.

Elbasiouny, H., Abowaly, M., Abu_Alkheir, A., and Gad, A. A. (2014). Spatial variation of soil carbon and nitrogen pools by using ordinary Kriging method in an area of north Nile Delta, Egypt. *Catena* **113**, 70-78.

Fidencio, P. H., Poppi, R. J., and de Andrade, J. C. (2002). Determination of organic matter in soils using radial basis function networks and near infrared spectroscopy. *Analytica Chimica Acta* **453**, 125-134.

Forkuor, G., Hounkpatin, O. K., Welp, G., and Thiel, M. (2017). High resolution mapping of soil properties using remote sensing variables in South-Western Burkina Faso: A comparison of machine learning and multiple linear regression models. *PloS one* **12**, e0170478.

Glowienka, E., Michalowska, K., Pekala, A., and Hejmanowska, B. (2016). Application of GIS and Remote Sensing Techniques in Multitemporal Analyses of Soil Properties in the Foreland of the Carpathians. *In* "IOP Conference Series: Earth and Environmental Science", Vol. 44, pp. 052044. IOP Publishing.

Gomez, C., Rossel, R. A. V., and McBratney, A. B. (2008). Soil organic carbon prediction by hyperspectral remote sensing and field vis-NIR spectroscopy: An Australian case study. *Geoderma* **146**, 403-411.

Griffin, M. K., Hsu, S. M., Burke, H.-h. K., Orloff, S. M., and Upham, C. A. (2005). "Examples of EO-1 Hyperion data analysis." MASSACHUSETTS INST OF TECH LEXINGTON LINCOLN LAB.

Hati, K. M., Swarup, A., Mishra, B., Manna, M., Wanjari, R., Mandal, K., and Misra, A. (2008). Impact of long-term application of fertilizer, manure and lime under intensive cropping on physical properties and organic carbon content of an Alfisol.

Havlin, J., Kissel, D., Maddux, L., Claassen, M., and Long, J. (1990). Crop rotation and tillage effects on soil organic carbon and nitrogen. *Soil Science Society of America Journal* **54**, 448-452.

Karmanov, I. (1970). Study of soils by the spectral composition of reflected radiation. *Pochvovedenie*, 34-47.

Klingebiel, A., Horvath, E., Moore, D., and Reybold, W. (1987). Use of Slope, Aspect, and Elevation Maps Derived from Digital Elevation Model Data in Making Soil Surveys 1. *Soil survey techniques*, 77-90.

Kumar, S. (2013). Soil organic carbon mapping at field and regional scales using GIS and remote sensing applications. *Advances in Crop Science and Technology*.

Lal, R. (2006). Enhancing crop yields in the developing countries through restoration of the soil organic carbon pool in agricultural lands. *Land Degradation & Development* **17**, 197-209.

Lillesand, T., Kiefer, R. W., and Chipman, J. (2014). "Remote sensing and image interpretation," John Wiley & Sons.

Liu, E., Teclemariam, S. G., Yan, C., Yu, J., Gu, R., Liu, S., He, W., and Liu, Q. (2014). Long-term effects of no-tillage management practice on soil organic carbon and its fractions in the northern China. *Geoderma* **213**, 379-384.

Lobell, D. B., and Asner, G. P. (2002). Moisture effects on soil reflectance. *Soil Science Society of America Journal* **66**, 722-727.

Ludwig, B., Geisseler, D., Michel, K., Joergensen, R., Schulz, E., Merbach, I., Raupp, J., Rauber, R., Hu, K., and Niu, L. (2010). Effects of fertilization and soil management on crop yields and carbon stabilization in soils. A review. *Agronomy for sustainable development*.

Lund, E., Christy, C., and Drummond, P. J. P. a. (1999). Practical applications of soil electrical conductivity mapping. **99**, 771-779.

Malo, D. D. (2016). Online Soil Survey Information –SoilWeb Application (SWA). *iGROW Corn: Best management practices (2016)*.

Malo, D. D. (2008). Online sources of basic soils information. *Soil Science Step-by-Step Field Analysis*, (soilsciencestep), 35-48.

Mathews, H., Cunningham, R., and Petersen, G. (1973). Spectral Reflectance of Selected Pennsylvania Soils 1. *Soil Science Society of America Journal* **37**, 421-424.

McCarty, G., Hively, W., Reeves, J., Lang, M., Lund, E., and Weatherbee, O. (2010). Infrared sensors to map soil carbon in agricultural ecosystems. *In* "Proximal Soil Sensing", pp. 165-176. Springer.

Melgani, F., and Bruzzone, L. (2004). Classification of hyperspectral remote sensing images with support vector machines. *IEEE Transactions on geoscience and remote sensing* **42**, 1778-1790.

Metternicht, G. I., and Zinck, J. (2003). Remote sensing of soil salinity: potentials and constraints. *Remote sensing of Environment* **85**, 1-20.

Nagler, P., Daughtry, C., and Goward, S. (2000). Plant litter and soil reflectance. *Remote Sensing of Environment* **71**, 207-215.

Narumalani, S., Hlady, J. T., and Jensen, J. R. (2002). Information extraction from remotely sensed data. *Manual of geospatial science and technology*, 288-324.

Nelson, D. W., and Sommers, L. E. (1996). Total carbon, organic carbon, and organic matter. *Methods of soil analysis part 3—chemical methods*, 961-1010.

Piekarczyk, J., Kaźmierowski, C., Królewicz, S., and Cierniewski, J. (2016). Effects of soil surface roughness on soil reflectance measured in laboratory and outdoor conditions. *IEEE Journal of Selected Topics in Applied Earth Observations and Remote Sensing* **9**, 827-834.

Post, W. M., Izaurralde, R. C., Mann, L. K., and Bliss, N. (2001). Monitoring and verifying changes of organic carbon in soil. *In* "Storing Carbon in Agricultural Soils: A Multi-Purpose Environmental Strategy", pp. 73-99. Springer.

Richards, J. A., and Richards, J. (1999). "Remote sensing digital image analysis," Springer.

Ronov, A., and Yaroshevsky, A. (1969). Chemical composition of the earth's crust. *The Earth's crust and upper mantle*, 37-57.

Saadat, H., Bonnell, R., Sharifi, F., Mehuys, G., Namdar, M., and Ale-Ebrahim, S. (2008). Landform classification from a digital elevation model and satellite imagery. *Geomorphology* **100**, 453-464.

Sarmadian, F., Ali, K., Antonia, O., Ghavamoddin, Z., and Hossein, J. (2014). Mapping of spatial variability of soil organic carbon based on radial basis functions method. *ProEnvironment* **7**, 3-9.

Schnitzer, M. (1982). Organic matter characterization. *Methods of Soil Analysis. Part 2. Chemical and Microbiological Properties*, 581-594.

Scudiero, E., Skaggs, T. H., and Corwin, D. L. (2014). Regional scale soil salinity evaluation using Landsat 7, western San Joaquin Valley, California, USA. *Geoderma Regional* **2**, 82-90.

Scull, P., Franklin, J., Chadwick, O., and McArthur, D. (2003). Predictive soil mapping: a review. *Progress in Physical Geography* **27**, 171-197.

Seelan, S. K., Laguette, S., Casady, G. M., and Seielstad, G. A. (2003). Remote sensing applications for precision agriculture: A learning community approach. *Remote Sensing of Environment* **88**, 157-169.

Singh, S. (2016). Remote sensing applications in soil survey and mapping: A Review. *International Journal of Geomatics and Geosciences* **7**, 192-203.

Soileau, J., and McCracken, R. (1967). Free Iron and Coloration in Certain Well-Drained Coastal Plain Soils in Relation to Their Other Properties and Classification 1. *Soil Science Society of America Journal* **31**, 248-255.

Stevens, A., Udelhoven, T., Denis, A., Tychon, B., Lioy, R., Hoffmann, L., and Van Wesemael, B. (2010). Measuring soil organic carbon in croplands at regional scale using airborne imaging spectroscopy. *Geoderma* **158**, 32-45.

Stohr, C., and West, T. (1985). Terrain and look angle effects upon multispectral scanner response. *Photogrammetric Engineering and Remote Sensing* **51**, 229-235.

Stoner, E. R., and Baumgardner, M. (1981). Characteristic Variations in Reflectance of Surface Soils 1. *Soil Science Society of America Journal* **45**, 1161-1165.

Studdert, G. A. (2000). Crop rotations and nitrogen fertilization to manage soil organic carbon dynamics. *Soil Science Society of America Journal* **64**, 1496-1503.

Swift, R. S. (2001). Sequestration of carbon by soil. *Soil science* **166**, 858-871.

Takiff Smith, D. (1991). "Agriculture and the environment the 1991 yearbook of agriculture." Department of Agriculture, Washington (EUA).

Teillet, P., Guindon, B., and Goodenough, D. (1982). On the slope-aspect correction of multispectral scanner data. *Canadian Journal of Remote Sensing* **8**, 84-106.

Thomasson, J., Sui, R., Cox, M., and Al–Rajehy, A. (2001). Soil reflectance sensing for determining soil properties in precision agriculture. *Transactions of the ASAE* **44**, 1445.

Tugel, A., Herrick, J., Brown, J., Mausbach, M., Puckett, W., and Hipple, K. (2005). Soil change, soil survey, and natural resources decision making. *Soil Science Society of America Journal* **69**, 738-747.

Twomey, S. A., Bohren, C. F., and Mergenthaler, J. L. (1986). Reflectance and albedo differences between wet and dry surfaces. *Applied Optics* **25**, 431-437.

Werninghaus, R. (2004). TerraSAR-X mission. *In* "SAR Image Analysis, Modeling, and Techniques VI", Vol. 5236, pp. 9-17. International Society for Optics and Photonics.

Wiegand, C. L., and Richardson, A. J. (1992). Relating spectral observations of the agricultural landscape to crop yield. *Food structure* **11**, 7.

Wu, J., Nellis, M., Ransom, M., Price, K., and Egbert, S. (1997). Evaluating soil properties of CRP land using remote sensing and GIS in Finney County, Kansas. *Journal of Soil and Water Conservation* **52**, 352-358.

Yong-Ling, W., Peng, G., and Zhi-Liang, Z. (2010). A spectral index for estimating soil salinity in the Yellow River Delta region of China using EO-1 Hyperion data. *Pedosphere* **20**, 378-388.

Zhang, K., Shu, A., Xu, X., Yang, Q., and Yu, B. (2008). Soil erodibility and its estimation for agricultural soils in China. *Journal of arid environments* **72**, 1002-1011.

Zhang, X. W., Kong, L. W., Cui, X. L., & Yin, S. (2016). Occurrence characteristics of free iron oxides in soil microstructure: evidence from XRD, SEM and EDS. *Bulletin of Engineering Geology and the Environment*, *75*(4), 1493-1503.

Zomer, R. J., Bossio, D. A., Sommer, R., and Verchot, L. V. (2017). Global sequestration potential of increased organic carbon in cropland soils. *Scientific Reports* **7**, 15554.

Zribi, M., Baghdadi, N., and Nolin, M. (2011). Remote sensing of soil. *Applied and Environmental Soil Science* **2011**.

Zribi, M., Kotti, F., Lili-Chabaane, Z., Baghdadi, N., Issa, N. B., and Amri, R. (2012). Analysis of soil texture using TERRASAR X-band SAR. *In* "Geoscience and Remote Sensing Symposium (IGARSS), 2012 IEEE International", pp. 7027-7030. IEEE.

CHAPTER 2: Materials and Methods

Study Sites

The fields selected for this research were located in Brookings County (3 fields), South Dakota and Lac qui Parle County (2 fields), Minnesota (see Table 2.1). The climatic information about studied fields is given in Table 2.2. The full USDA-NRCS taxonomic classification information for the named soil(s) in each soil mapping unit in each field used for the study is given in Tables 2.3 to 2.7 and in Figures 2.1 to 2.5.

Table 2.1 Research field locations

County	Field	Latitude***	Longitude***	MLRA+	Field Size ha (a)
Brookings*	A	44°23'17.1"N	96°56'32.5"W	102A	64.8 (160)
Brookings	B	44°27'37.0"N	96°50'35.5"W	102A	66.8 (165)
Brookings	C	44°25'54.2"N	96°51'47.0"W	102A	60.0 (148)
Lac qui Parle**	D	45°04'24.0"N	96°26'28.8"W	103	99.0 (245)
Lac qui Parle	E	45°05'27.6"N	96°26'42.4"W	103	83.0 (205)

*Brookings – South Dakota, ** Lac qui Parle – Minnesota, + MLRA – Major Land Resource Area (Stal, U. 1965), *** Latitude and Longitude values represent the center of each study field

Table 2.2 Climatic information for study fields

Location	Mean Annual Precipitation cm (in)*	Frost Free Days* (January- July)	Mean Annual Air Temperature °C (°F) *	Snowfall** cm (in)
Field A Brookings County	68.6 (27.0)	140	6.4 (43.5)	171 (67.3)
Field B Brookings County	68.6 (27.0)	140	6.4 (43.5)	171 (67.3)
Field C Brookings County	68.6 (27.0)	140	6.4 (43.5)	171 (67.3)
Field D Lac qui Parle County	66.0 (26.0)	145	6.9 (44.5)	149 (58.7)
Field E Lac qui Parle County	66.0 (26.0)	145	6.9 (44.5)	149 (58.7)

*Precipitation and Temperature (Abatzoglou, 2017), Frost free days = refer to number of days between last freezing temperature (0°, 32°F) in spring and first freezing temperature in fall (USDA-NRCS, 2018), ** Snow fall data represents mean of total snowfall from 2016 to 2018 was attained from Applied Climate Information System (RCC-ACIS, 2018).

Soil Sampling

For this research, grid cell sampling methods were used to determine soil sample locations (Wollenhaupt and Wolkowski, 1994). Each field was divided into 2.43 ha (6 acres) cells and soil samples were collected around the grid cell center. At least 10 soil samples were collected within 15m radius of the grid center and mixed (Figure 2.6). Soil samples were collected from 0 to 15cm (0-6in) depths using push probe auger in May 2018 after planting time and before germination. These soil samples were used to analyze soil texture, electrical conductivity (EC), pH, SOM, SOC concentration, soil moisture levels at time of sampling, sum of extractable cations (SOEC), Magnesium (Mg^{2+}), Sodium (Na^{+}), Calcium (Ca^{2+}), Potassium (K^{+}), nitrate nitrogen (NO_3^{-}-N), ammonium nitrogen (NH_4^{+}-N), and phosphorus as phosphate (PO_4^{-3}). The soil samples were air dried to 40^{O}C, ground, sieved (<2mm), and stored in paper bags.

Table2.3 Taxonomic classification of named soils for each soil mapping unit in field A*

Map Unit	Map Unit Name	Major Components	Soil Classification for Named Soil Series**	Area of Interest (%)
Ba	Badger silty clay loam, 0 to 1% slopes	Badger (90%) Minor Components (10%)	Fine, smectitic, frigid Vertic Argiaquolls	1.8
Co	Cubden -Badger silty clay loams, coteau, 0 to 2% slopes	Cubden (50%) Badger (40%) Minor Components (10%)	Fine-silty, mixed, superactive, frigid Aeric Calciaquolls Fine, smectitic, frigid Vertic Argiaquolls	30.2
Dn	Divide loam, 0 to 2% slopes	Divide (85%) Minor Components (15%)	Fine-loamy over sandy or sandy-skeletal, mixed, superactive, frigid Aeric Calciaquolls	2.9
KrB	Kranzburg-Brookings silty clay loams, 1 to 6% slope	Kranzburg (70%) Brookings (20%) Minor Components (10%)	Fine-silty, mixed, superactive, frigid Calcic Hapludolls Fine-silty, mixed, superactive, frigid Pachic Hapludolls	6.4
PbB	Poinsett-Buse-Waubay complex, 1 to 6% slopes	Poinsett (40%) Buse (30%) Waubay (20%) Minor Components (10%)	Fine-silty, mixed, superactive, frigid Calcic Hapludolls Fine-loamy, mixed, superactive, frigid Typic Calciudolls Fine-silty, mixed, superactive, frigid Pachic Hapludolls	19.6
PbC	Poinsett-Buse -Waubay complex, 2 to 9% slopes	Poinsett (40%) Buse (35%) Waubay (15%) Minor Components (10%)	Fine-silty, mixed, superactive, frigid Calcic Hapludolls Fine-loamy, mixed, superactive, frigid Typic Calciudolls Fine-silty, mixed, superactive, frigid Pachic Hapludolls	2.8
PwA	Poinsett-Waubay silty clay loams, 0 to 2% slopes	Poinsett (60%) Waubay (30%) Minor Components (10%)	Fine-silty, mixed, superactive, frigid Calcic Hapludolls Fine-silty, mixed, superactive, frigid Pachic Hapludolls	4.4
PwB	Poinsett-Waubay silty clay loams, 1 to 6% slopes	Poinsett (65%) Waubay (25%) Minor Components (10%)	Fine-silty, mixed, superactive, frigid Calcic Hapludolls Fine-silty, mixed, superactive, frigid Pachic Hapludolls	0.2
Z182B	Estelline silt loam, coteau, 2 to 6% slopes	Estelline (85%) Minor Components (15%)	Fine-silty over sandy or sandy-skeletal, mixed, superactive, frigid Calcic Hapludolls	31.7

** Soil map units, map unit names, and soil classification information from Web Soil Survey (USDA-NRCS, 2018).
*(44°23'17.1"N, 96°56'32.5"W, Brookings County, SD)

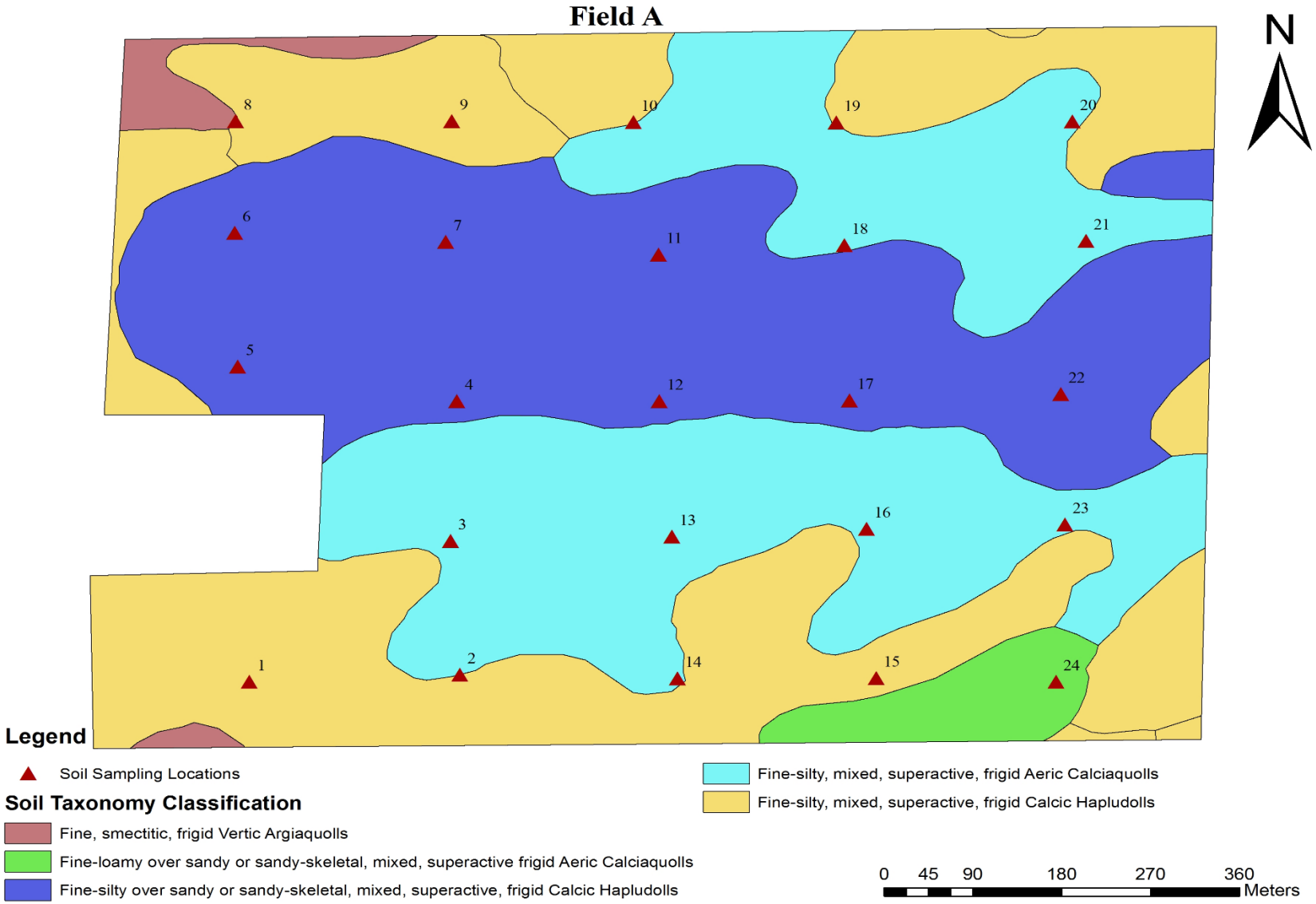

Figure 2.1 Spatial distribution of soil samples on field A (44°23'17.1"N, 96, °56'32.5"W, Brookings County, SD). Map Source: Web Soil Survey (WSS), USGS, USDA, NRCS (2018).

Table 2.4 Taxonomic classification of named soils for each soil mapping unit in field B*

Map Unit	Map Unit Name	Major Components	Soil Classification for Named Soil Series**	Area of Interest (%)
BbA	Barnes clay loam, 0 to 2% slopes	Barnes (80%) Minor Components (20%)	Fine-loamy, mixed, superactive, frigid Calcic Hapludolls	2.1
BbB	Barnes clay loam, 2 to 6% slopes	Barnes (80%) Minor Components (20%)	Fine-loamy, mixed, superactive, frigid Calcic Hapludolls	51.4
BgC	Buse-Barnes loams, 6 to 9% slopes	Buse (55%) Barnes (30%) Minor Components (15%)	Fine-loamy, mixed, superactive, frigid Typic Calciudolls Fine-loamy, mixed, superactive, frigid Calcic Hapludolls	0.4
Hb	Hamerly-Badger complex, 0 to 2% slopes	Hamerly (55%) Badger (30%) Minor Components (15%)	Fine-loamy, mixed, superactive, frigid Aeric Calciaquolls Fine, smectitic, frigid Vertic Argiaquolls	13.6
LnB	Lanona-Swenoda sandy loams, 2 to 6% slopes	Lanona (60%) Swenoda (25%) Minor Components (15%)	Coarse-loamy, mixed, superactive, frigid Calcic Hapludolls Coarse-loamy, mixed, superactive, frigid Pachic Hapludolls	25.8
SwA	Swenoda -Lanona sandy loams, 0 to 2% slopes	Swenoda (55%) Lanona (35%) Minor Components (10%)	Coarse-loamy, mixed, superactive, frigid Pachic Hapludolls Coarse-loamy, mixed, superactive, frigid Calcic Hapludolls	6.7

**Soil map units, map unit names, and soil classification information from Web Soil Survey (USDA-NRCS, 2018).
*44°27'37.0"N, 96°50'35.5"W, Brookings County, SD

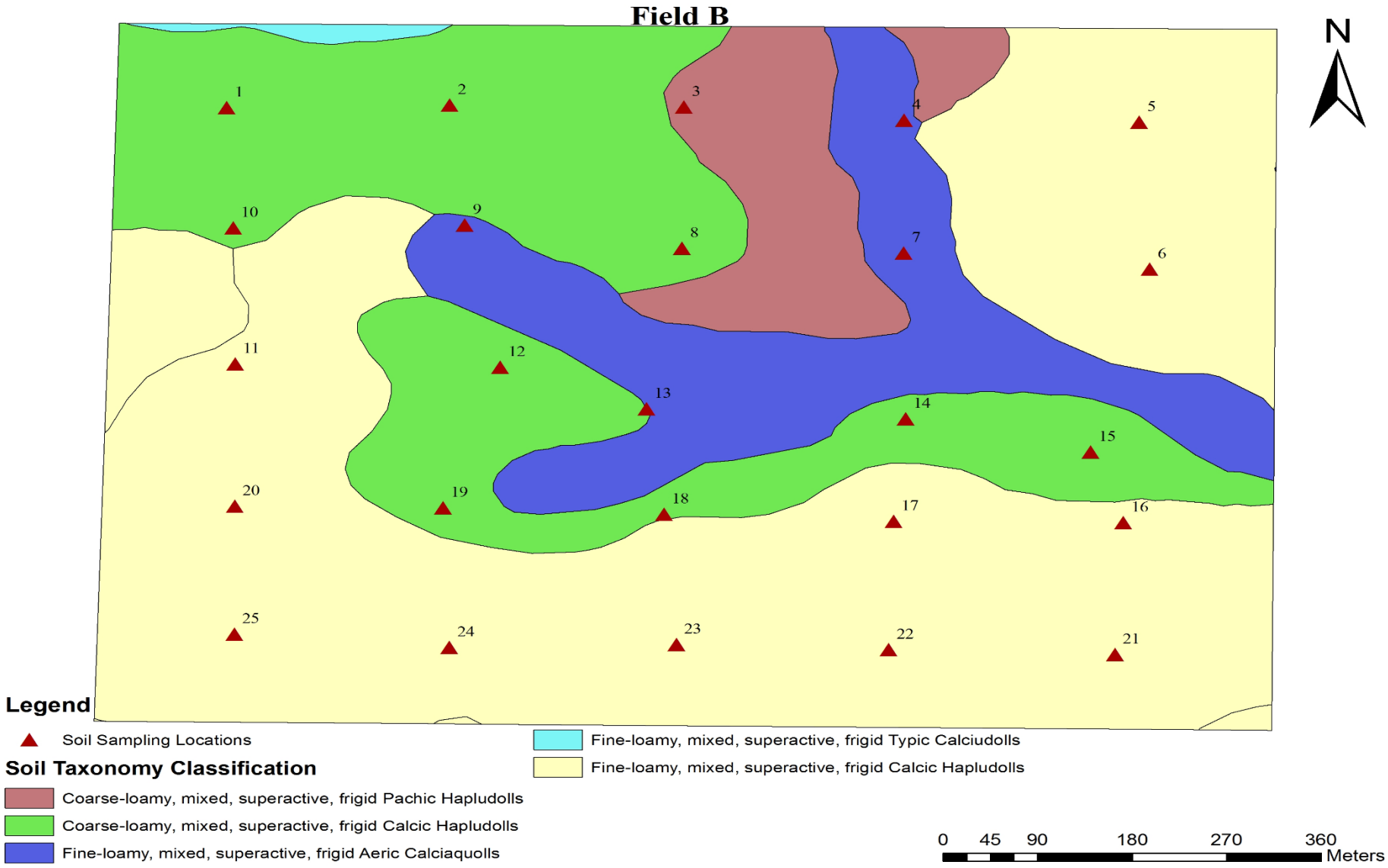

Figure 2.2 Spatial distribution of soil samples on field B (44°27'37.0"N, 96°50'35.5"W, Brookings County, SD), Map Source: Web Soil Survey (WSS), USGS, USDA, NRCS (2018).

Table 2.5 Taxonomic classification of named soils for each soil mapping unit in field C*

Map Unit	Map Unit Name	Major Components	Soil Classification for Named Soil Series**	Area of Interest (%)
DsA	Doland-Svea loams, 0 to 2% slopes	Doland (55%) Svea (25%) Minor Components (20%)	Fine-loamy, mixed, superactive, frigid Calcic Hapludolls Fine-loamy, mixed, superactive, frigid Pachic Hapludolls	0.2
EgB	Egeland-Embden complex, 2 to 6% slopes	Egeland (60%) Embden (30%) Minor Components (%10)	Coarse-loamy, mixed, superactive, frigid Calcic Hapludolls Coarse-loamy, mixed, superactive, frigid Pachic Hapludolls	47.2
LnB	Lanona-Swenoda sandy loams, 2 to 6% slopes	Lanona (60%) Swenoda (25%) Minor Components (15%)	Coarse-loamy, mixed, superactive, frigid Calcic Hapludolls Coarse-loamy, mixed, superactive, frigid Pachic Hapludolls	5.3
MaC	Maddock-Egeland sandy loams, 6 to 9% slopes	Maddock (65%) Egeland (25%) Minor Components (10%)	Sandy, mixed, frigid Entic Hapludolls Coarse-loamy, mixed, superactive, frigid Calcic Hapludolls	3.0
SrA	Strayhoss loam, 0 to 2% slopes	Strayhoss (85%) Minor Components (15%)	Fine-loamy over sandy or sandy-skeletal, mixed, superactive, frigid Calcic Hapludolls	0.1
VaA	Venagro-Svea loams, 0 to 2%t slopes	Venagro (60%) Svea (20%) Minor Components (20%)	Fine-loamy, mixed, frigid Udic Haploborolls Fine-loamy, mixed, superactive, frigid Pachic Hapludolls	44.2

**Soil map units, map unit names, and soil classification information from Web Soil Survey (USDA-NRCS, 2018).
*(44°25'54.2"N 96°51'47.0"W, Brookings County, SD).

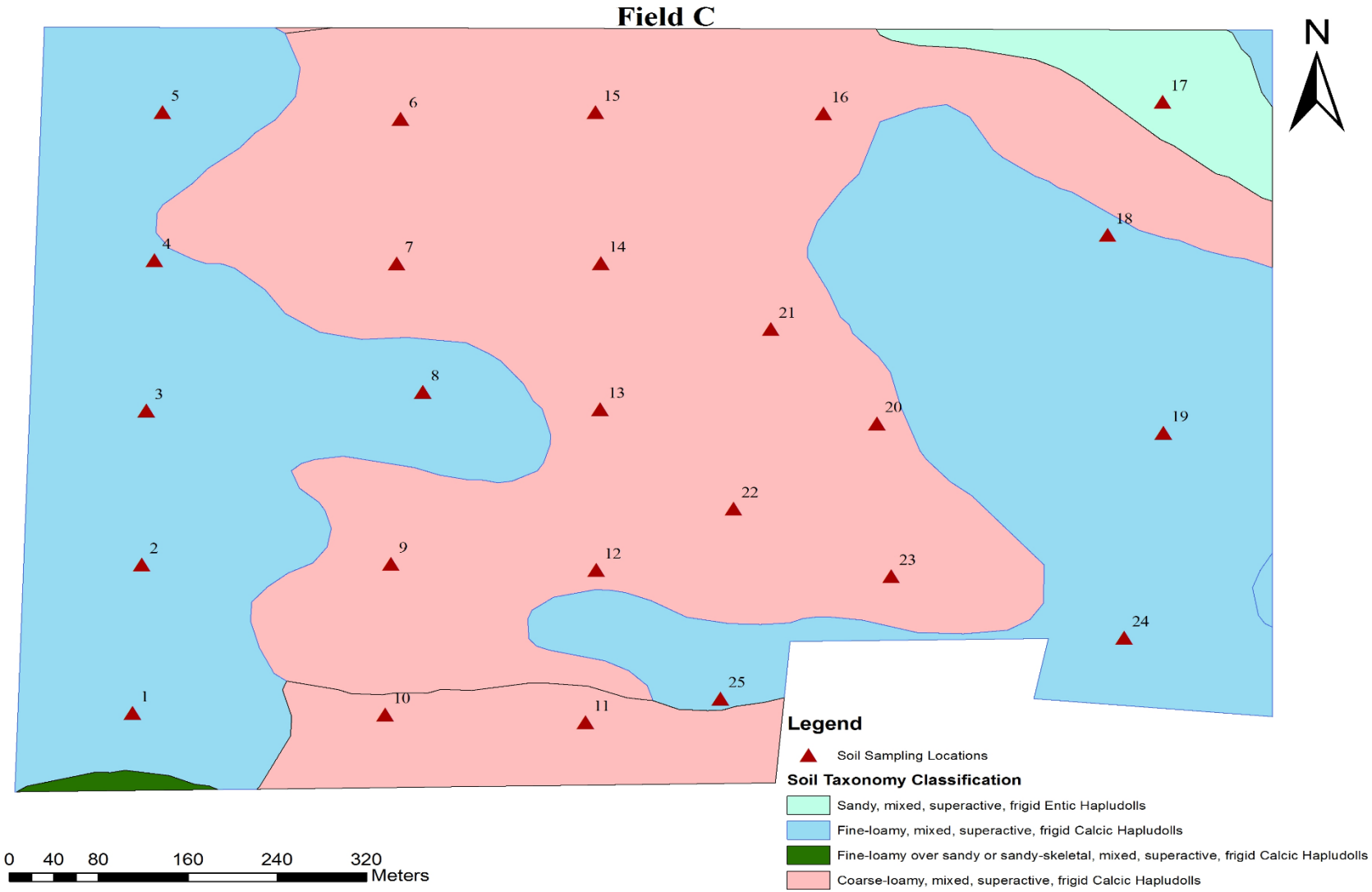

Figure 2.3 Spatial distribution of soil samples on field C (44°25'54.2"N, 96°51'47.0"W, Brookings County, SD), Map Source: Web Soil Survey (WSS), USGS, USDA, NRCS (2018).

Table 2.6 Taxonomic classification of named soils for each soil mapping unit in field D*

Map Unit	Map Unit Name	Major Components	Soil Classification for Named Soil Series**	Area of Interest (%)
51	La Prairie loam, 0 to 2% slopes, occasionally flooded	La Prairie (75%) Minor Components (25%)	Fine-loamy, mixed, superactive, frigid Cumulic Hapludolls	2.5
70	Svea loam, 1 to 3% slopes	Svea (85%) Minor Components (15%)	Fine-loamy, mixed, superactive, frigid Aquic Pachic Hapludolls	12.6
127B	Sverdrup sandy loam, 2 to 6% slopes	Sverdrup (70%) Minor Components (30%)	Sandy, mixed, superactive frigid Typic Hapludolls	2.6
141B	Egeland sandy loam, 2 to 6% slopes	Egeland (70%) Minor Components (30%)	Coarse-loamy, mixed, superactive, frigid Calcic Hapludolls	1.7
168B	Forman clay loam, 2 to 6% slopes	Forman (75%) Minor Components (%25)	Fine-loamy, mixed, superactive, frigid Calcic Argiudolls	3.7
184	Balaton-Hamerly complex, 1 to 4% slopes	Balaton (55%) Hamerly (30%) Minor Components (15%)	Fine-loamy, mixed, superactive, frigid Aquic Calciudolls Fine-loamy, mixed, superactive, frigid Aeric Calciaquolls	1.4
220D2	Langhei-Barnes, moderately eroded, complex, 12 to 20% slopes	Langhei (50%) Barnes (35%) Minor Components (15%)	Fine-loamy, mixed, superactive, frigid Typic Eutrudepts Fine-loamy, mixed, superactive, frigid Calcic Hapludolls	3.2
284B	Poinsett-Waubay silty clay loams, 1 to 6% slopes	Poinsett (65%) Waubay (25%) Minor Components (10%)	Fine-silty, mixed, superactive, frigid Calcic Hapludolls Fine-silty, mixed, superactive, frigid Pachic Hapludolls	0.2

Table 2.6 (continued)

Map Unit	Map Unit Name	Major Components	Soil Classification for Named Soil Series**	Area of Interest (%)
293B	Swenoda loam, 2 to 6% slopes	Swenoda (75%) Minor Components (25%)	Coarse-loamy, mixed, superactive, frigid Pachic Hapludolls	1.5
418	Lamoure silty clay loam, 0 to 2% slopes, occasionally flooded	Lamoure (80%) Minor Components (20%)	Fine-silty, mixed, superactive, calcareous, frigid Cumulic Endoaquolls	10.0
450	Rauville silty clay loam, 0 to 2% slopes, frequently flooded	Rauville (80%) Minor Components (20%)	Fine-silty, mixed, superactive, calcareous, frigid Cumulic Endoaquolls	0.2
748B	Hamlet loam, 1 to 4% slopes	Hamlet (70%) Minor Components (30%)	Fine-loamy, mixed, superactive, frigid Oxyaquic Hapludolls	16.0
769A	Mehurin clay loam, 0 to 2% slopes	Mehurin (75%) Minor Components (25%)	Fine, smectitic, frigid Aquic Argiudolls	13.7
777C2	Esmond-Sisseton-Heimdal, complex, 2 to 12% slopes, moderately eroded	Esmond (40%) Sisseton (30%) Heimdal (15%) Minor Components (15%)	Coarse-loamy, mixed, superactive, frigid Typic Calciudolls Coarse-loamy, mixed, superactive, frigid Typic Eutrudepts Coarse-loamy, mixed, superactive, frigid Calcic Hapludolls	5.3
942C2	Langhei-Barnes, moderately eroded, complex, 6 to 12% slopes	Langhei (55%) Barnes (30%) Minor Components (15%)	Fine-loamy, mixed, superactive, frigid Typic Eutrudepts Fine-loamy, mixed, superactive, frigid Calcic Hapludolls	3.6

Table 2.6 (continued)

Map Unit	Map Unit Name	Major Components	Soil Classification for Named Soil Series**	Area of Interest (%)
1233B	Esmond-Heimdal-Sisseton complex, 2 to 6% slopes	Esmond (40%) Heimdal (35%) Sisseton (15%) Minor Components (10%)	Coarse-loamy, mixed, superactive, frigid Typic Calciudolls Coarse-loamy, mixed, superactive, frigid Calcic Hapludolls	8.1
1938	Lakepark-Parnell, occasionally ponded, complex, 0 to 2% slopes	Lakepark (45%) Parnell (25%) Minor Components (30%)	Fine-loamy, mixed, superactive, frigid Cumulic Endoaquolls Fine, smectitic, frigid Vertic Argiaquolls	11.9
J105B	Arvilla sandy loam, Till Prairie, 2 to 6% slopes	Arvilla (85%) Minor Components (15%)	Sandy, superactive, mixed, frigid Calcic Hapludolls	1.8

** Soil map units, map unit names, and soil classification information from Web Soil Survey (USDA-NRCS, 2018).
*(45°04'24.0"N, 96°26'28.8"W, Lac qui Parle County, MN)

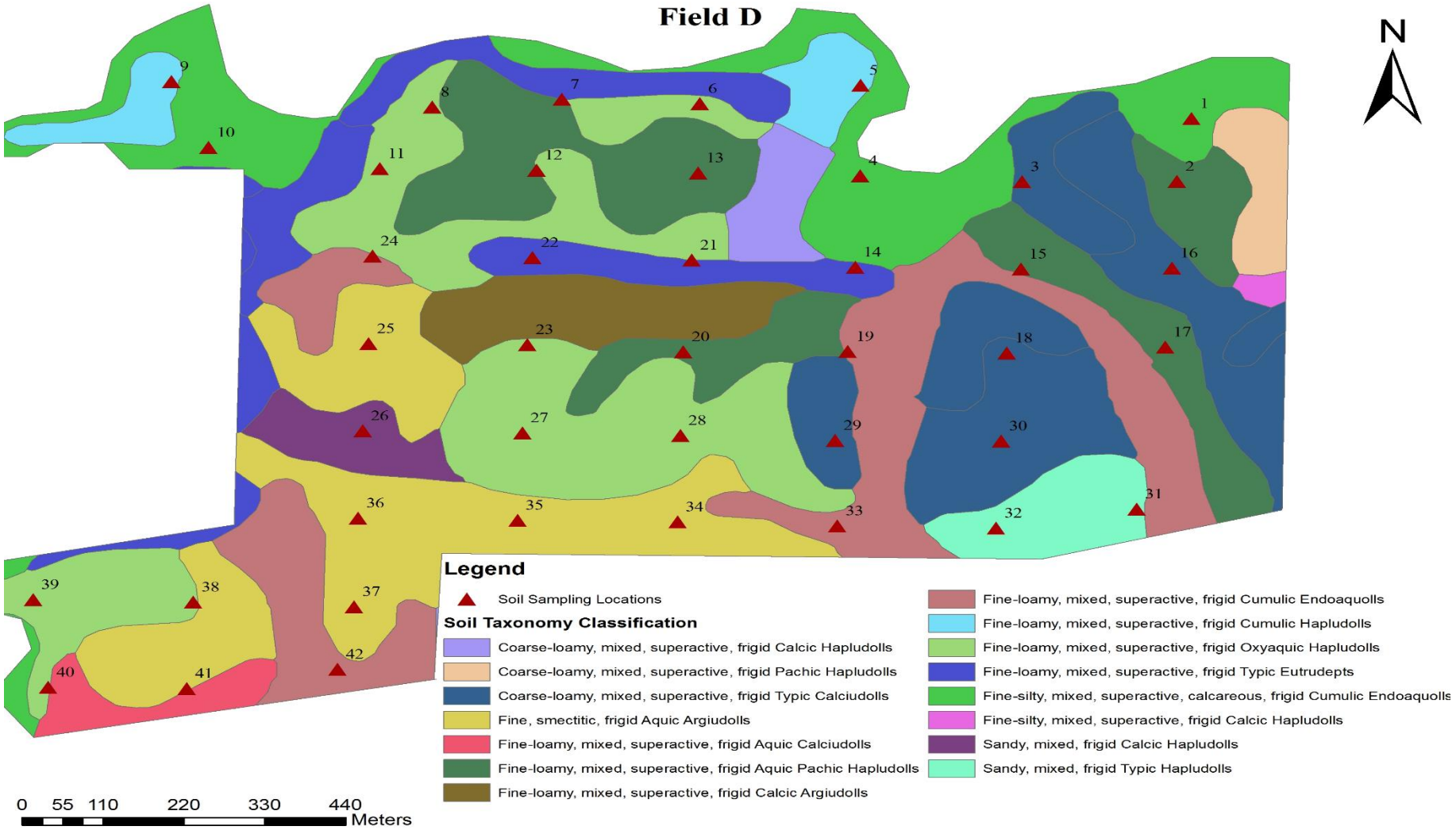

Figure 2.4 Spatial distribution of soil samples on field D (45°04'24.0"N, 96°26'28.8"W, Lac qui Parle County, MN), Map Source: Web Soil Survey (WSS), USGS, USDA, NRCS (2018).

Table 2.7 Taxonomic classification of named soils for each soil mapping unit in field E*

Map Unit	Map Unit Name	Major Components	Soil Classification for Named Soil Series**	Area of Interest (%)
34	Parnell silty clay loam, occasionally ponded, 0 to 1% slopes	Parnell (65%) Minor Components (35%)	Fine, smectitic, frigid Vertic Argiaquolls	3.5
47	Colvin silty clay loam 0 to 1% slopes	Colvin (75%) Minor Components (25%)	Fine-silty, mixed, superactive, frigid Typic Calciaquolls	14.6
70	Svea loam, 1 to 3% slopes	Svea (85%) Minor Components (15%)	Fine-loamy, mixed, superactive, frigid Aquic Pachic Hapludolls	2.2
127B	Sverdrup sandy loam, 2 to 6% slopes	Sverdrup (70%) Minor Components (30%)	Sandy, mixed,superactive, frigid Typic Hapludolls	18.5
127C	Sverdrup sandy loam, 6 to 12% slopes	Sverdrup (70%) Minor Components (30%)	Sandy, mixed,superactive, frigid Typic Hapludolls	2.2
141B	Egeland sandy loam, 2 to 6% slopes	Egeland (70%) Minor Components (30%)	Coarse-loamy, mixed, superactive, frigid Calcic Hapludolls	3.6
168B	Forman clay loam, 2 to 6% slopes	Forman (75%) Minor Components (25%)	Fine-loamy, mixed, superactive, frigid Calcic Argiudolls	0.8
184	Balaton-Hamerly complex, 1 to 4% slopes	Balaton (55%) Hamerly (30%) Minor Components (15%)	Fine-loamy, mixed, superactive, frigid Aquic Calciudolls Fine-loamy, mixed, superactive, frigid Aeric Calciaquolls	2.5
236	Vallers clay loam, 0 to 2% slopes	Vallers (85%) Minor Components (15%)	Fine-loamy, mixed, superactive, frigid Typic Calciaquolls	8.0
246	Marysland loam, 0 to 2% slopes	Marysland (75%) Minor Components (25%)	Fine-loamy over sandy or sandy-skeletal, mixed, superactive, frigid Typic Calciaquolls	11.1

Table 2.7 (continued)

Map Unit	Map Unit Name	Major Components	Soil Classification for Named Soil Series**	Area of Interest (%)
338	Waubay loam, 0 to 2% slopes	Waubay (90%) Minor Components (10%)	Fine-silty, mixed, superactive, frigid Pachic Hapludolls	1.5
347	Malachy loam 0 to 1% slope	Malachy (75%) Minor Components (25%)	Coarse-loamy, mixed, superactive, frigid Aquic Calciudolls	9.8
769A	Mehurin clay loam, 0 to 2% slopes	Mehurin (75%) Minor Components (25%)	Fine, smectitic, frigid Aquic Argiudolls	1.9
902B	Hokans-Buse complex, 2 to 6% slopes	Hokans (55%) Buse (23%) Minor Components (22%)	Fine-loamy, mixed, superactive, frigid Calcic Hapludolls Fine-loamy, mixed, superactive, frigid Typic Calciudolls	2.4
1938	Lakepark-Parnell, occasionally ponded, complex, 0 to 2% slopes	Lakepark (45%) Parnell (25%) Minor Components (30%)	Fine-loamy, mixed, superactive, frigid Cumulic Endoaquolls Fine, smectitic, frigid Vertic Argiaquolls	2.7
1994	Embden sandy loam 0 to 2% slope	Embden (75%) Minor Components (25%)	Coarse-loamy, mixed, superactive, frigid Pachic Hapludolls	5.7
J105A	Arvilla sandy loam, Till Prairie, 0 to 2% slopes	Arvilla (85%) Minor Components (15%)	Sandy, mixed, superactive, frigid Calcic Hapludolls	3.3
J105B	Arvilla sandy loam, Till Prairie, 2 to 6% slopes	Arvilla (85%) Minor Components (15%)	Sandy, mixed, superactive, frigid Calcic Hapludolls	4.5
J105C	Arvilla sandy loam, Till Prairie, 6 to 12% slopes	Arvilla (75%) Minor Components (25%)	Sandy, mixed, superactive, frigid Calcic Hapludolls	1.2

**Soil map units, map unit names, and soil classification information from Web Soil Survey (USDA-NRCS, 2018).
*(45°05'27.6"N 96°26'42.4"W, Lac qui Parle, County, MN).

Figure 2.5 Spatial distribution of soil samples on field E (45°05'27.6"N 96°26'42.4"W, Lac qui Parle, County, MN), Map Source: Web Soil Survey (WSS), USGS, USDA, NRCS (2018)

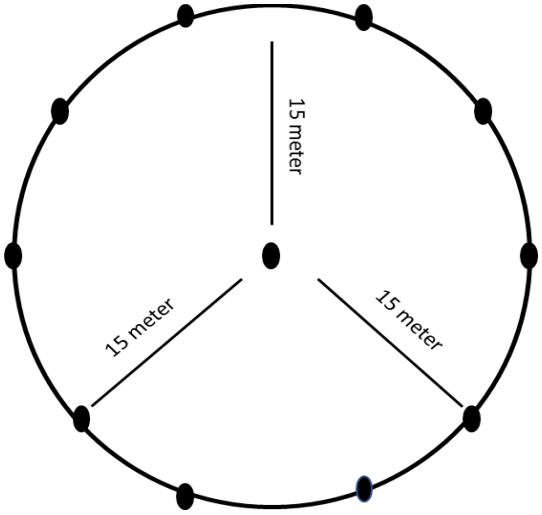

Figure 2.6 Illustration of soil sampling design

Lab Analysis

Soil Organic Matter

Soil organic matter was determined using the loss on ignition method in accordance with the SDSU Soil Testing and Plant Analysis Laboratory protocol (SDSU, 2006). Racks of 10mL crucibles were weighed before the analysis and recorded. Five g of < 2mm air-dried crushed soils were placed into each crucible. Check soils were used for quality assurance. Soil samples were placed in a furnace (Lindberg Hevi-Duty BPC) at 100^{O}C for two hours in order to remove all moisture from soil particles. Crucibles were removed from the oven and allowed to cool down for 15 min. After cooling crucibles were weighed to calculate weight loss. Soil samples were then returned to furnace for 2 hours and 10 minutes at 400^{O}C. After second heating, samples were removed from the furnace and weighed. Equations 2.1 to 2.3 were used to determine SOM. The conversion factor was 1.72 to convert from SOM to SOC (Pribyl, 2010).

Crucible Weight after 100°C (g) − Empty Crucible Weight (g) = Heated Weight (g) (HT) [2.1]

Crucible Weight after 400°C (g) − Empty Crucible Weight (g) = Ignition Weight (g) (IG) [2.2a]

HT – IG = Weight loss (g) [2.2b]

Weight Loss (g) / Heated Weight (g) (HT) × 100 = % Weight Loss [2.2c]

a + b (% Weight Loss) = % SOM [2.3]

Note: The coefficients, a and b in equation 2.3 are calculated by following the SDSU Soil Testing and Plant Analysis Laboratory (SDSU, 2006) protocols. Analysis was completed as two replicates.

Crop Residue Measurement

The crop residue on the land surface was measured using line transect method (Shelton et al., 1990). A 30.5m (100ft) tape measure was used for this method. The tape measure was laid on the ground diagonally to the row direction. At each 30.5cm (1.0ft) marker on same side of the tape I recorded the number of times plant residue was present at the designated tape locations. The recorded total number of intersections represent the percentage of surface residue. For instance, if 25 out of 100 points intersected with plant residue, then the residue on the ground is 25%.

Moisture Content

Soil moisture was determined as gravimetric moisture content following SDSU Soil Testing and Plant Analysis Laboratory protocol (SDSU, 2006). Soil samples were air dried at 40.5^{O}C for at least 5 days to reach air dry soil mass. Soil moisture content was calculated by the ratio of the mass lost using equation 2.4.

% soil moisture = [(wet soil wt.) – (dry soil wt.) / (dry soil wt.)] * 100% [2.4]

Particle Size

Before analyzing soil particle size by hydrometer method, SOM was removed from sample using 30% hydrogen peroxide (H_2O_2) (Malo et al., 2014). Fifty grams of soil was weighed in to 1-L Pyrex bottle and placed under the fume hood. Twenty mL of 30% H_2O_2 were added to the 1-L Pyrex bottle and the oxidation reaction was monitored to prevent effervescence from exiting the bottle. After reaction subsided, three to five drops of acetic acid were added to the 1-L Pyrex bottle in order to break iron related structural units (peds) and then the bottle was placed on the hot plate at $300^{O}C$. After that 15mL of 30%H_2O_2 was added to the 1-L Pyrex bottle. The bottles were monitored, and water added to prevent soil from drying out, especially in the bottom part. The H_2O_2 additions continued until there was no further color change of the soil sample (SOM removed from the soil). After removing SOM, bottles were placed in a forced air oven to dry at 105 ^{O}C overnight.

After oven drying, samples were removed from the oven and allowed to cool down until reaching room temperature in a moisture free container. The samples were weighed and 50mL dispersion solution (sodium hexametaphosphate and sodium carbonate) was added. The bottles were filled with 425mL DI water, capped, wrapped with cloth bag and placed in a reciprocating shaker to shake overnight. Soil samples were then transferred to 1-L graduated cylinders. All soil particles were rinsed from the Pyrex bottle to the cylinders and filled the cylinders with DI water until the 1 L mark. A wooden plunger was used to mix the sample for 60 seconds. As soon as, the samples were homogenized, a glass hydrometer was placed into the cylinders to record 40 second

reading (after mixing stopped). The solution temperature was measured just prior to mixing with plunger or after the 40 sec reading. After two hours of settling time, second hydrometer reading was taken, and the solution temperature was again recorded. Soil textural fractions were calculated using the equations 2.5 to 2.14. Soil textural class was determined using a soil textural triangle.

40 Second Temperature (^{O}C) − 20^{O}C = 40 Second Temperature Difference (^{O}C) [2.5]

40 Second Temperature Difference (^{O}C) × 0.36 g/L^{-1} = 40 Second Temperature Correction Factor [2.6]

(Hydrometer Reading – Dispersion correction factor) + 40 Second Temperature Correction Factor = Silt and Clay (g) [2.7]

Sample weight (g) − Silt and Clay (g) = Sand (g) [2.8]

(Sand (g) / Sample weight (g)) × 100% = % Sand [2.9]

2-Hour Measured Temperature (^{O}C) − 20 (^{O}C) = 2 Hour Temperature Difference (^{O}C) [2.10]

2-Hour Temperature Difference (^{O}C) × 0.36 g/L^{-1} = 2 Hour Temperature Correction Factor (^{O}C) [2.11]

(2-Hour Hydrometer Reading – Dispersion correction factor) − 2 Hour Temperature Correction Factor (^{O}C) = Clay (g) [2.12]

(Clay (g) / Sample Weight (g)) × 100% = % Clay [2.13]

100% − % Sand − % Clay = % Silt [2.14]

Soil pH and Electrical Conductivity (EC)

Soil samples from 0-15cm were air dried and grounded. Twenty g of soil was placed in a small beaker, 20mL of distilled water was added, and the suspension (the ratio of soil: water is 1:1) was stirred by hand for 60 seconds. After 30 minutes, the samples were again stirred with a glass rod before reading. Soil pH and EC was measured using the same probe all the time. The pH and EC meter were checked and calibrated for each set of 25 samples.

Sum of Extractable Cations

Sum of Extractable Cations (SOEC) was determined using the summation method in accordance with the SDSU Soil Testing and Plant Analysis Laboratory protocol (SDSU, 2006). Two g of soil was weighed and 20 mL of extracting solution 1*M* NH_4OA_c (ammonium acetate) were added to flask. The samples were then shaken for 5 minutes with oscillating shaker. The soil solutions were extracted through Whatman #40 filter paper. The samples were analyzed using Atomic Adsorption (AA) unit to determine potassium (K^+), calcium (Ca^{2+}), magnesium (Mg^{2+}) and sodium (Na^+). The centimoles of charge per kilogram ($cmol_c\ kg^{-1}$) of each ion were calculated using equations 2.15 and 2.16. When the soil pH was lower than 7, the SMP (Lime Requirement Test) pH buffer was used to measure exchangeable acidity in the SOEC calculations. For the SMP pH buffer test 10 g of soil was placed into plastic beakers and 10 mL of Nanopure water was added. The sample was stirred and allowed to sit for 5 minutes. Ten mL of SMP buffer was added to soil sample and shaken with oscillating shaker for 10 minutes. Lastly, the $cmol_c\ kg^{-1}$ of exchangeable acidity was calculated using equations 2.16. The pH was recorded using same probe. The final SOEC was calculated using equation 2.17

Conversion ppm to $cmol_c$, kg^{-1} [2.15]

ppm in soil K^+ / 390 = K^+ $cmol_c$ kg^{-1}

ppm in soil Ca^{2+} / 200 = Ca^{+2} $cmol_c$ kg^{-1}

ppm in soil Mg^{2+} / 120 = Mg^{+2} $cmol_c$ kg^{-1}

ppm in soil Na^+ / 230 = Na^+ $cmol_c$ kg^{-1}

$cmol_c$ exchangeable acidity /100_g =12 (7.0 – SMP buffer pH). When soil pH reading ≥ 7.0, [2.16]

the $cmol_c$ kg^{-1} exchangeable acidity = 0

Estimation of SOEC ($cmol_c$ kg^{-1}) is determined by following equation:

SOEC ($cmol_c$ kg^{-1}) = $cmol_c$ kg^{-1} (K^+, Na^+, Ca^{2+}, Mg^{2+}) + $cmol_c$ kg^{-1} H^+ [2.17]

Phosphorous as Phosphate (PO_3^{4-})

Total Orthophosphate (P, ortho), a form of inorganic phosphorus, in the sample was measured by direct colorimetric analysis procedure (O'Dell, 1993). Two g soil was placed in a 125 mL Erlenmeyer flask and 20 mL Ortho-Phosphate Extracting Solution (0.03 *M*NH_4F, 0.025 *M*HCl) was added. Flasks were then placed on reciprocating shaker for 15 min and filtered. Ammonium molybdate and antimony potassium tartrate react in an acid medium with dilute solutions of phosphorus to form an antimony-phospho-molybdate complex. This complex is reduced to an intensely blue-colored complex by ascorbic acid. The color is proportional to the phosphorus concentration in the solution. The solution was analyzed the same day as extracted using Astoria Nutrient Analyzer (Astoria-Pacific, Inc. Clackamas, OR).

Nitrate - N (NO_3^--N) and Ammonium -N (NH_4^+-N)

Ten of g soil was placed in a 125mL Erlenmeyer flask, and 100mL 1.0*M* KCl was added. Flasks were placed on reciprocating shaker for 60 min and the solution filtered (Kim et al., 2008). Nitrate (NO_3^--N) was determined by reduction to nitrite (NO_2^--N) via a cadmium reactor, diazotized with sulfanilamide and coupled to N-(1-Napthyl)-ethylenediamine dihydrochloride to form an azo-chromophore (red-purple in color) and measured spectrophotometrically at 520nm, using the Astoria Nutrient Analyzer (Astoria-Pacific, Inc. Clackamas, OR).

Ammonium (NH_4^+-N) was determined by the phenate method using the same soil extraction used for NH_3^--N. It is based on the reaction of NH_3^--N in alkaline solution with phenolate to produce a blue color (indophenol blue) in the presence of a strong oxidizing agent, like hypochlorite. The process is accelerated by heating the solution to 37^OC and measured spectrophotometrically using the Astoria Nutrient Analyzer (Astoria-Pacific, Inc. Clackamas, OR).

Statistical Analysis

Descriptive statistics were completed using R 3.5.0 (R Core Team, 2018). Pearson Correlation Matrix and Simple Linear Regressions were completed in JMP (SAS Institute Cary, NC).

Multiple linear regression (MLR) analysis was conducted in R 3.5.0. The Variance Inflation Factor (VIF) was calculated to detect multicollinearity problem. The general rule is that VIF values exceeding 4 warrant further examination, while VIF values exceeding 10 indicate serious multicollinearity requiring model modifications (Simon, 2004).

The VIF is defined in Equation 2.18 (Simon, 2004):

$$VIF = \frac{1}{1 - {R_k}^2} \quad [2.18]$$

${R_k}^2$ is the correlation coefficient between two independent variables, and VIF = Variance Inflation Factor.

Stepwise regression model selection was completed in R 3.5.0. Depending on VIF values, Principal Component Regression (PCR) which is the method of combining linear regression with principal component analysis (Liu et al., 2003) and Ridge Regression (RR) which minimize the sum of square error (Marquardt and Snee, 1975) were applied to build SOC prediction model.

To compare the prediction performance of different models, we presented the cross-validation values of the different models. For validation, we followed leave one out cross validation. The function estimator is trained on all the data of 150 points except for one point and a prediction model applied for that point.

Spatial Data Acquisition

The Operational Land Imager (OLI) on Landsat-8 is the most recent spacecraft launched by NASA Earth Observation Center into orbit on February 11, 2013. As Landsat-8 was being designed, scientists developed new focal plane technology that allows for a new class of enhanced and improved instruments to meet the needs of the Landsat community. Landsat 8 Operational Land Imager (OLI) and Thermal Infrared Sensor (TIRS) images consist of nine spectral bands with a spatial resolution of 30m for $Bands_L$ 1 to 7 and 9. The resolution for $Band_L$ 8 (panchromatic) is 15m. Thermal $bands_L$

10 and 11 are useful in providing more accurate surface temperatures and are collected at 100-meter resolution (See Table 2.8). The approximate scene size is 170km north-south by 183km east-west (106 mile by 114 miles).

Table 2.8 Wavelength and spatial resolution of different bands of Landsat 8 (Zanter, 2016).

Bands	Wavelength (µm)	SpatialResolution (m)
$Band_L$ 1 - Ultra Blue (coastal/aerosol)	0.435 - 0.451	30
$Band_L$ 2 - Blue	0.452 - 0.512	30
$Band_L$ 3 - Green	0.533 - 0.590	30
$Band_L$ 4 - Red	0.636 - 0.673	30
$Band_L$ 5 - Near Infrared (NIR)	0.851 - 0.879	30
$Band_L$ 6 - Shortwave Infrared (SWIR) 1	1.566 - 1.651	30
$Band_L$ 7 - Shortwave Infrared (SWIR) 2	2.107 - 2.294	30
$Band_L$ 8 - Panchromatic	0.503 - 0.676	15
$Band_L$ 9 - Cirrus	1.363 - 1.384	30
$Band_L$ 10 - Thermal Infrared (TIRS) 1	10.60 - 11.19	100 * (30)
$Band_L$ 11 - Thermal Infrared (TIRS) 2	11.50 - 12.51	100 * (30)

The PlanetScope Scene product is a Scaled Top of Atmosphere Radiance (at sensor) and sensor corrected product, providing imagery as seen from the spacecraft without correction for any geometric distortions inherent in the imaging process. Three PlanetScope satellite data images were acquired over the Brookings County, SD and Lac qui Parle County, MN in US. The date of acquisition for the imagery was in May 2018. The acquisition time was chosen to be cloud free and as close as possible to soil sampling time (just after planting in May). This was done to reduce the crop residue effect on soil reflectance values. Technical details of the PlanetScope Scene are shown in Table 2.9

Table 2.9 Wavelength and spatial resolution of different bands of PlanetScope scene (Team, 2017)

Bands	Wavelenght(μm)	Spatial Resolution(m)
$Band_P$ 1 (Blue)	0.455-0.515	~3.0 m
$Band_P$ 2 (Green)	0.500-0.590	~3.0 m
$Band_P$ 3 (Red)	0.590-0.670	~3.0 m
$Band_P$ 4 (Near-Infrared)	0.780-0.860	~3.0 m

Image Processing

The study area fields had some residue left on the soil surface depending on each farmer`s management system. We had corn and soybean residue in the study areas from the previous harvests. The fields were mostly bare and had no living vegetation at the time of sampling. To identify and estimate the SOC in the study area indices [the normalized difference vegetation index (NDVI), modified soil-adjusted vegetation index (MSAVI2), bare soil index (BSI), and Brightness Index (BI)] were considered and have proven useful for monitoring vegetation and SOC content These indices were developed to calculate more reliable soil brightness correction factors (Kumar, 2013; Zimmermann et al., 2006). In order to prepare the imagery for processing of various indices the Digital Number (DN) of the Landsat 8 imagery is converted to radiance at the beginning. Then, the DN is converted into spectral reflectance enabling the identification of the spectral properties of the pixels of the images. All the image processing was done using ArcGIS v10.4.1 (Environmental Systems Research Institute, Inc. Redlands, CA USA, ESRI).

In the first stage, DN values were converted into spectral radiance and later to the top of atmosphere reflectance. Landsat 8 imagery contains band-wise parameters like the band specific multiplicative rescaling factor, additive rescaling factor in the metadata file which are used for direct conversion of DN to Top of Atmosphere (TOA) reflectance

values (Alipour et al., 2003; Irons et al., 2012). Operational Land Imager bands were converted were to TOA spectral radiance using scaling factors from the metadata using equation 2.19 (Zanter, 2016).

$$L_\lambda = M_L Q_{cal} + A_L \quad [2.19]$$

where:

L_λ = TOA spectral radiance (Watts/(m^2 * srad * μm)),

M_L = Band-specific multiplicative rescaling factor from the metadata

(RADIANCE_MULT_BAND_x, where x is the band number),

A_L = Band-specific additive rescaling factor from the metadata

(RADIANCE_ADD_BAND_x, where x is the band number), and

Q_{cal} = Quantized and calibrated standard product pixel values (DN)

The TOA reflectance of the OLI bands were computed using the reflectance rescaling factors available from the metadata using equation 2.20 (Zanter, 2016)

$$P_\lambda' = M_\rho Q_{cal} + A_\rho \quad [2.20]$$

where:

ρ_λ' = TOA planetary reflectance, without correction for solar angle.

(Note that ρ_λ' does not contain a correction for the sun angle),

Mρ = Band-specific multiplicative rescaling factor from the metadata

(REFLECTANCE_MULT_BAND_x, where x is the band number),

Aρ = Band-specific additive rescaling factor from the metadata

(REFLECTANCE_ADD_BAND_x, where x is the band number), and

Q_{cal} = Quantized and calibrated standard product pixel values (DN)

Top of Atmospheric Reflectance with a correction for the sun angle is (see equation 2.21):

$$P_{\lambda=} \rho_{\lambda}^{'} / \boldsymbol{sin}\ (\boldsymbol{\theta_{SE}}) \qquad [2.21]$$

Where;

$\boldsymbol{\theta_{SE=}}$ Local sun elevation angle. The scene center sun elevation angle in degrees is provided in the metadata (SUN_ELEVATION).

The Normalized Difference Vegetation Index (NDVI) was developed to highlight the difference of the spectral responses of vegetation at the red and near infrared bands (Deng et al., 2015). NDVI (see equation 2.22) depicts the vegetation condition through the ratio of responses in near infrared ($Band_L$ 5) and visible bands ($Band_L$ 4) of the Landsat 8 datasets see Table 2.8 for Landsat 8 bands information). It is expressed as:

$$NDVI = (Band_L\ 5 - Band_L\ 4) / (Band_L\ 5 + Band_L\ 4) \qquad [2.22]$$

The Modified Second Adjusted Vegetation Indices 1 and 2 (MSAVI1, MSAVI2) were developed. MSAVI2 (Qi et al., 1994b) was developed to calculate a more reliable soil brightness correction factor. These indices are variants of Soil Adjusted Vegetation Index (SAVI), where the factor L is dynamically adjusted explaining how much vegetation there is. Modified Soil Adjusted Vegetation Index is expressed in the equation 2.23 and 2.23a.

$$MSAVI1 = \frac{(NIR - Red)(1 + L)}{\mathrm{NIR} + \mathrm{Red} + \mathrm{L}} \qquad [2.23]$$

In MSAVI1 the factor L is described by the following expression and WDVI is Weighted Difference Vegetation Index = NIR- aR.

$$L = 1- 2\times a\times NDVI\times WDVI \quad [2.23a]$$

MSAVI2 is an iterated version of MSAVI1, developed by substituting 1 - MSAVI(n-1) as the L factor in MSAVI(n), and then inductively solving MSAVI(n) = MSAVI(n-1) (Mróz and Sobieraj, 2004). See equation 2.24

$$MSAVI2 = \frac{2\text{NIR} + 1 - \sqrt{(2\text{NIR} + 1)^2 - 8(\text{NIR} - \text{Red})}}{2} \quad [2.24]$$

Bare soil index can be defined as the numerical indicator that combines blue, green, red and NIR bands to characterize the soil variations. The BSI is a normalized index of the difference sums of two separating bands of the satellite image (for the vegetation). Equation (2.25) used for calculating the BSI is given below (Jamalabad, 2004):

$$BSI = \frac{[(B5 + B3) - (B4 + B1)]}{[(B5 + B3) + (B4 + B1)]} \times 100 + 100 \quad [2.25]$$

where, BSI =bare soil index, B1 = Blue Band, B3 = Green Band, B4 =Red Band, and B5 = Near Infra-Red Band from Landsat 8. The comparison was done using NDVI with the bare soil index to estimate the barren areas in the fields. Moreover, The Red and Green bands were used for calculating the Brightness Index (BI) for Landsat 8 and PlanetScope imagery (see Table 2.10). The BI was used to identify salt affected spots in the study areas (Escadafal, 1989). Indices used for this study are shown in Table 2.10. The methodology used for spatial data and soil data processing is represented in Figure 2.7.

SoilWeb Data Acquisition

Digital soil data was collected from the USDA-NRCS Web Soil Survey (WSS) website (websoilsurvey.sc.egov.usda.gov, 2018) and the SoilWeb Application (SWA) from the University of California Davis, California Soil Resource Lab (casoilresource.lawr.ucdavis.edu/soilweb-apps/, 2018). The websites were used as sources for gathering soil special and numerical lab data. First of all, our soil test sampling locations were found using the WSS website and the accuracy of locations were checked. After that, soil test data for each sampling point lab data was obtained using the SoilWeb Application (SWA). The SWA website provides detailed information about map units and their components. After the soil map units covers our sampling locations were found, specific soil property information (e.g., % sand, % silt, % clay, bulk density, % TC, % OC, % OM, pH, base saturation, CEC [cation exchange capacity], % gypsum, % CaCO3 [lime], SAR [sodium adsorption ratio], soil series % in each map unit and others) was obtained using the Soil Data Explorer function of SWA.

Table 2.10 Detail of Derived Indices for Landsat 8 and PlanetScope

Index	Definition	Reference
NDVI	$\frac{\text{NIR} - \text{Red}}{\text{NIR} + \text{Red}}$	Rouse Jr et al. (1974)
BSI	$\frac{[(\text{Red} + \text{Green}) - (\text{Red} + \text{Blue})]}{[(\text{NIR} + \text{Green}) + (\text{Red} + \text{Blue})]} \times 100 + 100$	Kumar (2013)
MSAVI2	$\frac{2 \times \text{NIR} + 1 - \sqrt{(2 \times \text{NIR} + 1)^2 - 8 \times \rho\text{NIR} - \text{Red})}}{2}$	Qi et al. (1994)
BI	$\frac{\sqrt{(\text{Red} \times \text{Red}) + (\text{Green} \times \text{Green})}}{2}$	(Gholizadeh et al., 2018)

NDVI = Normalized Difference Vegetation Index, BSI = Bare Soil Index, MSAVI2 = Modified Soil Adjusted Vegetation Index 2, BI = Brightness Index.

The methodology used for spatial data and soil data processing is represented in Figure 2.7

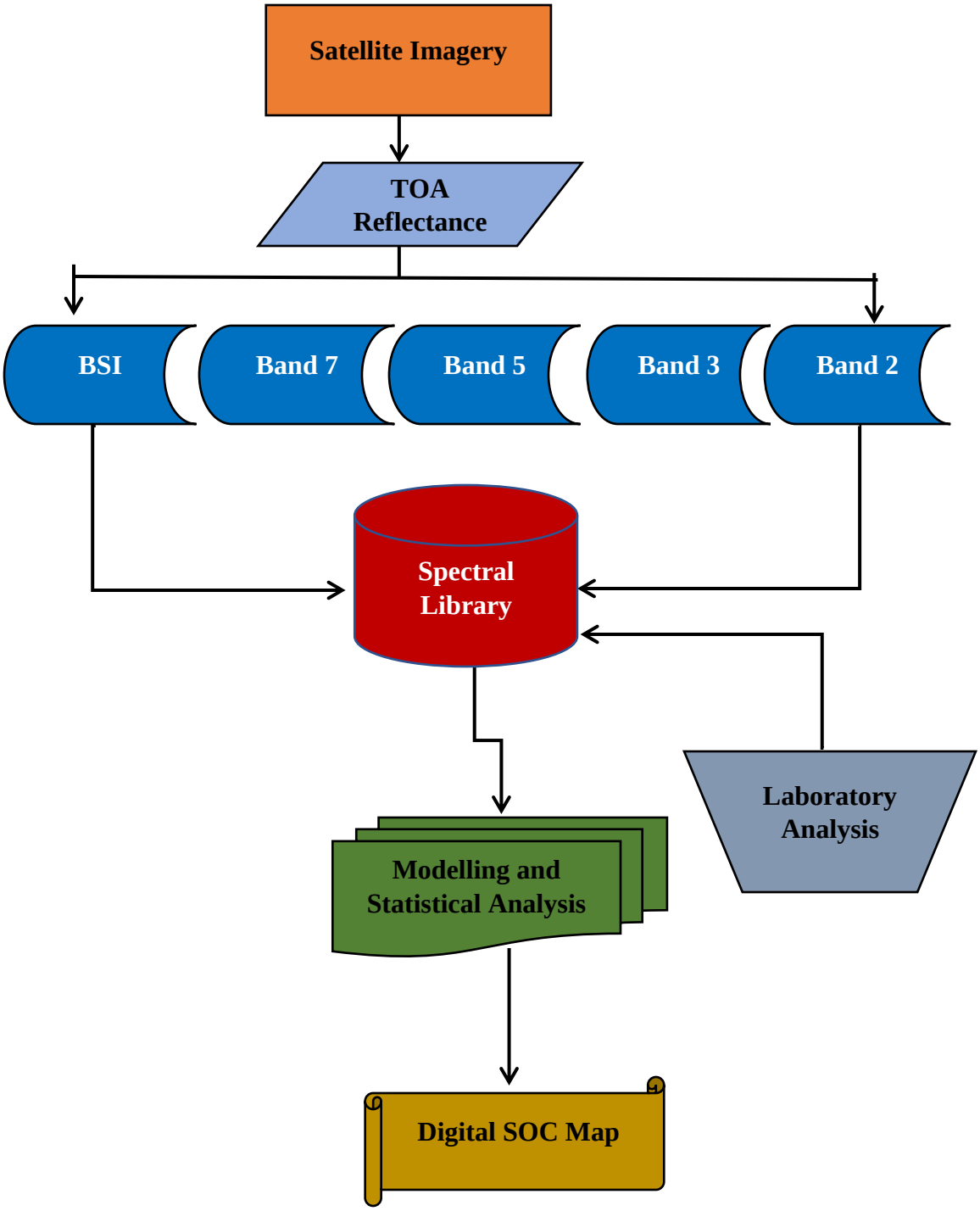

Figure 2.7 Landsat 8 flow chart of methodology for spatial data and soil data processing

REFERENCES

Abatzoglou, J. T., McEvoy, D. J., and Redmond, K. T. (2017). The west wide drought tracker: drought monitoring at fine spatial scales. *Bulletin of the American Meteorological Society*, *98*(9), 1815-1820.

Alipour, T., Sarajian, M. R., and Esmaeily, A. (2003). Land surface temperature estimation from thermal band of landsat sensor, case study: Alashtar city. *The International Achieves of the Photogrammetry, Remote Sensing and Spatial Information Sciences*, *38*(4).

Deng, Y., Wu, C., Li, M., and Chen, R. (2015). RNDSI: A ratio normalized difference soil index for remote sensing of urban/suburban environments. *International Journal of Applied Earth Observation and Geoinformation*, *39*, 40-48.

Escadafal, R. (1989). Remote sensing of arid soil surface color with Landsat thematic mapper. *Advances in space research* 9, 159-163.

Gholizadeh, A., Žižala, D., Saberioon, M., and Borůvka, L. (2018). Soil organic carbon and texture retrieving and mapping using proximal, airborne and Sentinel-2 spectral imaging. *Remote Sensing of Environment*, *218*, 89-103.

Irons, J. R., Dwyer, J. L., and Barsi, J. A. (2012). The next Landsat satellite: The Landsat data continuity mission. *Remote Sensing of Environment*, *122*, 11-21.

Jamalabad, M. (2004). Forest canopy density monitoring using satellite images. *In* "Geo-Imagery Bridging Continents XXth ISPRS Congress, Istanbul, Turkey, 2004".

Kim, K.-I., Clay, D., Carlson, C., Clay, S., and Trooien, T. (2008). Do synergistic relationships between nitrogen and water influence the ability of corn to use nitrogen derived from fertilizer and soil? *Agronomy Journal* 100, 551-556.

Kumar, S. (2013). Soil organic carbon mapping at field and regional scales using GIS and remote sensing applications. *Advances in Crop Science and Technology*.

Liu, R., Kuang, J., Gong, Q., Hou, X. J. C. m., and biomedicine, p. i. (2003). Principal component regression analysis with SPSS. **71**, 141-147.

Marquardt, D. W., and Snee, R. D. (1975). Ridge regression in practice. *The American Statistician*, *29*(1), 3-20.

Mróz, M., and Sobieraj, A. (2004). Comparison of several vegetation indices calculated on the basis of a seasonal SPOT XS time series, and their suitability for land cover and agricultural crop identification. *Technical Sciences*, *7*(7), 39-66.

Malo, D.D., Kumar, S., Chintala, R. 2014. Soil particle size methods. Pedology, Soil Chemistry, and Soil Physics Laboratories; Plant Science Department; South Dakota State University. Pedology Report 14-1.

Stal, U. (1965). Land resource regions and major land resource areas of the United States.

O'Dell, J. (1993). Determination of phosphorus by semi-automated colorimetry. Method 365.1. *Cincinnati, OH: Environmental Monitoring Systems Laboratory, Office of Research and Development. US Environmental Protection Agency*.

Pribyl, D. W. (2010). A critical review of the conventional SOC to SOM conversion factor. *Geoderma* 156, 75-83.

Qi, J., Kerr, Y., and Chehbouni, A. (1994). External factor consideration in vegetation index development. *Proc. of Physical Measurements and Signatures in Remote Sensing, ISPRS*, 723-730.

R Core Team (2018). R: A language and environment for statistical computing. R Foundation for Statistical Computing, Vienna, Austria *URL:(https://www. R-project. org)*.

RCC-ACIS (2018). RCC-ACIS. (n.d.). Retrieved October 18, 2018, from http://www.rcc-acis.org/index.html.

Rouse Jr, J. W., Haas, R., Schell, J., and Deering, D. (1974). Monitoring vegetation systems in the Great Plains with ERTS.

SDSU (2006). South Dakota State University. 2006. Soil testing procedures in use at the South Dakota State Soil Testing and Plant Analysis Laboratory. SDSU.

Shelton, D. P., Dickey, E. C., Jasa, P. J., Kanable, R., and Smydra Krotz, S. (1990). Using the Line-Transect Method to Estimate Percent Residue Cover.

Simon, L. J. (2004). Detecting multicollinearity using variance inflation factors. *Penn State Department of Statistics, The Pennsylvania State University*.

SoilWeb Apps. (2018). Retrieved October 18, 2018, from https://casoilresource.lawr.ucdavis.edu/soilweb-apps

Team, P. (2017). Planet Application Program Interface: In Space for Life on Earth. *San Francisco, CA*.

USDA-NRCS (2018). Soil Survey Staff, Natural Resources Conservation Service, United States Department of Agriculture. Web Soil Survey. Available online at the following link: https://websoilsurvey.sc.egov.usda.gov/App/WebSoilSurvey.aspx Accessed [10/12/2018].

Wollenhaupt, N., and Wolkowski, R. (1994). Grid soil sampling. *Better Crops* **78**, 6-9.

Zanter, K. (2016). Landsat 8 (L8) data users handbook. *Landsat Science Official Website. Available online: https://landsat. usgs. gov/landsat-8-l8-data-users-handbook (accessed on 20 January 2018)*.

Zimmermann, B., Elsenbeer, H., and De Moraes, J. M. (2006). The influence of land-use changes on soil hydraulic properties: implications for runoff generation. *Forest ecology and management*, *222*(1-3), 29-38.

CHAPTER 3: Results

Descriptive Statistics of the Soil Organic Carbon (SOC) and Soil Test Data

Pearson correlation and simple linear regression were applied to reveal correlations between SOC and other soil properties. The complete Pearson correlation matrices and soil test data by fields are given in Appendix A and Appendix E. All data were analyzed at the 95% confidence interval (α=0.05; p<0.05). The correlogram (Friendly, 2002) for the Pearson correlation matrix between soil test variables is shown in Figure 3.1. The linear regressions for SOC with fourteen other soil properties, Clay, Silt, Sand, Moisture, NO_3^--N, NH_4^+-N, pH, EC, SOEC, K^+, Ca^{2+}, Mg^{2+}, PO_4^{3-} , and Na^+ in the studied fields are presented in Table 3.1.

The SOC levels in cultivated areas were significantly affected by soil texture. While there is a positive correlation between SOC and silt and clay, there is a negative correlation with sand. Regression analyses were performed between SOC and clay, silt and sand (see equations [3.1], [3.2], and [3.3], respectively, in Table 3.1. Silt and clay have strong relationships with SOC due to texture's role in SOM turnover. Clay has been shown to significantly protect SOM from quick decomposition by improving macroaggregate (> 0.25mm) aggregation and SOC adsorption.

Figure 3.1 Correlogram of the Pearson correlation matrix between soil properties and soil organic carbon (SOC). Blue colder tones indicate a negative correlation; red and hotter tones represent a positive correlation between soil test data and SOC. EC = electrical conductivity, dS = deciSiemens, SOEC = sum of extractable cations, n (number of observations) = 150.

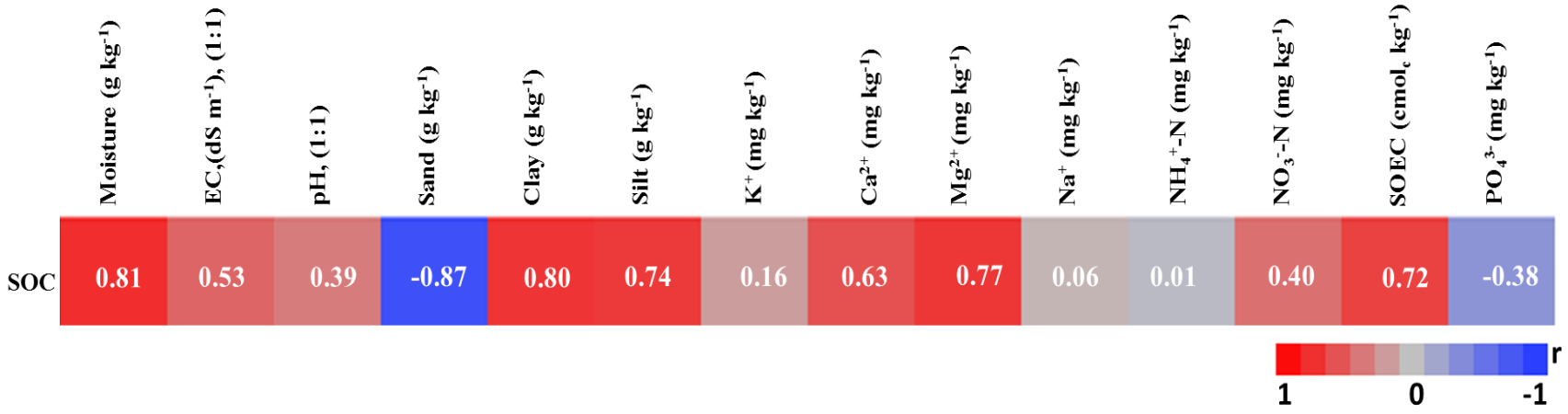

Table 3.1 Linear regression between soil organic carbon (SOC) and soil test data, EC = electrical conductivity, SOEC = sum of extractable cations, dS = decisiemens, SOC_p = predicted soil organic carbon, n (number of observations) = 150.

Equations	Soil Variables	R^2	Equation Number
$SOC_p = 0.963 + (0.0563 \times Clay)$	Clay (g kg^{-1})	0.64	[3.1]
$SOC_p = 1.24 + (0.0481 \times Silt)$	Silt (g kg^{-1})	0.54	[3.2]
$SOC_p = 4.05 - (0.0337 \times Sand)$	Sand (g kg^{-1})	0.76	[3.3]
$SOC_p = 0.96 + (0.0879 \times Moisture)$	Moisture (g kg^{-1})	0.66	[3.4]
$SOC_p = 2.12 + (0.0132 \times NO_3^-\text{-N})$	NO_3^--N (mg kg^{-1})	0.16	[3.5]
$SOC_p = 2.53 + (0.000300 \times NH_4^+\text{-N})$	NH_4^+-N (mg kg^{-1})	0.001	[3.6]
$SOC_p = 0.730 + (0.283 \times pH_{1:1})$	$pH_{1:1}$	0.15	[3.7]
$SOC_p = 1.72 + (1.37 \times EC_{1:1})$	$EC_{1:1}$ (dS m^{-1})	0.28	[3.8]
$SOC_p = 1.45 + (0.0582 \times SOEC)$	SOEC ($cmol_c$ kg^{-1})	0.52	[3.9]
$SOC_p = 2.32 + (0.000900 \times K^+)$	K^+ (mg kg^{-1})	0.02	[3.10]
$SOC_p = 1.67 + (0.000300 \times Ca^{2+})$	Ca^{2+}(mg kg^{-1})	0.40	[3.11]
$SOC_p = 1.52 + (0.00200 \times Mg^{2+})$	Mg^{2+}(mg kg^{-1})	0.60	[3.12]
$SOC_p = 2.47 + (0.00230 \times Na^+)$	Na^+(mg kg^{-1})	0.004	[3.13]
$SOC_p = 2.93 - (0.00710 \times PO_4^{3-})$	PO_4^{-3} (mg kg^{-1})	0.11	[3.14]

Silt increases the plant available water holding capacity controlling the climate and ecosystem in soil (Burke et al., 1989; Gelaw et al., 2015; Koroleva et al., 2017). The determination of coefficient (R^2) of the linear regression models is 0.64 (r = 0.80, *p<0.0001*) and 0.54 (r = 0.74, *p<0.0001)* for clay and silt, respectively. Nearly 64% and 54% of the variance of SOC distribution can be estimated by clay and silt, respectively. The results (see Figure 3.1) also showed that there is a significant relationship between SOC and sand content (r=-0.87, *p<0.0001*). Moreover, the highest R^2 was found between sand content and SOC (see equation [3.3] in Table 3.1). Soil moisture also showed a statistically positive relationship (see Figure 3.1) with SOC (r = 0.81, *p*<0.0001). SOC levels increased with increasing soil moisture levels in the soils studied. Nearly 66% of the variance of SOC can be estimated by this variable (see equation [3.4] in Table 3.1).

SOC was positively affected by nitrate nitrogen, NO_3^--N (see Figure 3.1) r = 0.40 and *p*<0.0001, while there was no significant correlation between SOC and ammonium nitrogen NH_4^+-N (see Figure 3.1), r = 0.01 and *p*= 0.9056 (also see Table 3.1 equations [3.5] and [3.6]). Nitrogen fertilization has helped to maintain SOC levels in cultivated areas. The source of N is the N that comes from pre-plant or post-plant farmers' fertilizer applications. Studdert (2000) reported that there is a significant difference in SOC levels between fertilized and unfertilized crop areas.

A positive correlation between SOC and SOEC (r = 0.72, *p*<0.0001) was observed (see Figure 3.1). One half of the variance of the SOC can be explained with this variable (see Table 3.1, equation [3.9]). SOC is linearly associated with Magnesium (Mg^{2+}) and Calcium (Ca^{2+}) in the soils studied (see Table 3.1, equations [3.11] and [3.12]). Positive statistically significant correlations were found between SOC and Mg^{2+} (r = 0.77,

$p<0.0001$) and Ca^{2+} (r = 0.63, $p<0.0001$). There were no significant correlations, or regression relationships with Potassium (K^{+}) or Sodium (Na^{+}) (see Figure 3.1 and equations [3.10] and [3.13] in Table 3.1). Weak correlations were found between SOC and pH, PO_4^{3-} and EC (see Figure 3.1, r = 0.39, $p<0.0001$, r = 0.38, $p<0.0001$ and r = 0.53, $p<0.0001$; respectively). Weak regression relationships between pH, EC, and PO_4^{3-} were found (see Table 3.1 equations [3.7], [3.8], and [3.14], respectively). The descriptive statistics obtained for the soil variables examined in the study area are presented in Table 3.2a and Table 3.2b.The data presented in Table 3.2 shows the relatively wide range of values for the soil properties were studied [SOC (1.05 to 4.38 g kg^{-1}), Sand (10 to 75.6 g kg^{-1}) SOEC (4.5 to 37.5 $cmol_c$ kg^{-1}), Clay (8.1 to 48.61 g kg^{-1}), Silt (10.9 to 51.1 g kg^{-1}) and Moisture (7.3 to 36.2 g kg^{-1})].

Table 3.2a Soil test data descriptive statistics physical properties. EC = electrical conductivity, dS = deciSiemens, SOEC = sum of extractable cations, SOC = soil organic carbon, n (number of observations) = 150

Parameters	SOC ($g\ kg^{-1}$)	pH (1:1)	Sand ($g\ kg^{-1}$)	SOEC ($cmol_c\ kg^{-1}$)	Moisture ($g\ kg^{-1}$)	EC ($dS\ m^{-1}$) (1:1)	Clay ($g\ kg^{-1}$)	Silt ($g\ kg^{-1}$)
Mean	2.54	6.39	44.8	18.7	18.0	0.60	28.1	27.1
Std. Error	0.05	0.07	1.3	0.6	0.5	0.02	0.7	0.8
Median	2.48	6.38	45.3	17.4	16.3	0.55	28.2	25.7
Std.* Deviation	0.60	0.83	15.7	7.5	5.6	0.23	8.6	9.3
Kurtosis	-0.11	-1.16	-0.2	0.1	0.5	-1.22	-0.7	0.3
Skewness	0.03	0.07	-0.4	0.7	0.9	0.16	-0.2	0.9
Range	3.33	3.04	65.6	33.0	29.0	0.85	40.5	40.2
Minimum	1.05	4.94	10.0	4.5	7.3	0.14	8.1	10.9
Maximum	4.38	7.98	75.6	37.5	36.2	0.99	48.6	51.1

*Std = Standard

Table 3.2b Soil test data descriptive statistics, chemical properties. K^+ = potassium, Ca^{2+} = calcium, Mg^{2+} = magnesium, Na^+ = sodium, NH_4^+-N=ammonium nitrogen, NO_3^--N = nitrate nitrogen, and PO_4^{3-} = phosphate, n (number of observations) = 150.

Parameters	K^+ (mg kg^{-1})	Ca^{2+} (mg kg^{-1})	Mg^{2+} (mg kg^{-1})	Na^+ (mg kg^{-1})	NH_4^+-N (mg kg^{-1})	NO_3^--N (mg kg^{-1})	PO_4^{3-} (mg kg^{-1})
Mean	251	2730	513	33	26	32	55
Std.* Error	9	98	19	1	2	1	3
Median	220	2480	446	28	22	27	47
Std. Deviation	112	120	235	16	18	18	33
Kurtosis	19	0.2	3.6	4.88	-0.2	0.7	2.7
Skewness	4	0.8	1.4	2.02	0.8	1.1	1.1
Range	869	5513	1543	99	82.	89	205
Minimum	129	607	122	14	5	0	0
Maximum	998	6120	1664	113	87	89	205

*Std = Standard

Soil Data Multiple Linear Regression:

This section considers the soil properties data and analyzes their effect on the SOC. The results of the global F test are presented in Table 3.3. We tested:

$$\begin{cases} H_0: \ none\ of\ the\ regressors\ are\ important\ in\ predicting\ SOC\ response \\ H_a: at\ least\ one\ regressor\ is\ important\ in\ predicting\ SOC\ response \end{cases}$$

The observed value for the F-statistic is 74.2 (p <0.0001) and p value is less than 0.05 which means that there is sufficient evidence to reject H_0 and that at least one regressor variable is important in predicting SOC, the response variable. As can be seen from the Table 3.3, the coefficients of Sand and pH are significantly different from 0 and these independent regressors can be used to predict SOC with high degree of confidence. Please note that soil moisture was not used in model development even though significant correlations were noted in Figure 3.1 and Table 3.1. This decision was due to extreme changes in soil moisture on a daily or weekly basis and thus meaningful SOC predictions are less useful using soil moisture.

Table 3.3 Model output of SOC prediction using all soil test data. Significant at α = 0.05. EC = electrical conductivity, dS = deciSiemens, SOEC = sum of extractable cations, and n (number of observations) = 150.

Parameters	Estimate	Std Error	t Ratio	Prob>|t|
Intercept	4.38	0.38	11.49	<0.0001
$EC_{1:1}$ (dS m^{-1})	0.220	0.15	1.48	0.1408
$pH_{1:1}$	-0.300	0.056	-5.31	<0.0001
Sand (g kg^{-1})	-0.0200	0.0037	-6.57	<0.0001
Clay (g kg^{-1})	-0.0100	0.0073	-1.77	0.0788
K^+ (mg kg^{-1})	-0.00200	0.0017	-1.47	0.1441
Ca^{2+} (mg kg^{-1})	-0.00600	0.003	-1.84	0.0682
Mg^{2+} (mg kg^{-1})	-0.0100	0.0054	-1.8	0.0735
Na^+ (mg kg^{-1})	-0.000400	0.0033	-0.12	0.9028
NH_4^+-N (mg kg^{-1})	-0.000300	0.0014	-0.25	0.8003
NO_3^--N (mg kg^{-1})	0.000900	0.0015	0.62	0.5382
SOEC ($cmol_c$ kg^{-1})	1.24	0.645	1.92	0.0569
PO_4^{-3} (mg kg^{-1})	-0.000200	0.0011	-0.16	0.8748

When all parameters where used the value of the R^2 is 0.867 and this means that regressor variables explained approximately 86.7 % of SOC variation. However, in linear regression model development, R^2 is always increased by adding regressor variables even though those variables may not have a statistically significant relationship with the response variable. The adjusted $R^2$is used to compare goodness of the fit for regression models. Basically, the adjusted R^2 decreases when variables do not improve the model by an acceptable amount (Miles, 2014). In this study, the adjusted R^2 was expected to be close R^2. The adjusted R^2 is 0.855 and was 1.1 percent less than R^2. Mean square error is 0.053 which is very good when compared to the range of the data studied. Since, there are variables in our regression model that are not significant, we reduced the model to include only the important variables. We used the stepwise sequential procedure to determine the best model (see Table 3.4).

Table 3.4 Ordinary Least Square (OLS) model output of SOC_P based on important variables. Significant at $\alpha = 0.05$, SOEC = some of extractable cations, n = 150 (number of observations)

Parameters	Estimate	Std Error	t Ratio	Prob>|t|
Intercept	3.99	0.221	18.1	<0.0001*
$pH_{1:1}$	-0.206	0.0541	-3.81	0.0002*
Sand (g kg^{-1})	-0.0227	0.0020	-11.3	<0.0001*
SOEC ($cmol_c$ kg^{-1})	0.0475	0.00740	6.42	<0.0001*

The value of the R^2 for the reduced model is 0.827 and this means that regressor variables can explain approximately 82.7% of variation in response variable, but we know that R^2 always increases as additional regressor variables are added to the model. So, we calculated the adjusted R^2 which is 0.823 and this value was 0.36 percent less than R^2. Mean square error is 0.063 which is very good when compared to the range of the data studied.

Since the regressors are highly correlated, we suspected that there might be multicollinearity problem in the data. Multicollinearity is a linear association among the regressor variables and exists when two or more regressors have high empirical correlation (Farrar et al., 1967; Wold et al., 1984). Multicollinearity problem can appear in big data sets. Multicollinearity can be calculated using the Variance Inflation Factor (VIF). The convention is that if VIF exceeds 4 , further investigation is needed (Simon, 2004). The results of the Variance Inflation Factor (VIF) for this study are presented in Table 3.5:

Table 3.5 Variance Inflation Factor (VIF) results for soil parameters studied, SOEC = sum of extractable cations, SOC = soil organic carbon, EC = electrical conductivity, dS = deciSiemens, n (number of observations) = 150.

Full Model		Reduced Model	
Parameter	VIF*	Parameter	VIF
$EC_{1:1}$ (dS m^{-1})	3.5	$pH_{1:1}$	4.7
$pH_{1:1}$	6.5	Sand (g kg^{-1})	2.3
Sand (g kg^{-1})	9.2	SOEC ($cmol_c$ kg^{-1})	7.1
Clay (g kg^{-1})	11		
K^+ (mg kg^{-1})	96		
Ca^{2+} (mg kg^{-1})	42000		
Mg^{2+} (mg kg^{-1})	44500		
Na^+ (mg kg^{-1})	8.0		
NH_4^+-N (mg kg^{-1})	2.0		
NO_3^--N (mg kg^{-1})	2.0		
SOEC ($cmol_c$ kg^{-1})	65000		
PO_4^{3-} (mg kg^{-1})	3.310		

*VIF values > 4 indicate possible multicollinearity problems

As seen in Table 3.5, there are many variables with the VIF greater than 4. Thus, there is a multicollinearity problem in our data set. Multicollinearity can be explained as one predictor variable in regression model also can be estimated from other predictors (Farrar et al., 1967). It is assumed that the quality of the fit and prediction capability of model is not compromised. To avoid multicollinearity problems an alternative is to use a biased form of estimation and two common approaches are: Ridge regression (RR), and Principle component regression (PCR). Ridge regression and Principal Component Analysis (PCA).

In order to look at the prediction capability of our model, we randomly selected five soil samples from each field for validation. In order to measure the error of different developed models, we used a cross validation (CV) approach (Shao, 1993).

To compare the prediction performance of different models, the cross-validation values of the different models developed are given in Table 3.6.

Table 3.6 Prediction performance of the models, PC = Principal Component, PCs = Principle Components used, CV= Cross-Validation, n (number of observations) = 150.

Model	CV
Regression (Full model)	0.060
Regression (Reduced model)	0.066
Ridge Regression (Reduced model, k*= 1.3837)	0.066
Principal Component Regression (Reduced model, # PCs=2)	0.071

*k = Ridge parameter.

Based on the observed cross validation values, the regression full model and ridge regression model are very close to the CV values of the reduced model. However, the regression model has multicollinearity making that model weak. In this regard, we can conclude that the ridge regression is the best model using equation [3.15]:

$$SOC_p = 3.98 - (0.210 \times pH) - (0.220 \times Sand\ g\ kg^{-1}) + (0.0403 \times SOEC\ cmol_c\ kg^{-1}) \quad [3.15]$$

Where; SOC_p = predicted soil organic carbon, pH = soil pH, Sand = soil sand content, and SOEC = sum of extractable cations.

Figure 3.2 The linear relationship between measured and predicted soil organic carbon (SOC) from soil test data.

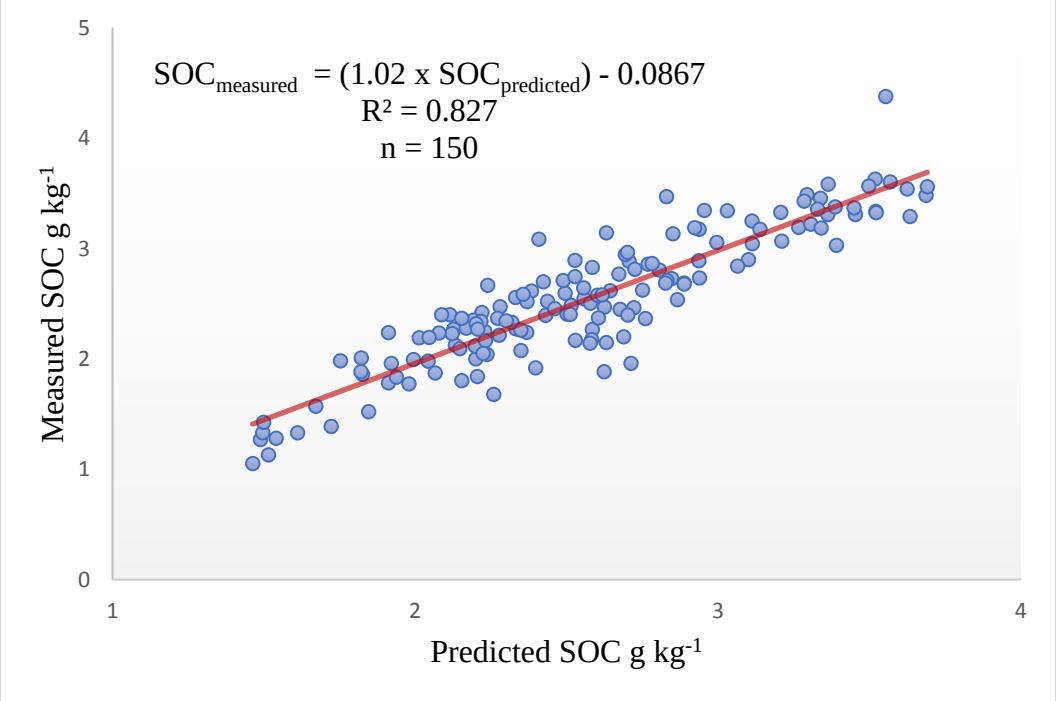

Figure 3.2 shows the results of predicted versus measured SOC using soil test data. The approach showed very good agreement between measured SOC and predicted SOC with R^2= 82.7 %, p<0.0001 and confidence level was 0.05.

Relationship Between SOC and Landsat 8 Data

Soil Line Concept to Indicate Bareness of the Study Areas

Soil line can be explained as the relationship between the NIR band and the Red band of bare soil including the slope and intercept of the relationship (Fox et al., 2004). This relationship was first discovered (see equation [3.16]) by Richardson and Wiegand (1977) :

$$NIR = \beta_1 + \beta_0 \qquad [3.16]$$

where β_1 is the slope of soil line and + β_0 is the intercept. Results from test field data are shown below (see equation 3.17):

$$\text{NIR band} = 0.00802 + (1.54 \times \text{Red band}) \quad [3.17]$$

The R^2 was found as 0.866. The detailed density plot was demonstrated in Figure 3.3.

Figure 3.3 Soil line representing the observed linear relationship between Band 5 (NIR) (0.851 - 0.879 µm) and Band 4 (red band) (0.636 - 0.673 µm) reflectance from Landsat 8 or image intensity of bare soil in the present study sites.

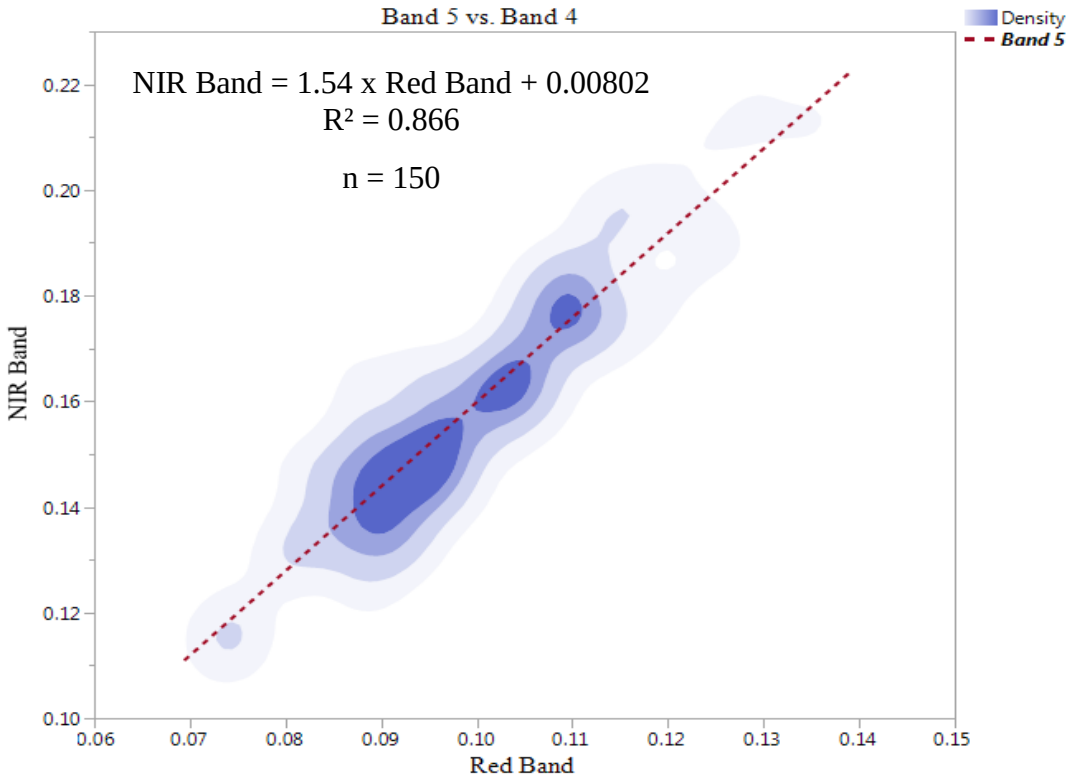

The upper part of graph which has high reflectance showed the brighter soil due to lack of moisture and increased plant residue impacts. The soil samples in the upper part of the graph have coarser textures (more sand) and also these samples had more post-harvest residue. Koroleva et al. (2017) mentioned that the soil data where the density is high in the graph had darker soil color due to high SOM content, more moisture, and less crop residue.

Correlation Between SOC and Spatial Data from Landsat 8

Pearson correlation and simple linear regression were applied to show correlations between SOC and spatial data from Landsat 8. All the data was analyzed at the 95% confidence interval ($\alpha = 0.05$; $p<0.05$). The complete Pearson correlation matrix and Landsat 8 data are given in Appendix B and Appendix E. To demonstrate the relationships of Landsat 8 bands and spectral indices, the correlogram map between variables and SOC was built (Figure 3.4).

The correlogram map identifies which indices and which spectral bands of Landsat 8 (see Tables 2.8 and 2.10 for Landsat 8 bands and indices descriptions) were the most statistically significant in predicting SOC in the test fields. When the map is evaluated, the highest statistical correlations were obtained between $MSAVI2_L$ ($r = -0.54$, $p<0.0001$), $Band_L$ 6 ($r = -0.54$, $p<0.0001$) and $Band_L$ 5 ($r = -0.52$, $p<0.0001$). The remaining bands and indices were BSI_L ($r = -0.44$, $p<0.0001$) $Band_L$ 7 ($r = -0.44$, $p<0.0001$), $Band_L$ 4 ($r = -0.42$, $p<0.0001$), BI_L ($r = -0.39$, $p<0.0001$), $NDVI_L$ ($r = -0.39$, $p<0.0001$), $Band_L$ 3 ($r = -0.35$, $p<0.0001$), and $Band_L$ 2 ($r = -0.24$, $p=0.0026$. The SOC prediction equations and R^2 for each variable were calculated (see Table 3.7).

Figure 3.4 Correlogram of the Pearson correlation matrix between soil organic carbon (SOC) and extracted bands from Landsat 8 (see Table 2.8 for Landsat 8 band descriptions) and different calculated indices (see Table 2.10). Blue color tones indicate negative correlations between SOC and spatial data (the values in the box show correlation coefficients at the 0.05 level), $Band_L$ = Landsat 8 bands, n (number of observations) = 150.

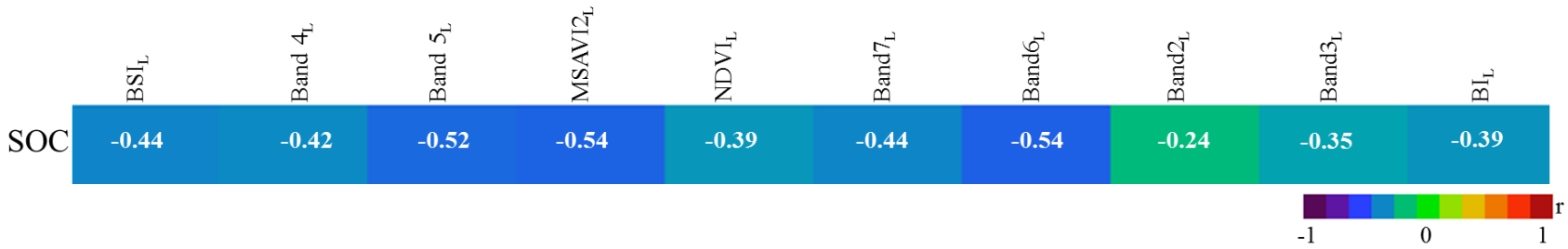

Table 3.7 Linear regressions between SOC and Landsat 8 Spatial Data, SOCp = Predicted soil organic carbon, $Band_L$ = Landsat 8 bands, BSI_L = Bare Soil Index, $NDVI_L$ = Normalized Difference Vegetation Index, $MSAVI2_L$ =Modified Soil-Adjusted Vegetation Index, BI_L = Brightness Index, n (number of observations) = 150.

Equations	Indices and Spectral Bands*	R^2	Equation Number
$SOC_p = 26.0 - 0.242 \times BSI_L$	BSI_L	0.19	[3.18]
$SOC_p = 4.42 - 19.4 \times MSAVI2_L$	$MSAVI2_L$	0.29	[3.19]
$SOC_p = 4.70 - 9.42 \times NDVI_L$	$NDVI_L$	0.15	[3.20]
$SOC_P = 4.56 - 30.1 \times BI_L$	BI_L	0.15	[3.21]
$SOC_p = 5.00 - 23.6 \times Band\ 2_L$	Band 2_L	0.04	[3.22]
$SOC_p = 4.64 - 23.3 \times Band\ 3_L$	Band 3_L	0.12	[3.23]
$SOC_p = 4.44 - 19.1 \times Band\ 4_L$	Band 4_L	0.17	[3.24]
$SOC_p = 4.75 - 13.9 \times Band\ 5_L$	Band 5_L	0.27	[3.25]
$SOC_p = 5.63 - 10.9 \times Band\ 6_L$	Band 6_L	0.29	[3.26]
$SOC_p = 4.91 - 9.42 \times Band\ 7_L$	Band 7_L	0.19	[3.27]

* See Table 2.8 and 2.10 for Landsat 8 bands and indices descriptions.

Multiple Linear Regression for Landsat 8

In this section, we only considered the all spatial information data that was obtained from Landsat 8 and analyzed their effect on the SOC. Results of the global F test are presented in Table 3.8. We tested:

$$H_0: \textit{none of the regressors are important in predicting the response}$$
$$H_a: \textit{at least one regressor is important in predicting the response}$$

The calculated F-statistic was 12.50 and p value was $p<0.0001$ (less than 0.05) and thus rejected the H_0. There is at least one of the regressor variable important in predicting SOC. As seen in Table 3.8, the p values of BSI_L, $Band_L$ 5, $Band_L$ 4, $MSAVI2_L$, $Band_L$ 3, and BI_L, $Band_L$ 2 are significantly different from 0.

Table 3.8 Ordinary Least Square (OLS) model output of SOC prediction using all spatial data from Landsat 8. BSI_L = Bare Soil Index, $NDVI_L$ = Normalized Difference Vegetation Index, $MSAVI2_L$ = Modified Soil-Adjusted Vegetation Index, BI_L = Brightness Index, n (number of observations) = 150.

Parameters	**Estimate**	**Std Error**	**t Ratio**	**Prob>|t|**
Intercept	-120	46.8	-2.56	0.0116*
BSI_L**	1.38	0.490	2.81	0.0056*
Band 4_L	3330	1520	2.19	0.0302*
Band 5_L	693	289	2.40	0.0178*
$MSAVI2_L$	-426	196	-2.17	0.0319*
$NDVI_L$	-12.9	15.7	-0.82	0.4113
Band 7_L	-13.2	8.6	-1.54	0.1267
Band 6_L	7.78	11.0	0.71	0.4815
Band 2_L	334	108	3.10	0.0024*
Band 3_L	3481	1538	2.26	0.0252*
BI_L	-11300	4538	-2.48	0.0144*

* See Tables 2.8 and 2.10 for Landsat 8 bands and indices descriptions.
**Confidence level was set at 0.05.

The value of the R^2 is 0.474 when all Landsat 8 variables were used, and this means that regressor variables can explain approximately 47.4% of variation in SOC. The adjusted R^2 is 0.436 which is almost 4 percent less than R^2, a large difference. Mean square error (MSE) was found as 0.206 which is very good compared to the range of the data studied. Since, we have a lot of variables as regressors that were not significant, we reduced the model to include only the important variables. The stepwise sequential regression procedure was used to select the best model (see Table 3.9).

Table 3.9 Ordinary Least Square (OLS) model output of soil organic carbon (SOC) prediction based on important Landsat 8 data. Significant at $\alpha = 0.05$, BSI_L = Bare Soil Index, n (number of observations) = 150.

Parameters	**Estimate**	**Std Error**	**t Ratio**	**Prob>|t|**
Intercept	-100	22.7	-4.42	<0.0001*
BSI_L*	1.10	0.240	4.47	<0.0001*
Band 5_L	-23.0	6.00	-3.81	0.0002*
Band 7_L	-4.50	2.19	-2.06	0.0409*
Band 2_L	289	58.4	4.95	<0.0001*
Band 3_L	-272	60.4	-4.50	<0.0001*

*See Table 2.8 and 2.10 for Landsat 8 bands and indices descriptions

The value of the R^2 for the reduced model is 0.423 and this means that regressor variables can explain approximately 42.3% of variation in SOC. The adjusted R^2 is 0.403 and that value was 2 percent less than R^2, a big significant difference. Mean square error is 0.21 which is acceptable when compared to the range of the data. VIF values were calculated for the both models in the following Table 3.10

Table 3.10 Variation Inflation Factor (VIF) values of Landsat 8 bands and indices, $Band_L$ = Landsat 8 bands, BSI_L = Bare Soil Index, $NDVI_L$ = Normalized Difference Vegetation Index, $MSAVI2_L$ =Modified Soil-Adjusted Vegetation Index, BI_L = Brightness Index, n (number of observations) = 150.

Full Model		**Reduced Model**	
Parameters	**VIF**	**Parameters**	**VIF**
BSI_L*	206	BSI_L	45.0
Band 5_L	291000	Band 5_L	13.0
Band 4_L	31100	Band 7_L	3.0
$MSAVI2_L$	7940	Band 2_L	91.0
$NDVI_L$	113	Band 3_L	207
$Band2_L$	326		
$Band3_L$	14200		
$Band6_L$	81.0		
$Band7_L$	43.0		
BI_L	933000		

* See Table 2.8 and 2.10 for Landsat 8 bands and indices description.

As seen from Table 3.10, VIF values of all variables in the full model are much greater than 4. There is a multicollinearity problem among the regressor variables in the full model. To deal with this problem, we followed the same statistical methods used for soil test data model development (Ridge Regression and Principle Component Regression). To compare the prediction performance of different models, we present the cross-validation values of the different models (see Table 3.11).

Table 3.11 Prediction performance of the reduced model. k: Ridge parameter, PCs: Principal components, CV = Cross validation, n (number of observations) = 150.

Model	**CV**
Regression (Reduced model)	0.228
Ridge Regression (Reduced model, k=0.0001)	0.246
Principal Component Regression (Reduced model, # PCs = 3)	0.262

When the observed cross validation values are evaluated, the ridge regression was selected as the best model to use since it was not affected by multicollinearity problem.

We can conclude that by using Landsat 8 data, 37.0% of the variance of SOC distribution can be estimated from the RR model equation (see equation 3.28 and Figure 3.5):

$$SOC_p = -26.7 + (0.310 \times BSI_L) - (23.2 \times Band_L\ 5) + (75.8 \times Band_L\ 2) - (51.1 \times Band_L\ 3) - (3.05 \times Band_L\ 7) \quad [3.28]$$

The scatterplot in Figure 3.5 represents the results of predicted versus measured SOC using Landsat 8 imagery data. The approach showed good agreement between measured SOC and predicted SOC with R^2= 37.0 %, p<0.0001 and confidence level was set 0.05. As seen from the R^2 of OLS and RR, there is a difference. Ridge Regression (RR) gives an estimate which minimizes the sum of square error (SSE) and a penalty on the size of β (standardized regression coefficient). As a result, RR model is more numerically stable. Predicted SOC maps of studied area using Landsat 8 data are presented in Figures 3.6 to 3.10.

Figure 3.5 The linear relationship between measured and predicted soil organic carbon (SOC) from Landsat 8.

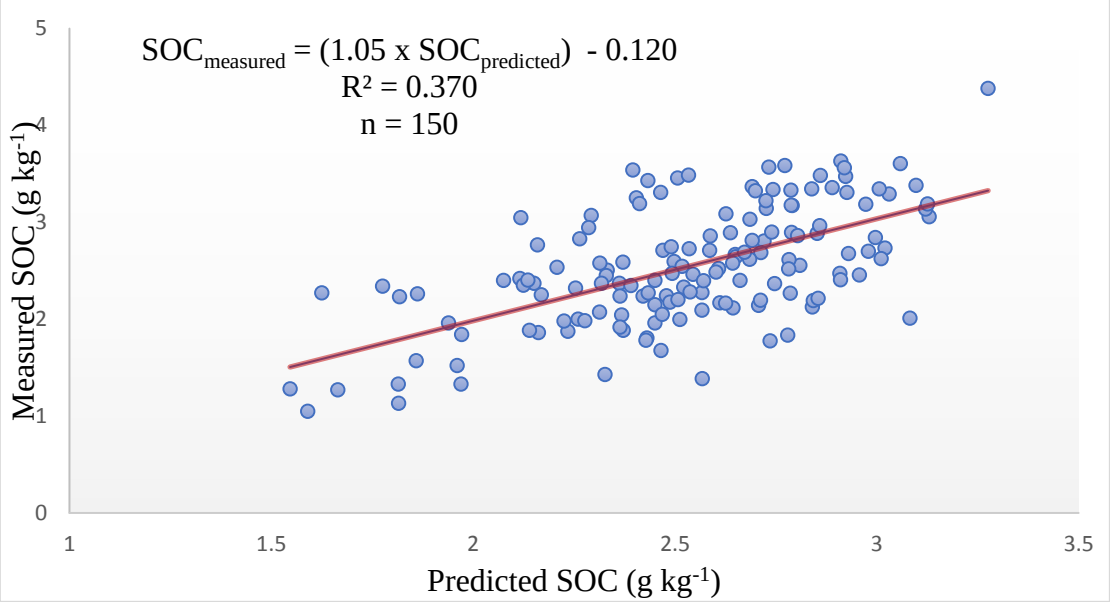

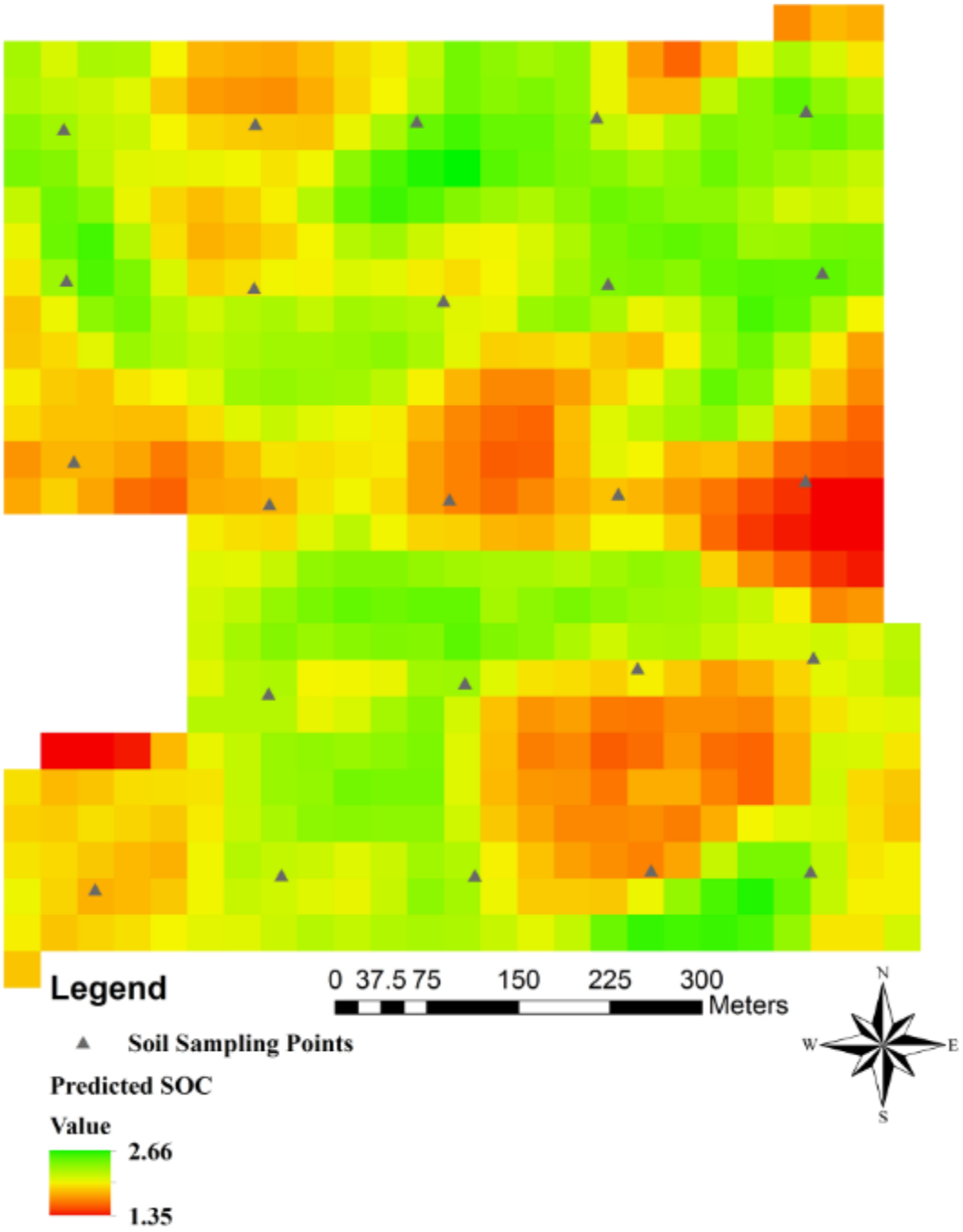

Figure 3.6 Predicted SOC map from Landsat 8 satellite imagery for field A (Brookings County, SD). Map sources = Landsat 8 OLI (2018).

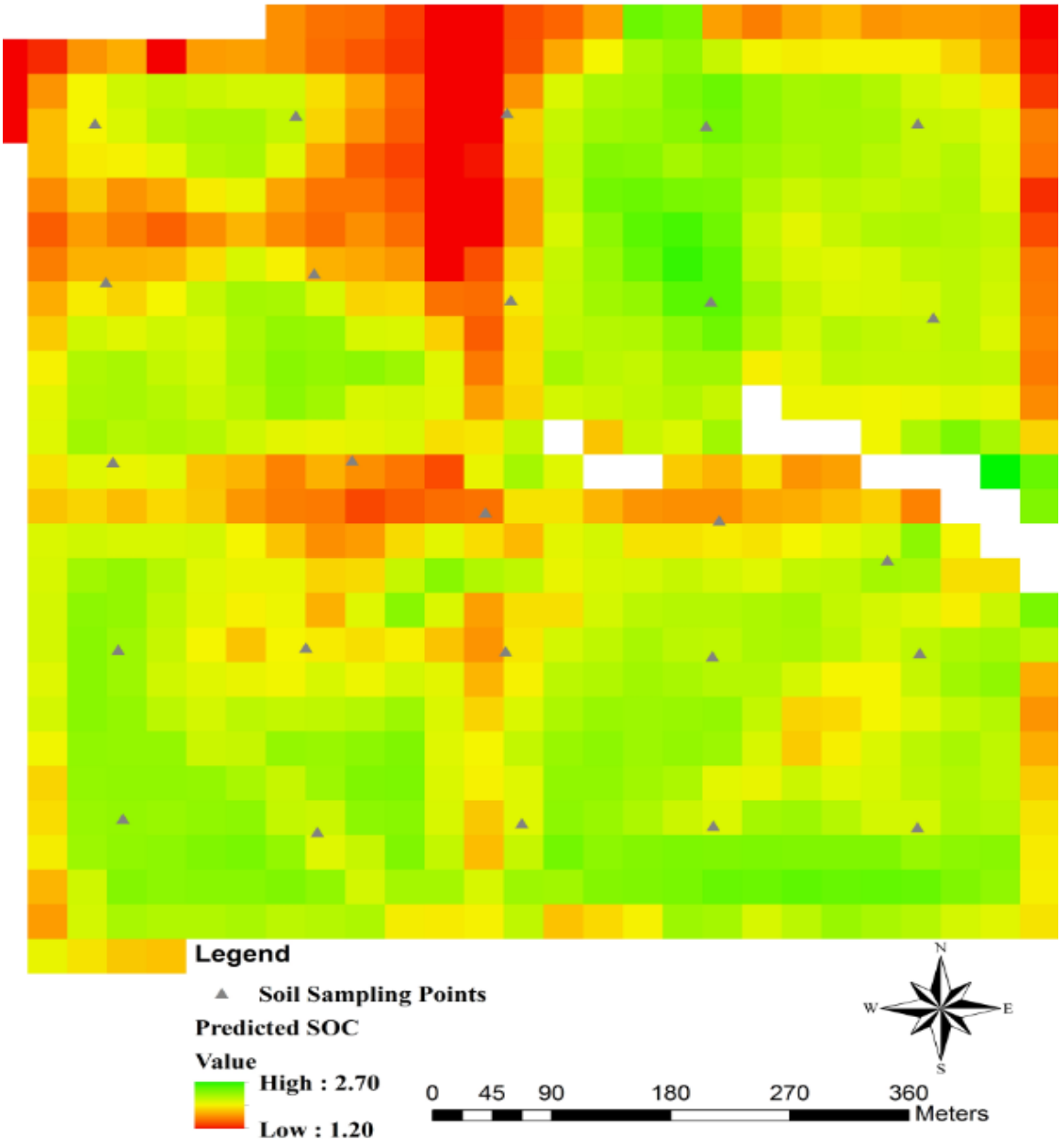

Figure 3.7 Predicted SOC map from Landsat 8 satellite imagery for field B (Brookings County, SD). Map sources = Landsat 8 OLI (2018).

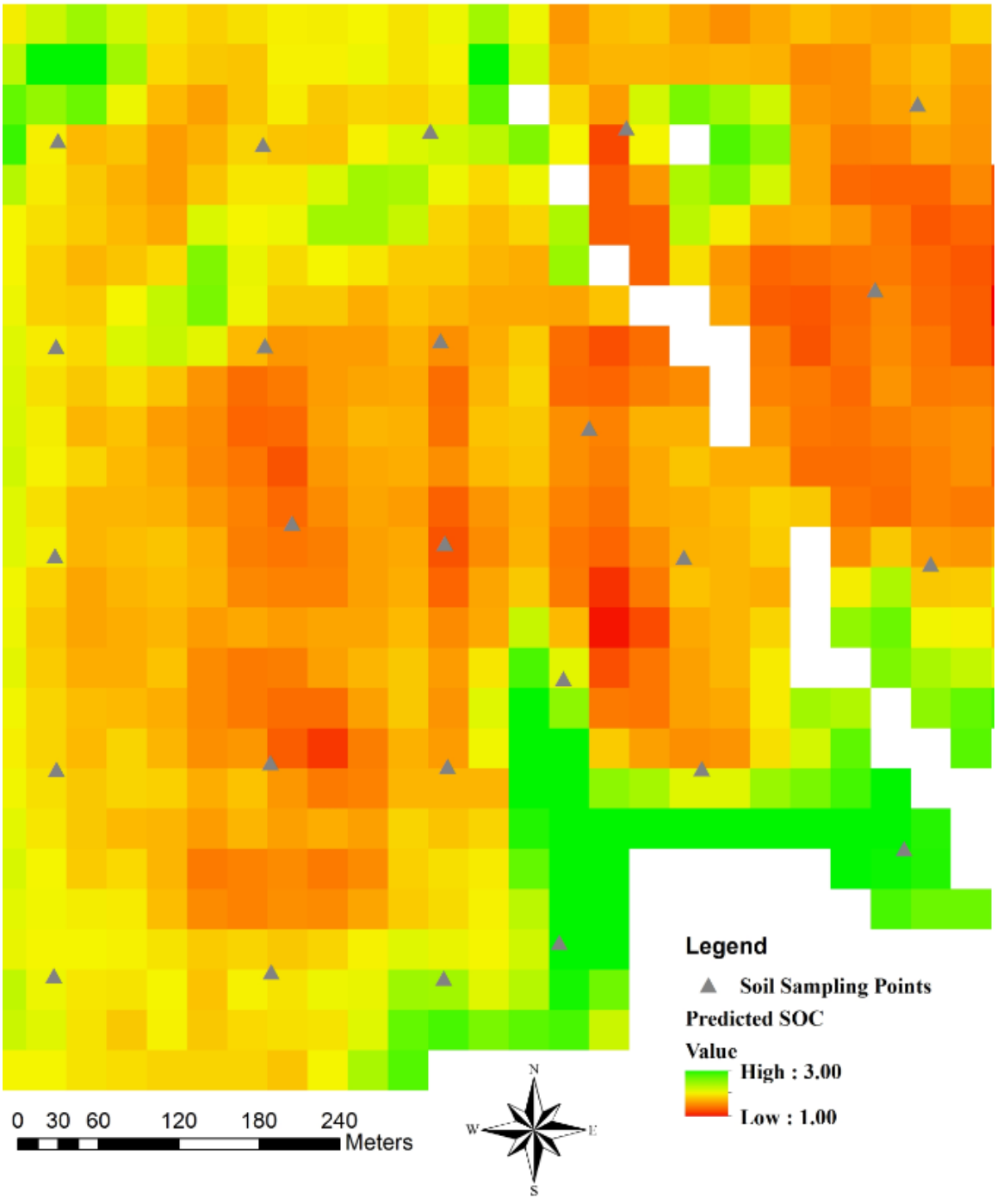

Figure 3.8 Predicted SOC map from Landsat 8 satellite imagery for field C (Brookings County, SD). Map sources = Landsat 8 OLI (2018).

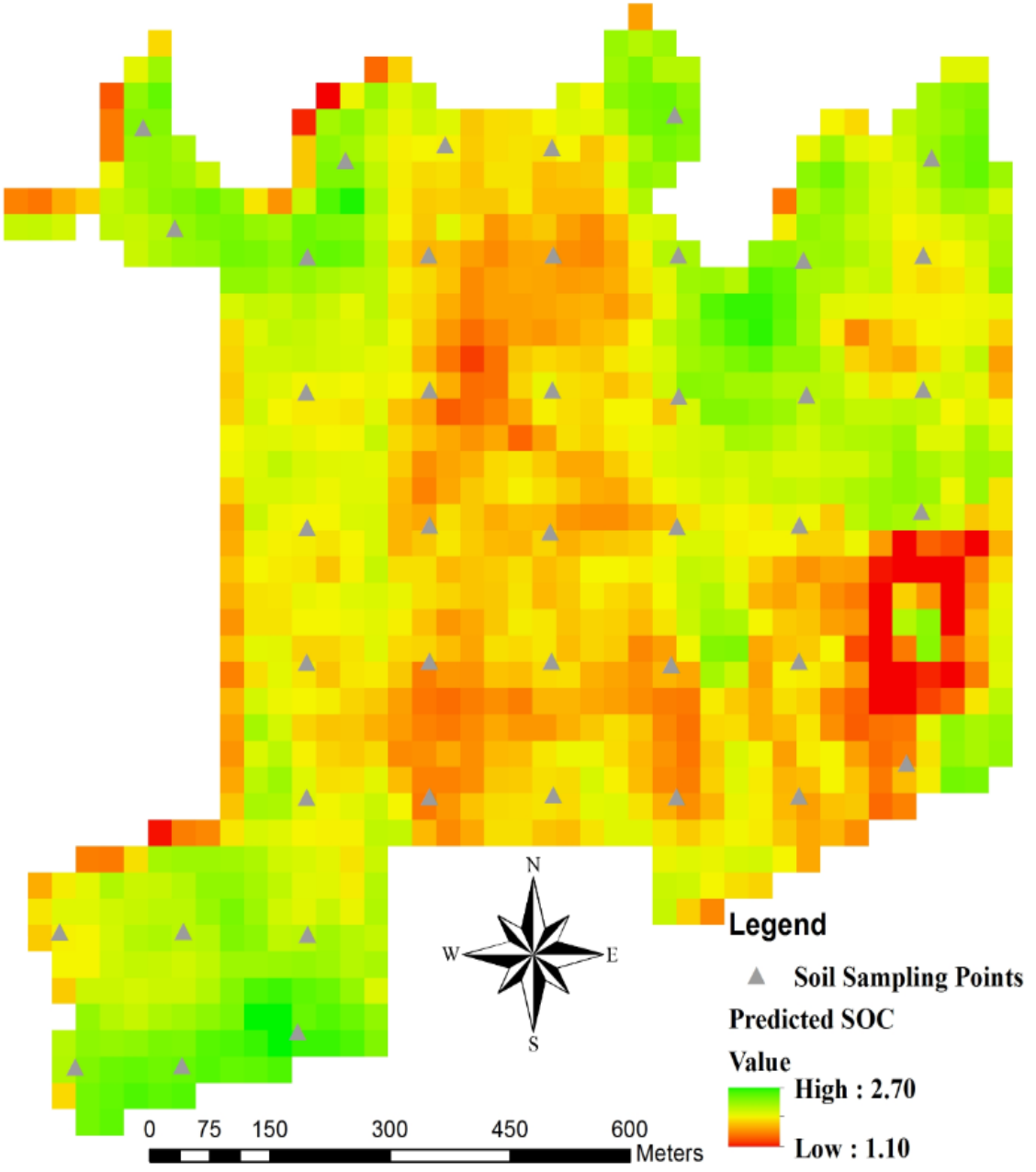

Figure 3.9 Predicted SOC map from Landsat 8 satellite imagery for field D (Lac qui Parle County, MN). Map sources = Landsat 8 OLI (2018).

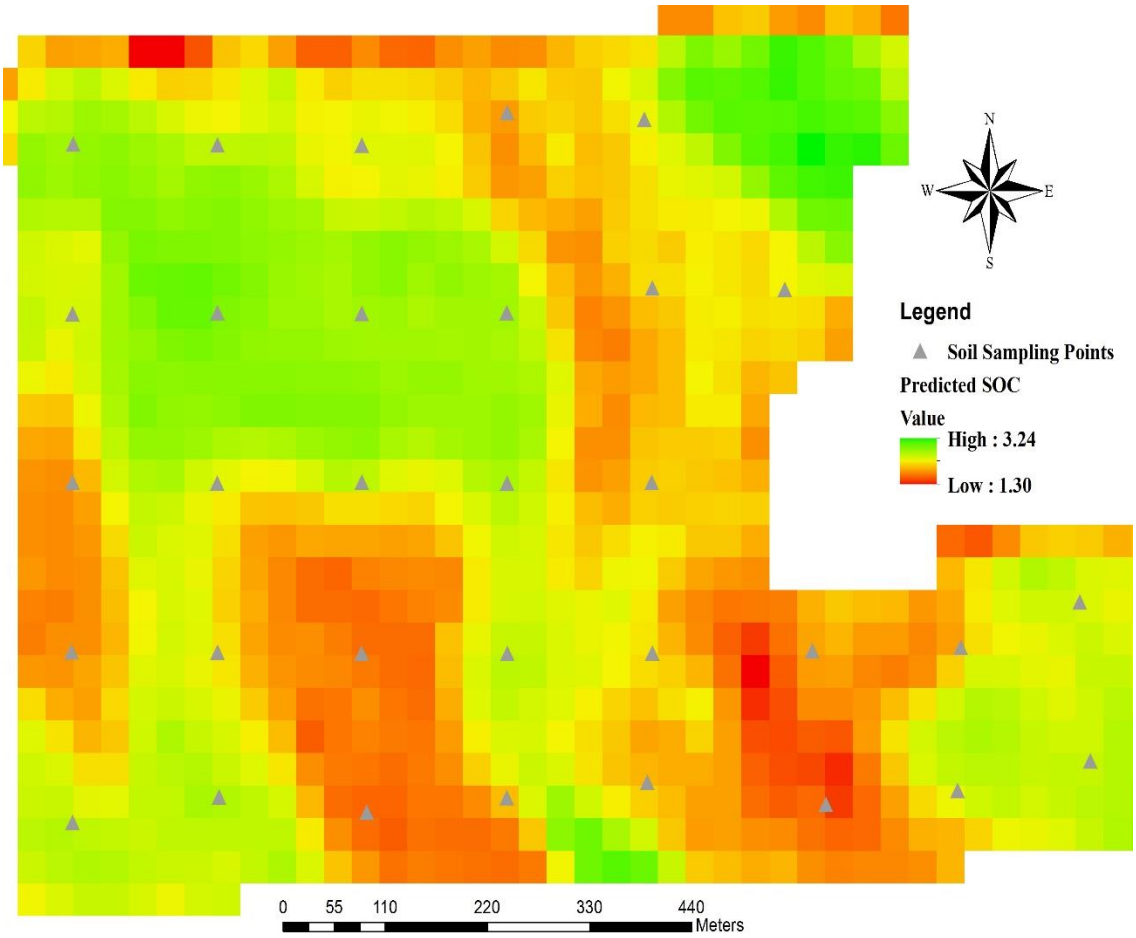

Figure 3.10 Predicted SOC map from Landsat 8 satellite imagery for field E (Lac qui Parle County, SD). Map sources = Landsat 8 OLI (2018).

Relationship SOC and PlanetScope Data

Soil Line Concept to Indicate Bareness of the Study Areas

Soil line concept was demonstrated again in this section by using PlanetScope data (Team, 2017). The soil line concept is used to reveal bareness of the studied area. In this case we used high resolution imagery and R^2 was found as 88.5 %. This result showed that the studied area was bare considering post-harvest plant residue. The detailed density plot is demonstrated in Figure 3.11

Figure 3.11 Soil line concept representing the observed linear relationship between NIR (0.780-0.860 µm) and Red (0.590-0.670 µm) band reflectance (see Table 2.9) from PlanetScope.

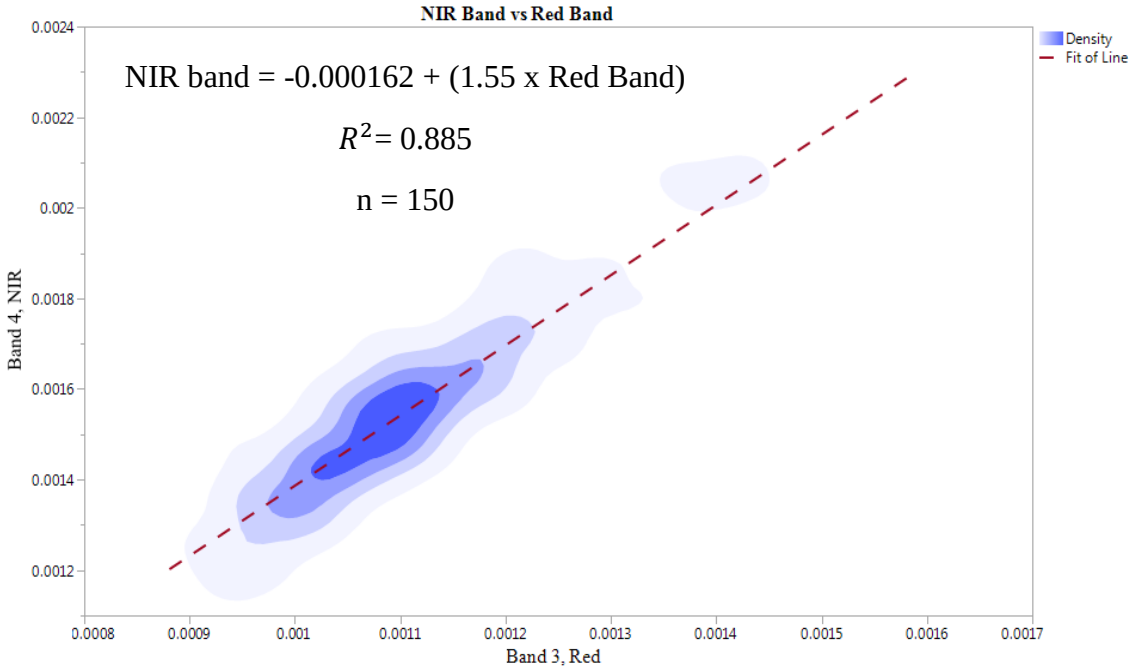

Correlation Between SOC and Spatial Data from Planet Scope

Pearson Correlation and simple linear regression were applied to show correlation between SOC and spatial data from PlanetScope. All the data was analyzed at the 95% confidence interval (α=0.05; $p<0.05$). The complete Pearson correlation matrix and PlanetScope data are given Appendix C and Appendix E. To demonstrate the relationship of PlanetScope bands and spectral indices, the correlation map between variables and SOC was done (Figure 3.12).

Significant correlations were found between SOC and PlanetScope Bands (see Figure 3.12). The correlogram identifies which indices and spectral bands of PlanetScope were statistically significant in the prediction of SOC for the test fields studied. The highest significant correlations were with $Band_P$ 4 (r = -0.74, $p<0.0001$), $Band_P$ 3 (r = -0.69, $p<0.0001$), BI_p (r = -0.68, $p<0.0001$), $Band_P$ 2 (r = -0.65, $p<0.0001$), $Band_P$ 1 (r = -0.74, $p<0.0001$) and this pattern was followed by $MSAVI2_P$ (r = -0.54, $p<0.0001$), $NDVI_P$ = -0.44, $p<0.0001$), and BSI_P (r = -0.35), $p<0.0001$). The SOC linear regression prediction equations and R^2 for each PlanetScope variable are shown in Table 3.12. When comparing Landsat 8 and PlanetScope data, PlanetScope imagery data is more strongly correlated to SOC than Landsat 8 due to higher spatial resolution (30m vs 3.125m).

Figure 3.12 The correlogram (correlation color map) of soil organic carbon (SOC) vs extracted bands from PlanetScope (see Table 2.9) and different calculated indices (Table 2.10). Blue color tones indicate negative correlations between SOC and spatial data (the values in the box show correlation coefficients at the 0.05 level), $Band_P$ = PlanetScope bands, n (number of observations) = 150.

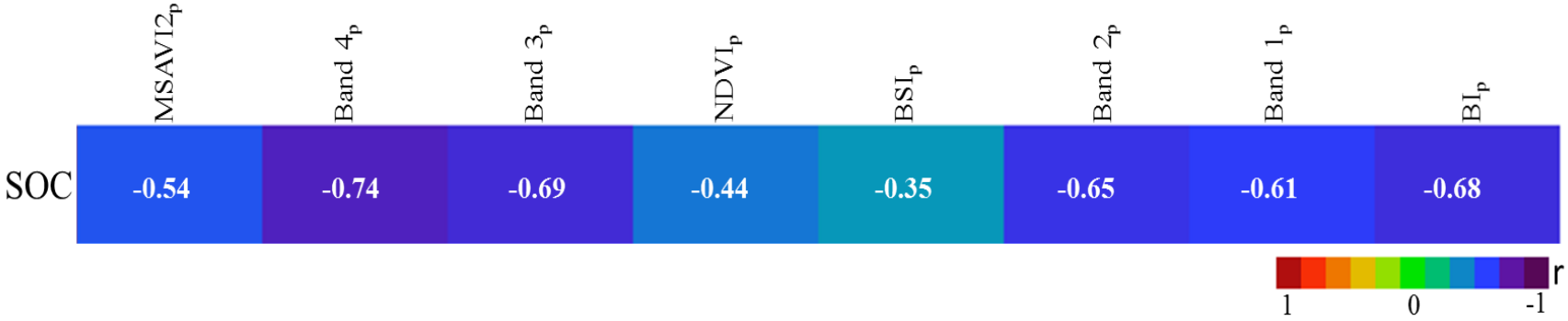

Table 3.12 Linear regression between SOC and Spatial Data Derived from PlanetScope, SOCp = Predicted soil organic carbon, $Band_p$= PlanetScope bands, BSI_P = Bare Soil Index, $NDVI_P$ = Normalized Difference Vegetation Index, $MSAVI2_P$ =Modified Soil-Adjusted Vegetation Index, BI_P = Brightness Index, n (number of observations) = 150.

Equations	**Indices and Spectral Bands**	**R^2**	**Equation Number**
$SOC_p = 39.2 – (0.370 \times BSI_P)$	BSI_P*	0.120	[3.29]
$SOC_p = 4.42 – (19.4 \times MSAVI2_P)$	$MSAVI2_P$	0.290	[3.30]
$SOC_p = 4.64 – (12.7 \times NDVI_P)$	$NDVI_P$	0.190	[3.31]
$SOC_p = 6.40 – (4930 \times BI_P)$	BI_P	0.460	[3.32]
$SOC_p = 6.22 – (33100 \times Band_P\ 2)$	Band 2_p	0.430	[3.33]
$SOC_p = 6.47 – (3550 \times Band_P\ 3)$	Band 3_p	0.480	[3.34]
$SOC_p = 6.13 – (2310 \times Band_P\ 4)$	Band 4_p	0.550	[3.35]
$SOC_p = 7.41 – (4220 \times Band_P\ 1)$	Band 1_p	0.370	[3.36]

* See Table 2.9 and 2.10 for PlanetScope bands and indices descriptions.

When all variables are included in the model, the F-statistic was 28.8 and *p*- value was $p<0.0001$. Since *p*- value is < 0, at least one regressor variable is important in predicting SOC. As seen from the Table 3.13, the coefficient of BSI, and Band 1 are significantly different from 0.

Table 3.13 Ordinary Least Square (OLS) model output of SOC prediction based on all spatial data from PlanetScope (Table 2.9). *Confidence level was set at 0.05, $Band_p$= PlanetScope ands, BSI_P = Bare Soil Index, $NDVI_P$ = Normalized Difference Vegetation Index, $MSAVI2_P$ =Modified Soil-Adjusted Vegetation Index, BI_P = Brightness Index, n (number of observations) = 150.

Parameter	Estimate	Std Error	t Ratio	Prob>|t|
Intercept	-27.1	8.10	-3.35	0.0010*
$MSAVI2_P$	-2.45	2.52	-0.97	0.3340
Band 4_p	-210.	2250	-0.09	0.9259
Band 3_p	-19410	37100	-0.52	0.6020
$NDVI_P$	-8.39	7.18	-1.17	0.2445
BSI_P	0.349	0.0826	4.22	<0.0001*
Band 2_p	-20304	41500	-0.49	0.6256
Band 1_p	3735	1880	1.99	0.0487*
BI_P	47145	110000	0.43	0.6692

* See Table 2.9 and 2.10 for PlanetScope bands and indices description.

The value of the R^2 is 0.620 and this means that PlanetScope regressor variables can explain approximately 62.0% of variation in SOC. The adjusted R^2 is 0.599 and the value was approximately 2 percent less than R^2, and is considered a large difference. Mean square error (MSE) was found as 0.146 which is very good when compared to the range of the data. Variance Inflation Factors (VIF) were calculated for each variable and are presented in Table 3.14.

Table 3.14 Variation Inflation Factor (VIF) values of PlanetScope, $Band_P$= PlanetScope Bands, BSI_P = Bare Soil Index, $NDVI_P$ = Normalized Difference Vegetation Index, $MSAVI2_P$ =Modified Soil-Adjusted Vegetation Index, BI_P = Brightness Index, n = 150 (number of observations)

Full Model		Reduced Model	
Parameter	VIF	Parameter	VIF
$MSAVI2_P$	1.84	$Band_P$ 4	1.92
$Band_P$ 4	195	BSI_P*	1.92
$Band_P$ 3	19500		
$NDVI_P$	23.8		
BSI_P	2.30		
$Band_P$ 2	25200		
$Band_P$ 1	27.6		
BI_P	85700		

* See Table 2.9 and 2.10 for PlanetScope bands and indices description.

Since, we have a lot of variables as our regressors that are not significant, we reduced the model to include only the significant variables and used the stepwise sequential procedure to choose the best model (see Table 3.15)

Table 3.15 Ordinary Least Square (OLS) model output of SOC prediction based on important PlanetScope. *Confidence level was set at 0.05, Bandp= PlanetScope Bands, BSIP = Bare Soil Index, n (number of observations) = 150. See Table 2.9 and 2.10 for PlanetScope bands

Parameters	Estimate	Std Error	t Ratio	Prob>|t|
Intercept	-25.1	7.26	-3.46	0.0007*
$Band_P$ 4	-2980	225	-13.26	<0.0001*
BSI_P*	0.327	0.0760	4.30	<0.0001*

* See Table 2.9 and 2.10 for PlanetScope bands and indices description.

The value of the R^2 is 0.601 and this means that regressor variables can explain approximately 60.1% of variation in response variable but, it is known that R^2 always increases as additional regressor variables are added to the model. The calculated adjusted R^2 is 0.596 and is 0.5 percent less than R^2, a small difference. Mean square error (MSE) was found as 0.147 which is very good for the range of the data studied.

Cross-Validation (CV) was calculated as 0.15 to measure performance of the model. Variance Inflation Factor (VIF) was used to show collinearity for each variable. The results of the VIF is presented in Table 3.14 and the full model has high multicollinearity problem. As for reduced model, the VIF values are lower than 4 indicating that there is no collinearity problem for reduced model. In this case, there is no need to run PCR and RR for the full model. We can conclude that using PlanetScope spatial data, 60.1% of the variance of SOC distribution can be estimated (see equation [3.37]).

$$SOC_p = -25.1 + (2980 \times \text{Band 4}) + (0.327 \times \text{BSI}) \quad [3.37]$$

Figure 3.13 reveals the results of predicted SOC versus measured SOC using Planet Scope imagery data. The approach showed good agreement between measured SOC and predicted SOC with R^2= 60%, p<0.0001 and confidence level was 0.05. Predicted SOC maps of studied area are presented in Figure 3.14 to 3.18.

Figure 3.13 The linear relationship between measured and predicted soil organic carbon (SOC) from PlanetScope data, n = 150 (number of observations)

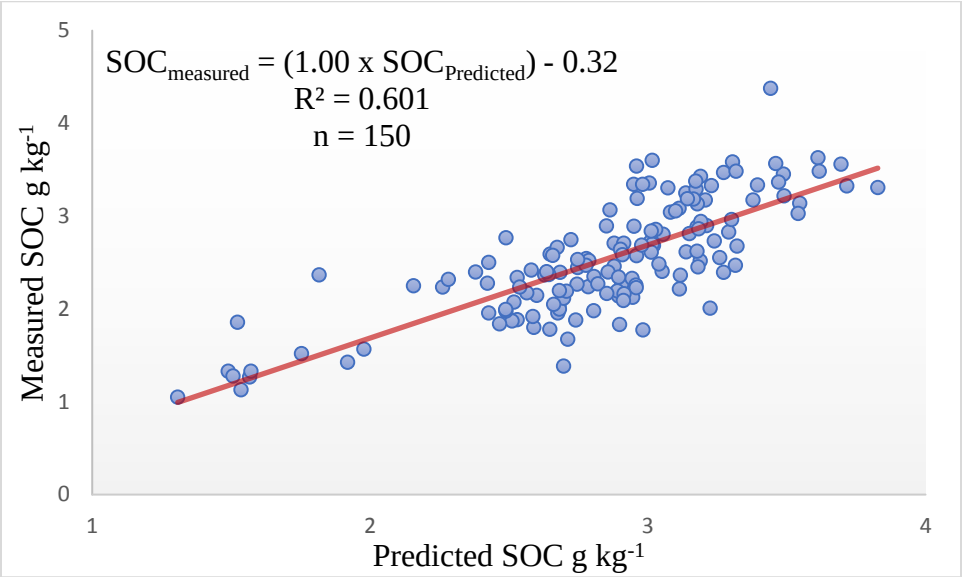

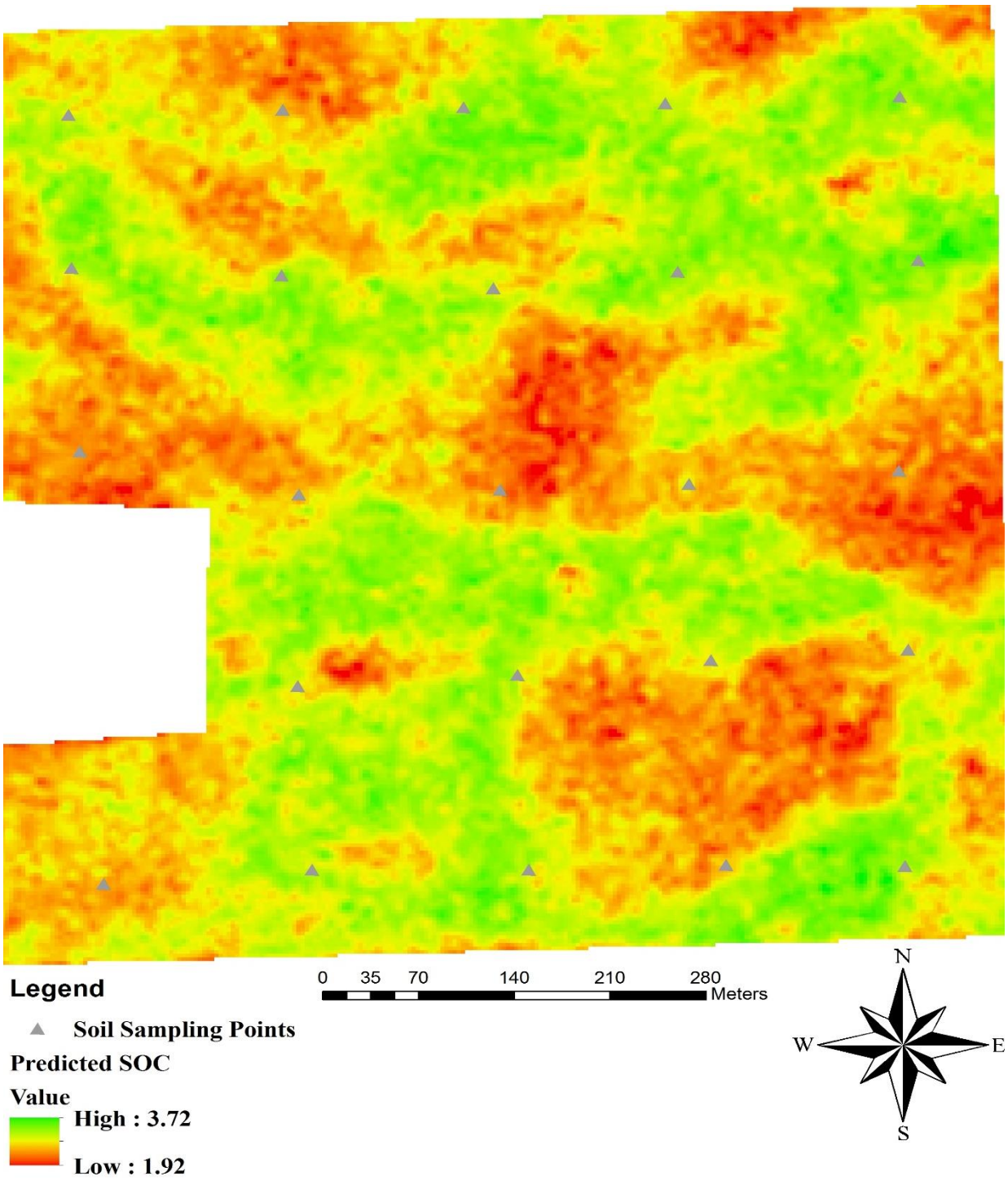

Figure 3.14 Predicted SOC map from PlanetScope satellite imagery for field A (Brookings County, SD). Map sources = PlanetScope (2018).

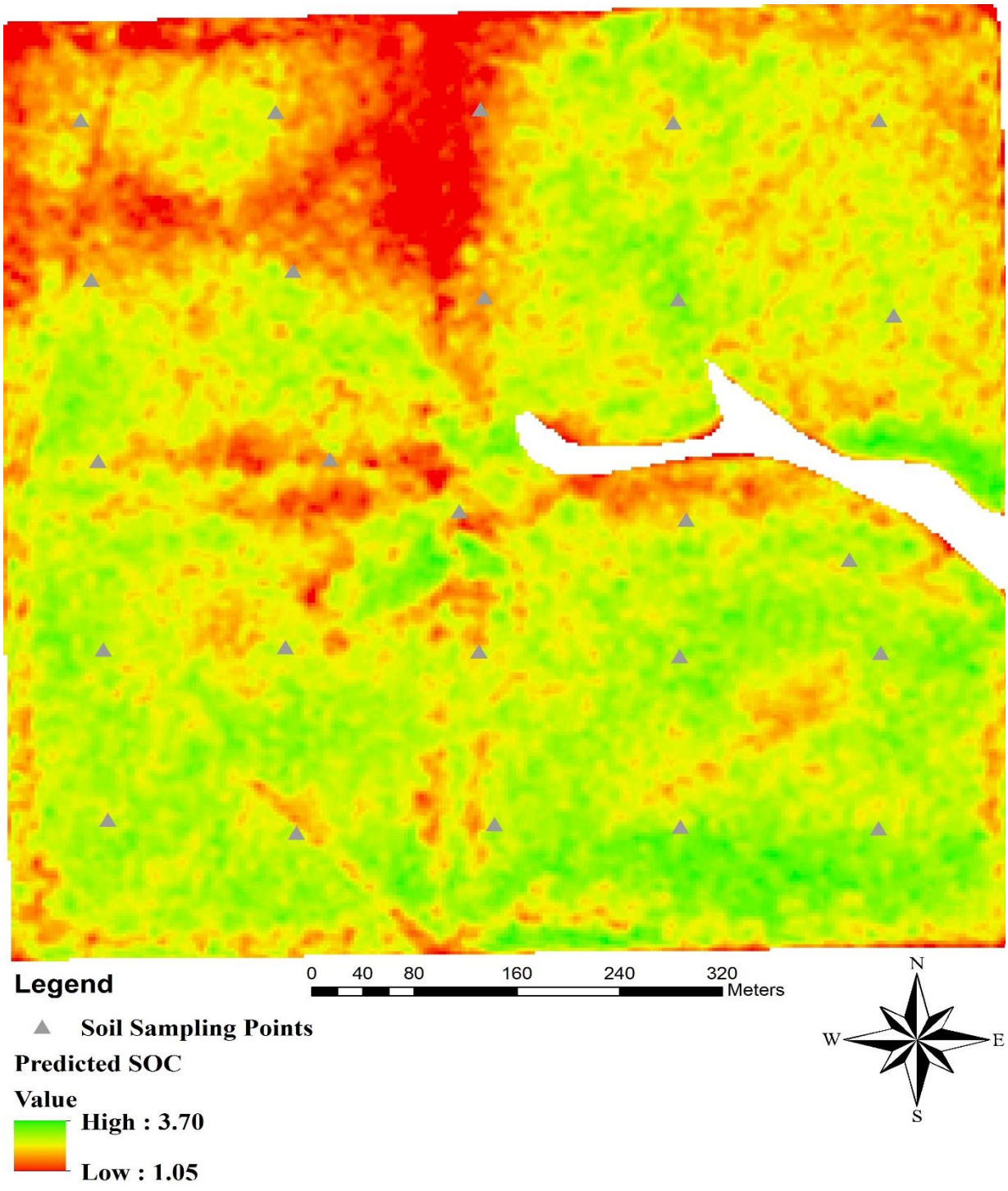

Figure 3.15 Predicted SOC map from PlanetScope satellite imagery for field B (Brookings County, SD). Map sources = PlanetScope (2018).

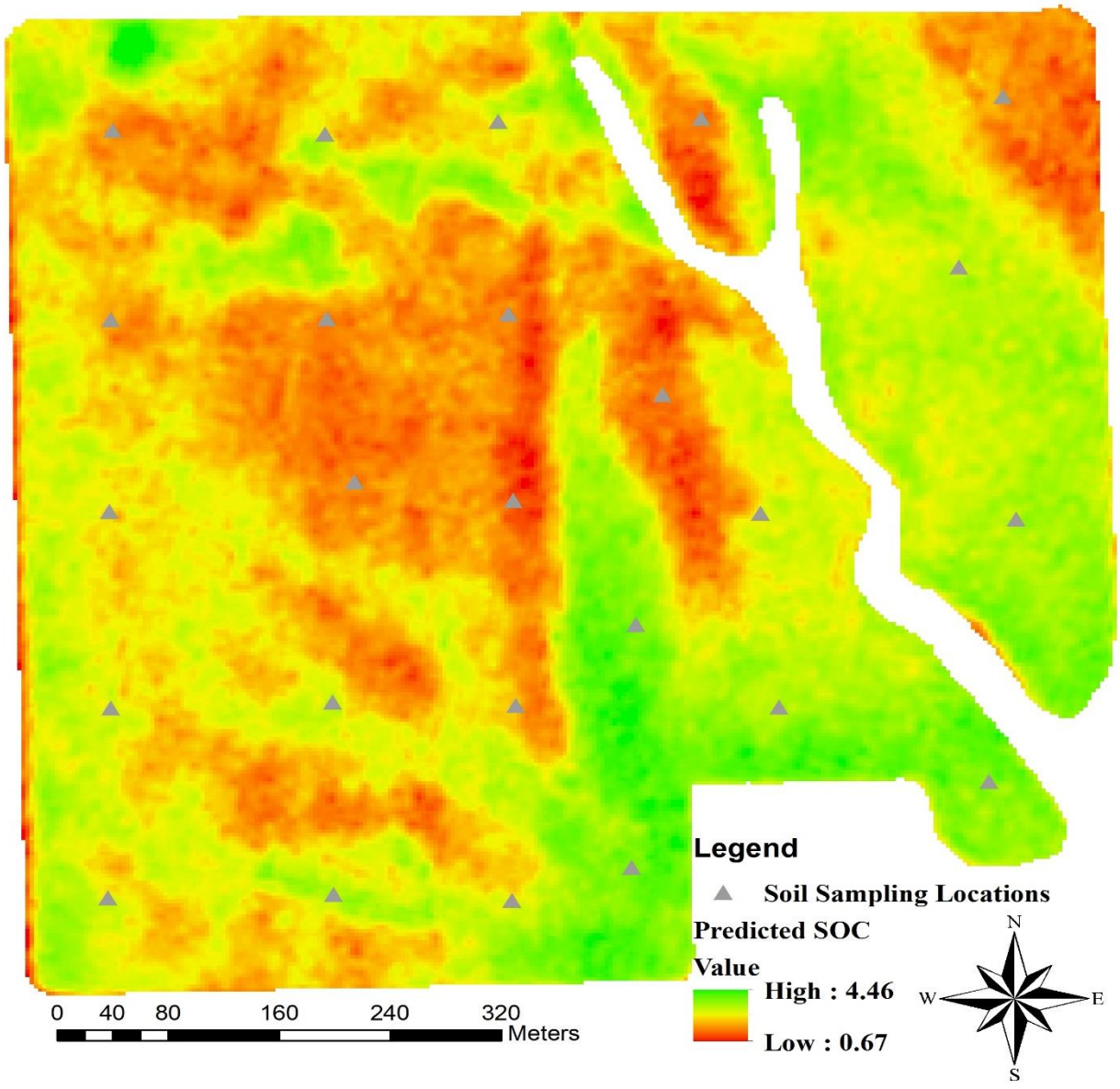

Figure 3.16 Predicted SOC map from PlanetScope satellite imagery for field C (Brookings County, SD). Map sources = PlanetScope (2018).

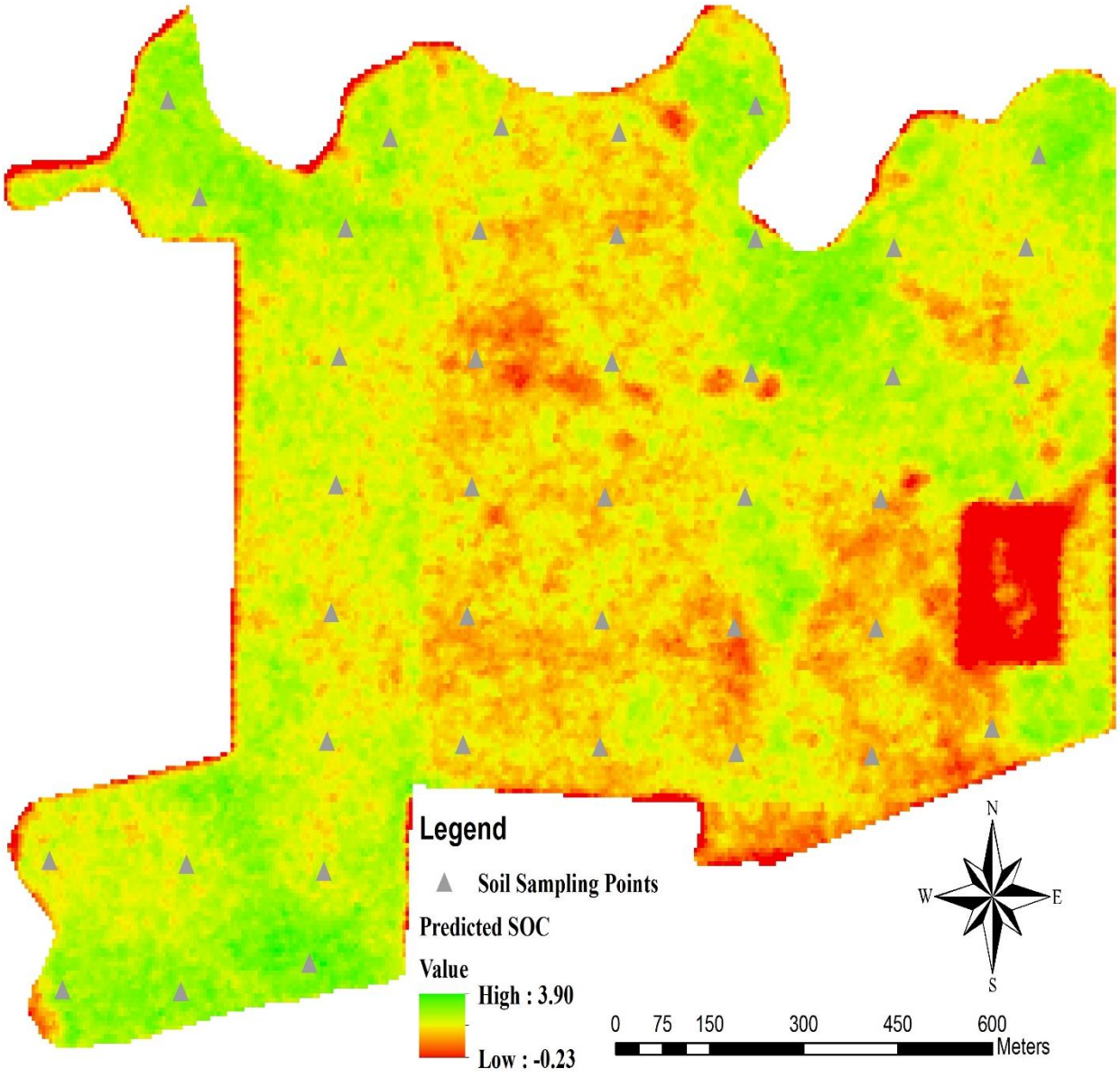

Figure 3.17 Predicted SOC map from PlanetScope satellite imagery for field D (Lac qui Parle County, MN). Map sources = PlanetScope (2018).

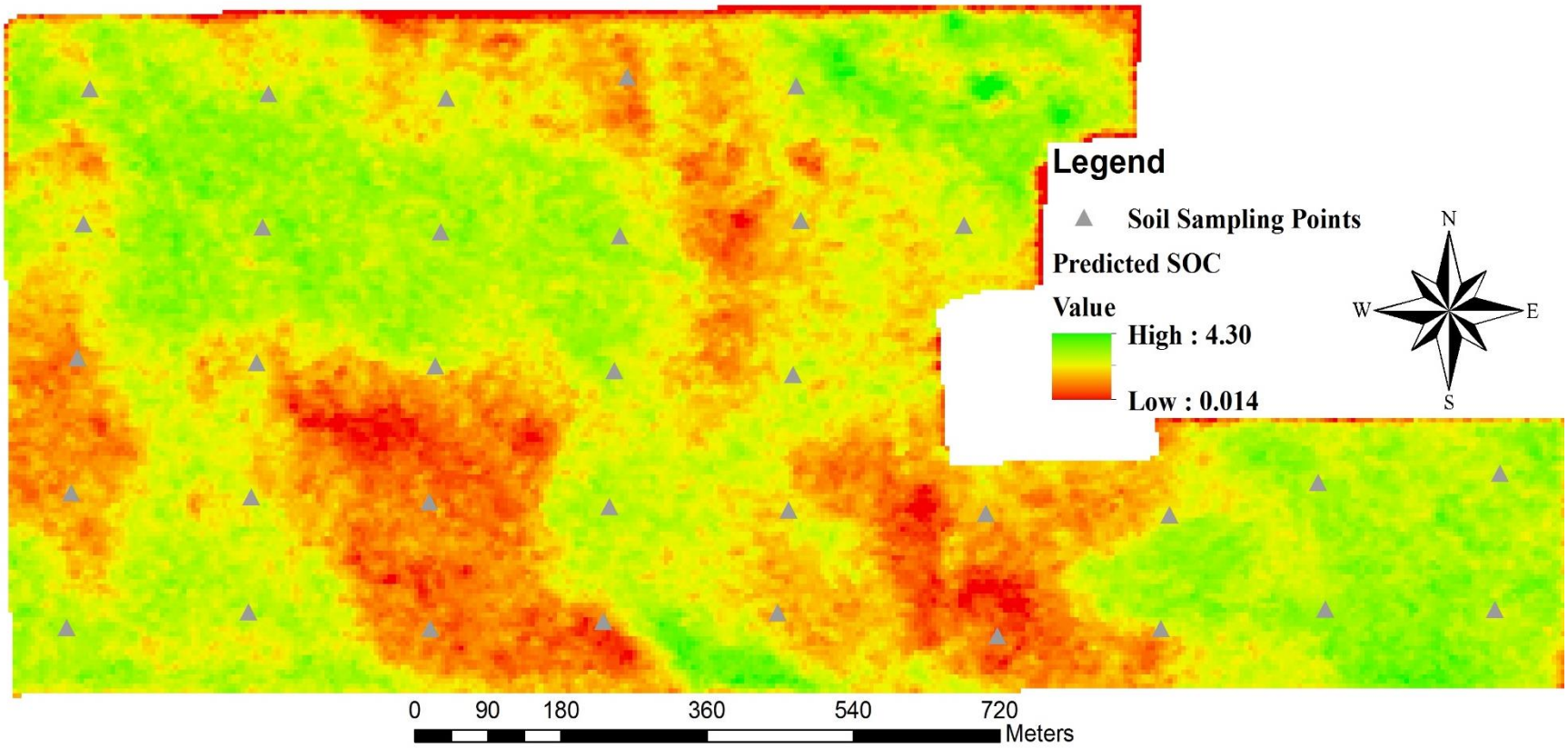

Figure 3.18 Predicted SOC map from PlanetScope satellite imagery for field E (Lac qui Parle County, MN). Map sources = PlanetScope (2018).

Model Development with Spatial Data and Web Soil Survey Data (WSS)

Model Development Using only WSS Data

Pearson correlation and simple linear regression were applied to show correlation between SOC and Web Soil Survey (WSS) data using SoilWeb App (Casoilresource.lawr.ucdavis.edu, 2018) All the data was analyzed at the 95% confidence interval ($\alpha = 0.05$; $p<0.05$). The complete Pearson correlation and WSS data are given in Appendix D and Appendix E. To demonstrate the relationships of selected WSS data and SOC a correlogram was built (see Figure 3.19)

Figure 3.19 The correlogram (correlation color map) of soil organic carbon (SOC) vs selected Web Soil Survey (WSS) data. Purple color tones indicate negative correlations between SOC, and spatial data and green colors show positive correlation (the values in the box show correlation coefficients at the 0.05. CEC = cation exchange capacity, n (number of observations) = 150

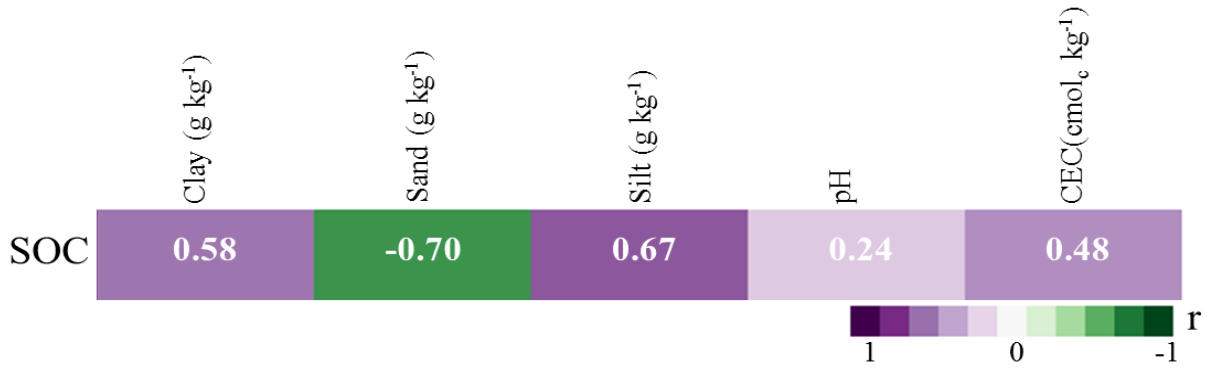

Significant correlations were found between SOC and WSS data. According to the color map, Sand ($r = -0.70$, $p<0.0001$) was highly negatively correlated, while Silt ($r = 0.67$, $p<0.0001$) and Clay ($r = 0.58$, $p<0.0001$) were strongly positively correlated to SOC, similar to soil test results found earlier in this publication. Moderate correlations were found between SOC and CEC ($r = 0.48$, $p<0.0001$). Lastly, weak correlation was

found between SOC and pH (r = 0.24, p= 0.0023). The linear regression results for each variable are shown in Table 3.16.

Table 3.16 Linear regression between soil organic carbon (SOC) and selected Web Soil Survey (WSS) data. CEC = cation exchange capacity, n (number of observations) = 150.

Equations	Variables	R^2	Equation Number
$SOC_p = 1.32 + (0.0540 \times Clay)$	Clay (g kg^{-1})	0.330	[3.38]
$SOC_p = 3.37 – (0.0210 \times Sand)$	Sand (g kg^{-1})	0.489	[3.39]
$SOC_p = 1.58 + (0.0260 \times Silt)$	Silt (g kg^{-1})	0.450	[3.40]
$SOC_p = -0.00850 + (0.365 \times pH_{1:1})$	$pH_{1:1}$	0.060	[3.41]
$SOC_p = 1.33 + (0.0590 \times CEC)$	CEC ($cmol_c$ kg^{-1})	0.240	[3.42]

In order to develop a model using WSS data, the stepwise sequential procedure performed, and the model is shown in Table 3.17.

Table 3.17 Model output of soil organic carbon (SOC) prediction based on Web Soil Survey (WSS) data. *Confidence level was set at 0.05, n (number of observations) = 150.

Parameters	Estimate	Std Error	t Ratio	Prob>|t|
Intercept	3.37	0.0778	43.28	<.0001*
Sand_WSS	-0.0206	0.00173	-11.92	<.0001*

The value of the R^2 is 0.490 and this means that regressor variable can explain approximately 49.0% of variation in response variable. The calculated adjusted R^2 is 0.486, 0.04 percent less than R^2. Mean square error (MSE) was found as 0.18 which is very good when compared to the range of the data. CV was found as 0.188. Using WSS data can explain 49.0% of the variance of SOC distribution can be estimated (see equation [3.43]).

$$SOC_p = 3.37 + (-0.0206 \times Sand\_WSS\ [g\ kg^{-1}]) \quad [3.43]$$

Figure 3.20 shows the results of predicted versus measured SOC WSS data. The approach showed good agreement between measured SOC and predicted SOC with R^2= 49.0%, p<0.0001 and confidence level was 0.05.

Figure 3.20 The linear relationship between measured and predicted soil organic carbon (SOC) from Web Soil Survey (WSS) data, n (number of observations) = 150.

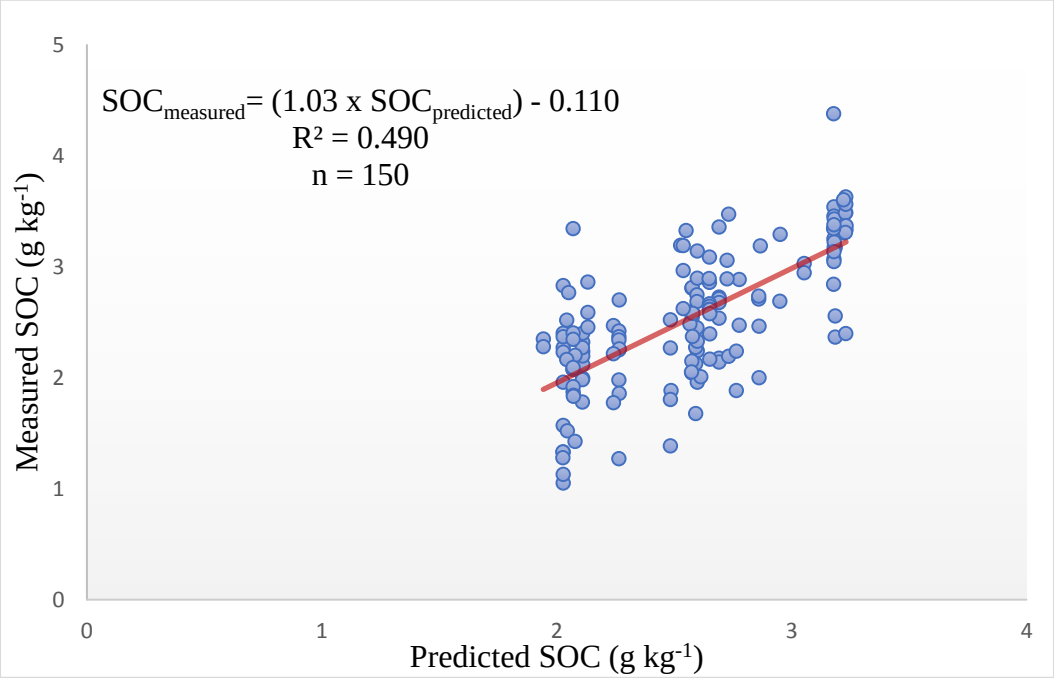

Model Development Using Landsat 8, Planet Scope and WSS Data

Since we started to work on this project, we have tried to develop a SOC prediction model for precision agriculture use. The idea was to build model which reduced the number of sample sites and the cost of laboratory analysis. In order to do that, we used public free information from Landsat 8 and WSS data.

Since, we have a lot of variables as our regressors that are not significant, we reduced the model to include only important variables. Stepwise sequential procedure was used to choose the best model for this part (see Table 3.18)

Table 3.18 Ordinary Least Square (OLS) model output of soil organic carbon (SOC) prediction based on Landsat 8 and Web Soil Survey (WSS) data. Significant at $\alpha = 0.05$, $Band_L$= Landsat 8 bands, VIF = variance inflation factor, n (number of observations) = 150.

Parameters	Estimate	Std Error	t Ratio	Prob>|t|	VIF
Intercept	4.58	0.338	13.55	<.0001*	.
$Band_L$ 3*	-14.1	3.83	-3.68	0.0003*	1.05
Sand_WSS	-0.0193	0.00170	-11.35	<.0001*	1.05

* See Table 2.8 for the Landsat 8 bands descriptions.

The value of the R^2 is 0.533 and this means that regressor variables can explain approximately 53.3 % of variation in SOC. The calculated adjusted R^2 is 0.527, approximately 0.5 percent less than R^2. Mean square error (MSE) was 0.16 which is very good when compared to the range values for the soil properties studied. Variation Inflation Factor values were calculated (see Table 3.18) for each variable and the values are lower than 4 which means there is no collinearity problem in this model. Cross Validation was found as 0.178. Using data providing by those two public free sources, 53.3 % of the variance of SOC distribution can be estimated (see equation [3.44]).

$$SOC_p = 4.58 - (14.1 \times Band_L\ 3) - (0.0193 \times Sand\ [g\ kg^{-1}]) \quad [3.44]$$

Figure 3.21 The linear relationship between measured and predicted soil organic carbon (SOC) from Web Soil Survey (WSS) and Landsat 8 data, n (number of observations) = 150.

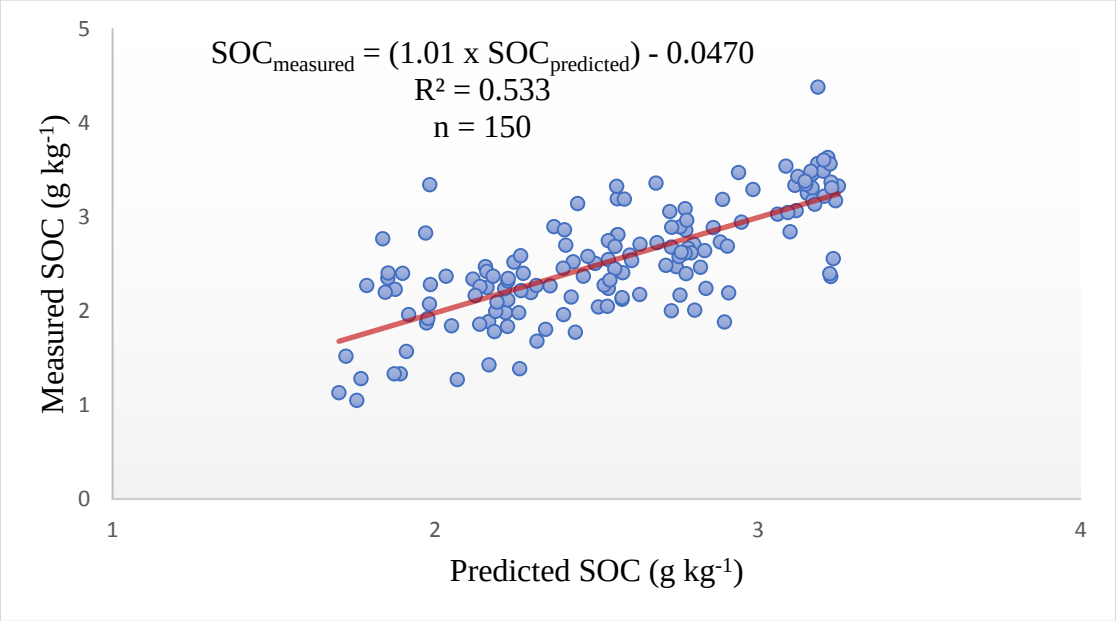

Figure 3.21 shows the results of predicted versus measured SOC using Landsat 8 imagery data. The approach showed good agreement between measured SOC and predicted SOC with R^2= 53.3%, p<0.0001 and confidence level was 0.05. As seen from the result we were able to increase our R^2 from approximately 0.370 (RR model) to 0.533 (OLS model) by adding WSS data in to the Landsat only model.

We also developed a SOC prediction model using PlanetScope and WSS data. In this part, high resolution imagery (PlanetScope) data was used to build model with WSS data (see Table 3.19).

Table 3.19 Ordinary Least Square (OLS) model output of soil organic carbon (SOC) prediction based on PlanetScope and WSS data. Significant at $\alpha = 0.05$, VIF = variance inflation factor, $Band_P$ = PlanetScope bands, BSI = bare soil index, n (number of observations) = 150.

Parameters	Estimate	Std Error	t Ratio	Prob>|t|	VIF
Intercept	-21.7	6.9	-3.15	0.0020*	.
Sand (g kg^{-1})	-0.00733	0.00227	-3.22	0.0016*	2.776
CEC ($cmol_c$ kg^{-1})	0.0168	0.00782	2.15	0.0334*	1.966
Band 4_P	-2270	252	-9.01	<0.0001*	3.042
BSI_P	0.281	0.0718	3.91	0.0001*	2.174

*See Table 2.9 and 2.10 for PlanetScope bands and indices descriptions.

The value of the R^2 is 0.688 and this means that regressor variables can explain approximately 68.8% of variation in SOC. The adjusted is R^2 which 0.680 or 0.8 percent less than R^2. Mean square error (MSE) was found as 0.115 which is very good when compared to the range of soil property values studied. The variance inflation factor for each variable. VIF values are lower than 4 which means there is no collinearity problem in this model. Cross Validation was found as 0.119. Basically, we can conclude that using data providing by WSS and Planet Scope data, we were able to increase correlation coefficient from 60.1% to 68.8%. The SOC distribution can be estimated by the following prediction expression:

$$SOC_p = -21.7 - (0.00733 \times \text{Sand g } kg^{-1}) + (0.0168 \text{ CEC } cmol_c\ kg^{-1}) \quad [3.45]$$

$$- (2270 \times \text{Band 4}) + (0.281 \times \text{BSI})$$

Figure 3.22 shows the results of predicted versus measured SOC using PlanetScope imagery data. The approach showed good agreement between measured SOC and predicted SOC with R^2= 68.8%, p<0.0001 and confidence level was 0.05.

Figure 3.22 The linear relationship between measured and predicted soil organic carbon (SOC) from Web Soil Survey (WSS) and PlanetScope data, n (number of observations) = 150.

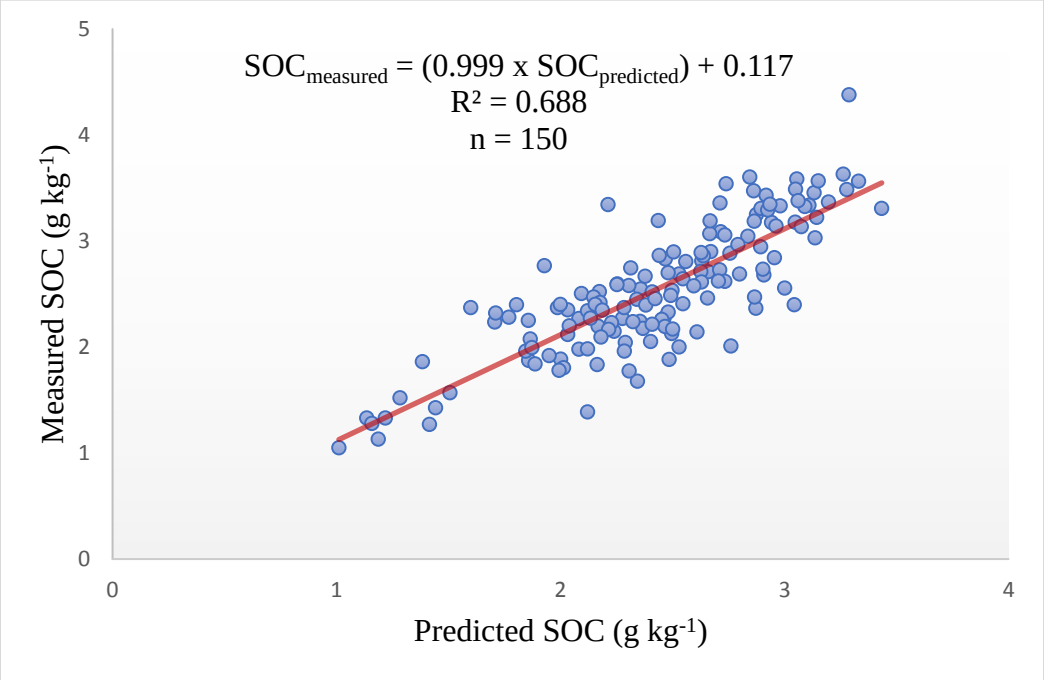

REFERENCES

Burke, I. C., Yonker, C. M., Parton, W. J., Cole, C. V., Schimel, D., and Flach, K. (1989). Texture, climate, and cultivation effects on soil organic matter content in US grassland soils. *Soil science society of America journal* **53**, 800-805.

Farrar, D. E., and Glauber, R. R. (1967). Multicollinearity in regression analysis: the problem revisited. *The Review of Economic and Statistics*, 92-107.

Fox, G. A., Sabbagh, G., Searcy, S., and Yang, C. (2004). An automated soil line identification routine for remotely sensed images. *Soil Science Society of America Journal* **68**, 1326-1331.

Friendly, M. (2002). Corrgrams: Exploratory displays for correlation matrices. *The American Statistician*, *56*(4), 316-324.

Gelaw, A. M., Singh, B., and Lal, R. (2015). Organic carbon and nitrogen associated with soil aggregates and particle sizes under different land uses in Tigray, Northern Ethiopia. *Land Degradation & Development* **26**, 690-700.

Koroleva, P., Rukhovich, D., Rukhovich, A., Rukhovich, D., Kulyanitsa, A., Trubnikov, A., Kalinina, N., and Simakova, M. (2017). Location of bare soil surface and soil line on the RED–NIR spectral plane. *Eurasian Soil Science* **50**, 1375-1385.

Miles, J. (2014). R squared, adjusted R squared. *Wiley StatsRef: Statistics Reference Online*.

Richardson, A. J., and Wiegand, C. (1977). Distinguishing vegetation from soil background information. *Photogrammetric engineering and remote sensing* **43**, 1541-1552.

Shao, J. (1993). Linear model selection by cross-validation. *Journal of the American statistical Association*, *88*(422), 486-494.

Simon, L. J. (2004). Detecting multicollinearity using variance inflation factors. *Penn State Department of Statistics, The Pennsylvania State University*.

SoilWeb Apps. (n.d.). Retrieved October 18, 2018, from https://casoilresource.lawr.ucdavis.edu/soilweb-apps

Studdert, G. A. (2000). Crop rotations and nitrogen fertilization to manage soil organic carbon dynamics. *Soil Science Society of America Journal* **64**, 1496-1503.

Team, P. (2017). Planet Application Program Interface: In Space for Life on Earth. *San Francisco, CA*.

Wold, S., Ruhe, A., Wold, H., and Dunn, III, W. J. (1984). The collinearity problem in linear regression. The partial least squares (PLS) approach to generalized inverses. *SIAM Journal on Scientific and Statistical Computing*, *5*(3), 735-743.

CHAPTER 4: Discussion and Conclusion

Discussion:

The soil organic carbon (SOC) prediction model using soil test data gives satisfactory results in the study area. As seen from Figure 3.1, SOC level is mainly controlled by textural classes. Goidts and van Wesemael (2007) found that there is no correlation between SOC and soil texture. However, our study did show that in the selected regions, soil texture significantly impacts SOC level in the 0-15cm depth. McGrath and Zhang (2003) and Mondal et al. (2017) found that there is a significant correlation between SOC and silt (r = 0.74, $p<0.0001$) plus clay (r = 0.80, $p<0.0001$); and a negative correlation between SOC and sand (r = -0.87, $p<0.0001$), similar to our study. Moreover, there was a strong correlation between SOC and Soil Moisture Content (SMC) (r = 0.81, $p<0.0001$) content in surface soil materials. This result is due to the climatic conditions which are present in the A horizons across the North American Great Plains region (Brady and Weil, 2017). Some previous studies have found the association between SOC and SMC (Hudson and Conservation, 1994; Hugar et al., 2012; Manns et al., 2016). In contrast, Parajuli and Duffy (2013) found very weak correlation between SOC and SMC.

Due to the effect of soil pH on species, organism size, and microbial activities in the soil profile, soil pH can be responsible for SOC decomposition and enhance soil C density (Pietri et al., 2009). Some previous studies showed that SOC levels are significantly correlated with pH (Ou et al., 2017; Suarez and Gonzalez-Rubio, 2017). In our case, pH (1:1) was statistically correlated (pH r = 0.39, $p<0.0001$) with SOC. This result could be coming from the association of soil pH and SOC content due to increasing

use of N fertilization and the presence of high lime parent materials. Studdert (2000) discussed the impact of N fertilization for farming purposes with continuous or without continuous N application on sustaining or enhancing SOC levels in cultivated areas.

A statistically high correlation was found between SOC and SOEC ($r = 0.72$, $p<0.0001$) in our study. Manrique et al. (1991) and Sullivan et al. (2006) mentioned that SOC can contribute to the CEC of the soil and values increases at higher pH levels. Moreover, Brady and Weil (2017) mentioned that the soil colloidal system consists of organic (humus) and mineral parts (clay). Soil organic matter is responsible for most of the CEC in soil surface, meanwhile, clay is responsible for most of the CEC in deeper parts of the soil profile. In a previous study, Caravaca et al. (1999) found that CEC of the soil is associated with SOC content of the same soil. The correlation between SOC and Clay was lower than with CEC. However, in our case, we found that SOC concentration is more strongly related to clay content than with CEC. The silicate clays in our soil are smectitic and our soils are young which supports our findings.

Principle Component Regression (PCR), Ridge Regression (RR), and Ordinary Least Square (OLS) were applied to the data set in order to deal with multicollinearity problems and to compare the prediction performance of different models. We presented the cross-validation values of the different models (see Table 3.5). Cross-validation (CV) showed that RR is slightly better than OLS. Considering the multicollinearity problem in our data set, PCR and OLS did not give the satisfactory results. However, adding the k constant in RR made model stronger since there is no multicollinearity problem with RR (Vigneau et al., 1997). Another study conducted by Shin (1990) mentioned that the ability of overcoming multicollinearity problems based on using RR which was better

than Ordinary Least Square (OLS). We did not focus on all soil variables. We only focused on soil variables that were used in reduced model.

Soil organic carbon is associated with soil color, nutrient-holding capacity, and helps to maintain soil composition (Ismail et al., 2012). In this regard, soil color and image intensity relationships were established between SOC concentration and satellite imagery data. Considering and evaluating the correlation color map (correlogram) and the performance of derived indices and single bands from satellite imagery (see Figure 3.4 and 3.7), the specific bands and indices of $Band_L$ 6 (1.566-1.651 µm), $MSAVI2_L$, $Band_L$ 5 (0.851 - 0.879 µm), $Band_L$ 7 (2.107 - 2.294 µm), BSI_L; followed by $Band_L$ 4 (0.636 - 0.673 µm) and BI_L for the Landsat 8; $Band_P$ 4 (0.780-0.860 µm), $Band_P$ 3 (0.590-0.670 µm) and BI_P for Planet Scope showed the highest correlation with SOC. Typical absorption features for SOC around the VIS and SWIR spectral region were attributed to these results (Viscarra Rossel et al., 2011). Soil with dark hues have higher SOC contents when compared to the soil with bright hues in the case of equal moisture and the same parent materials (Castaldi et al., 2016). However, there were some differences between studied fields such as moisture content and density of plant residue. Pimstein et al. (2011) explained that soils have different features such as moisture content during the data acquisition which can affect the spectral response. The amount of reflected and emitted spectra from soil surface is affected by soil humidity by decreasing reflectance values (Nocita et al., 2013). The OLS model from Landsat 8 and Planet Scope, include BSI as prediction parameters (see Table 3.9 and 3.15). BSI for both satellites was statistically correlated with SOC; high BSI areas were associated with low SOC, while low BSI was associated with high SOC. Kumar et al. (2016) found similar patterns with BSI which is

in agreement with our results. Frazier and Cheng (1989) obtained an R^2 value of 0.98 for SOC prediction equation using the Thematic Mapper (TM) fifth and fourth bands. Their results were much higher than our study (0.42 $R^2$for OLS model, 0.36 R^2 for RR model from Landsat 8 and 0.60 R^2 for OLS model from PlanetScope). On the other hand, Nanni and Demattê (2006) only used TM`s seventh and second bands using spectral reflectance (SR) in the model and found R^2 of 0.52. The reason for low R^2 was the bareness of the study areas. Nanni and Demattê (2006) obtained the soil line (NIR vs Red band) as R^2 of 0.96 but in our case, the relationship was R^2 of 0.866 for Landsat 8. According to Fox et al. (2004), the high R^2 represents more bare soil and soil line can be related to soil surface conditions within a field. Moreover, PCR and RR were used to deal with dimensionality of the data. Our results for Landsat 8 data showed that RR was better than PCR in terms of Cross-Validation (CV) results. In contrast, (Fox and Metla, 2005) suggested that PC1 within PCA were highly correlated to soil organic matter (SOM). To assist numerous agricultural applications and environmental activities, satellite data or drone data would be the efficient and non-intrusive way to assist in soil mapping and soil management. It is important to note that results of relationships between SOC and reflectance data is the same globally. Given these conditions, soil sampling should be done, and new statistical model developed for every geographic or study area to be mapped as managed. Soil characteristics would be required information from the study area in order to develop predictive model between SOC and reflectance data. It means that in order to obtain a good relationship between SOC and image reflectance local environmental conditions must be considered when developing a sampling methodology condition (Ladoni et al., 2010).

Web Soil Survey (WSS) data was useful for the SOC prediction in the present study. Data from WSS; Sand, Clay, Silt, pH, and CEC showed similar trends with the soil test data (see Figure 3.1 and 3.9). Sand % (r = -0.87 for soil test data, r = -0.70 for WSS data) was highly correlated in both situations. As seen in Table 3.18 and Table 3.19, WSS significantly contributed to increase the coefficient of determination (R^2) for our models.

Conclusions:

Soil organic carbon (SOC) is an important soil health property and needs to be monitored methodically and quantitatively. Remote sensing is one of the functional and inexpensive tools available to map SOC. In this study, SOC distribution in selected soils were estimated using soil test data, satellite imagery (Landsat 8 and PlanetScope) and Web Soil Survey (WSS) data. The main aim was to reduce the number of soil sampling points to build a cost-effective SOC prediction model using soil test data and free public data. The SOC prediction accuracy was improved by using selected soil test, satellite, and WSS data.

Soil test data was highly correlated to SOC. The full model explained 86.7% of the variation in SOC, however, the model was not free of multicollinearity with all soil variables. Even with the reduced model using SOEC, Sand, and pH which explained 82.7% of the variation in SOC the model still had multicollinearity problems. To deal with multicollinearity, principal component regression (PCR) and ridge regression (RR) methods were used. The best methods were decided based on observed cross-validation (CV) result and RR was selected as the best model. As for WSS data, the relationship between soil variables and SOC showed similar pattern with soil test data but without

multicollinearity problems. The WSS Sand data was highly correlated to SOC and the final WSS model explained 49.0% of variation in SOC.

Estimation of SOC levels in surface soil from remotely sensed data showed good agreement with the other studies. The best SOC and Landsat 8 spectral bands and indices correlations were obtained from $Band_L$ 5, $Band_L$ 6, and $MSAVI2_L$. After stepwise selection, ordinary least squared model (OLS) with $Band_L$ 7, $Band_L$ 5, $Band_L$ 3, $Band_L$ 2, and BSI_L explained 42.3% of the variation in SOC. However, due to multicollinearity, RR and PCR were applied. Ridge regression was the best model (37.0% of variation explained) to estimate SOC using Landsat 8 data and was not affected by multicollinearity. PlanetScope data ($Band_P$ 4, $Band_P$ 3, and BI_P) with higher spectral resolution provided the highest correlations with SOC. Stepwise selection produced OLS model which was not affected by multicollinearity with BSI_P and $Band_P$ 4 explaining 60.0% of the variation in SOC. WSS data also was included into model with both Landsat 8 and PlanetScope data. The results showed that WSS data improved the accuracy of the model and help estimation model of SOC using Landsat 8 data to remove multicollinearity problem. While the 53.3% of the variation explained by the WSS and Landsat 8 model, OLS model was expressed 68.0% of the variation in SOC by PlanetScope with WSS data.

The models developed in this study can be used for estimating the crop production inputs and their impacts on available SOC. Future work is needed to determine the number of soil samples needed to accurately predict SOC levels for an area. Another crucial part would be the acquisition time for the satellite imagery and the amount surface crop residue which affects reflectance. Sampling time and acquisition

time should be same day or very close. Adding drone imagery is another step in this project. As for crop residue, some remote sensing indices can be used to distinguish soil and plant residue. These situations would provide more accurate results. Moreover, as more quality and quantifiable soil data is added to the WSS data base, more precise predictions will be possible. The results of the research will improve and provide more precise soil data. Our research will assist scientists and farm managers determine the best management practices for their research, farm operations, and aid in conserving SOC levels and enhance precision agriculture farming systems. In the near future, there will be more free data available which will impact soil data quality positively to monitor soil variables.

REFERENCES

Brady, N and Weil, R. 2017. The Nature and Property of Soils. Harlow, England. Pearson Education Limited

Caravaca, F., Lax, A., & Albaladejo, J. (1999). Organic matter, nutrient contents and cation exchange capacity in fine fractions from semiarid calcareous soils. *Geoderma*, *93*(3-4), 161-176.

Castaldi, F., Palombo, A., Santini, F., Pascucci, S., Pignatti, S., & Casa, R. (2016). Evaluation of the potential of the current and forthcoming multispectral and hyperspectral imagers to estimate soil texture and organic carbon. *Remote Sensing of Environment*, *179*, 54-65.

Fox, G. A., & Metla, R. (2005). Soil property analysis using principal components analysis, soil line, and regression models. Soil Science Society of America Journal, 69(6), 1782-1788.

Fox, G. A., Sabbagh, G. J., Searcy, S. W., & Yang, C. (2004). An automated soil line identification routine for remotely sensed images. *Soil Science Society of America Journal*, *68*(4), 1326-1331..

Frazier, B. E., & Cheng, Y. (1989). Remote sensing of soils in the eastern Palouse region with Landsat Thematic Mapper. *Remote Sensing of Environment*, *28*, 317-325.

Goidts, E., and van Wesemael, B. J. G. (2007). Regional assessment of soil organic carbon changes under agriculture in Southern Belgium (1955–2005). **141**, 341-354.

Hudson, B. D. (1994). Soil organic matter and available water capacity. *Journal of Soil and Water Conservation*, *49*(2), 189-194.

Hugar, G. M., Sorganvi, V., Hiremath, G. M., & Hugar, G. M. (2012). Effect of Organic Carbon on Soil Moisture. *Indian Journal Of Natural Sciences International Bimonthly ISSN*, *976*, 0997.

Ismail, M., & Yacoub, R. K. (2012). Digital soil map using the capability of new technology in Sugar Beet area, Nubariya, Egypt. *The Egyptian Journal of Remote Sensing and Space Science*, *15*(2), 113-124.

Kumar, P., Pandey, P. C., Singh, B. K., Katiyar, S., Mandal, V. P., Rani, M., ... & Patairiya, S. (2016). Estimation of accumulated soil organic carbon stock in tropical forest using geospatial strategy. *The Egyptian Journal of Remote Sensing and Space Science*, *19*(1), 109-123.

Ladoni, M., Bahrami, H. A., Alavipanah, S. K., & Norouzi, A. A. (2010). Estimating soil organic carbon from soil reflectance: a review. *Precision Agriculture*, *11*(1), 82-99.

Manns, H. R., Parkin, G. W., & Martin, R. C. (2016). Evidence of a union between organic carbon and water content in soil. *Canadian Journal of Soil Science*, *96*(3), 305-316.

Manrique, L. A., Jones, C. A., & Dyke, P. T. (1991). Predicting cation-exchange capacity from soil physical and chemical properties. *Soil Science Society of America Journal*, *55*(3), 787-794.

McGrath, D., & Zhang, C. (2003). Spatial distribution of soil organic carbon concentrations in grassland of Ireland. *Applied Geochemistry*, *18*(10), 1629-1639.

Mondal, A., Khare, D., Kundu, S., Mondal, S., Mukherjee, S., & Mukhopadhyay, A. (2017). Spatial soil organic carbon (SOC) prediction by regression kriging using remote sensing data. *The Egyptian Journal of Remote Sensing and Space Science*, *20*(1), 61-70.

Nanni, M. R., & Demattê, J. A. M. (2006). Spectral reflectance methodology in comparison to traditional soil analysis. *Soil Science Society of America Journal*, *70*(2), 393-407.

Nocita, M., Stevens, A., Noon, C., & van Wesemael, B. (2013). Prediction of soil organic carbon for different levels of soil moisture using Vis-NIR spectroscopy. *Geoderma*, *199*, 37-42.

Ou, Y., Rousseau, A. N., Wang, L., & Yan, B. (2017). Spatio-temporal patterns of soil organic carbon and pH in relation to environmental factors—A case study of the Black Soil Region of Northeastern China. *Agriculture, Ecosystems & Environment*, *245*, 22-31.

Parajuli, P. B., & Duffy, S. (2013). Evaluation of soil organic carbón and soil moisture content from agricultural fields in Mississippi. *Open Journal of Soil Science*, *3*(02), 81.

Pietri, J. A., & Brookes, P. C. (2009). Substrate inputs and pH as factors controlling microbial biomass, activity and community structure in an arable soil. *Soil Biology and Biochemistry*, *41*(7), 1396-1405.

Pimstein, A., Notesco, G., & Ben-Dor, E. (2011). Performance of three identical spectrometers in retrieving soil reflectance under laboratory conditions. *Soil Science Society of America Journal*, *75*(2), 746-759.

Shin, M. Y. (1990). The use of ridge regression for yield prediction models with multicollinearity problems. *Journal of Korean Forestry Society*, *79*(3), 260-268.

Studdert, G. A. (2000). Crop rotations and nitrogen fertilization to manage soil organic carbon dynamics. *Soil Science Society of America Journal*, *64*(4), 1496-1503.

Suarez, D. L., & Gonzalez-Rubio, A. (2017). Effects of the dissolved organic carbon of treated municipal wastewater on soil infiltration as related to sodium adsorption ratio and pH. *Soil Science Society of America Journal*, *81*(3), 602-611.

Sullivan, T. J., Fernandez, I. J., Herlihy, A. T., Driscoll, C. T., McDonnell, T. C., Nowicki, N. A., ... & Sutherland, J. W. (2006). Acid-base characteristics of soils in the Adirondack Mountains, New York. *Soil Science Society of America Journal*, *70*(1), 141-152.

Vigneau, E., Devaux, M. F., Qannari, E. M., & Robert, P. (1997). Principal component regression, ridge regression and ridge principal component regression in spectroscopy calibration. *Journal of Chemometrics: A Journal of the Chemometrics Society*, *11*(3), 239-249.

Viscarra Rossel, R. A., Chappell, A., De Caritat, P., & McKenzie, N. J. (2011). On the soil information content of visible–near infrared reflectance spectra. *European Journal of Soil Science*, *62*(3), 442-453.

APPENDICEES

Appendix A

Table A.1 The complete Pearson correlation matrix for soil test data (n= 150)

Parameters	SOC	Moisture	EC (1:1)	pH (1:1)	Sand	Clay	Silt	K^+	Ca^{2+}	Mg^{2+}	Na^+	NH_4^+-N	NO_3^--N	SOEC	PO_4^{3-}
SOC (g kg^{-1})	1.00														
Moisture (g kg^{-1})	**0.81**	1.00													
$EC_{1:1}$ (dS m^{-1})	**0.53**	**0.46**	1.00												
$pH_{1:1}$	**0.39**	**0.46**	**0.69**	1.00											
Sand (g kg^{-1})	**-0.87**	**-0.72**	**-0.46**	**-0.31**	1.00										
Clay (g kg^{-1})	**0.80**	**0.64**	**0.65**	**0.45**	**-0.87**	1.00									
Silt (g kg^{-1})	**0.74**	**0.63**	0.18	0.10	**-0.89**	0.**54**	1.00								
K^+ (mg kg^{-1})	0.16	0.07	0.21	0.03	-0.04	0.12	-0.04	1.00							
Ca^{2+} (mg kg^{-1})	**0.64**	**0.67**	**0.75**	**0.85**	**-0.54**	**0.69**	**0.27**	0.05	1.00						
Mg^{2+} (mg kg^{-1})	**0.77**	**0.73**	**0.53**	**0.58**	**-0.76**	**0.75**	**0.59**	0.00	**0.67**	1.00					
Na^+ (mg kg^{-1})	0.06	0.01	-0.04	0.18	0.07	-0.10	-0.02	0.02	0.01	0.08	1.00				
NH_4^+-N (mg kg^{-1})	0.01	**-0.29**	0.14	-0.19	-0.07	**0.25**	-0.12	0.15	-0.15	-0.03	0.04	1.00			
NO_3^--N (mg kg^{-1})	**0.40**	**0.26**	**0.28**	0.16	**-0.52**	**0.32**	**0.59**	-0.03	0.14	**0.35**	-0.13	-0.02	1.00		
SOEC ($cmol_c$ kg^{-1})	**0.72**	**0.74**	**0.75**	**0.84**	**-0.63**	**0.75**	**0.37**	0.08	**0.98**	**0.80**	0.04	-0.12	0.20	1.00	
PO_4^{3-} (mg kg^{-1})	**-0.39**	**-0.47**	**-0.37**	**-0.61**	**0.38**	**-0.43**	-0.24	**0.43**	**-0.63**	**-0.51**	**-0.25**	0.09	-0.03	**-0.63**	1.00

All values in **bold print** are significant (P<0.05). SOEC = Sum of Extractable Cation, EC = Electrical Conductivity, SOC= Soil Organic Carbon. Soils from 0-15cm depth.

Table A.2 Field A (Brookings County, SD) soil test data set

Sample No	Latitude (^{O}N)	Longitude (^{O}W)	SOC (g kg^{-1})	Moisture (g kg^{-1})	pH (1:1)	EC (dS m^{-1}) (1:1)	K^{+} (mg kg^{-1})	Ca^{2+} (mg kg^{-1})	Mg^{2+} (mg kg^{-1})
1	44.3849033	-96.9461351	3.5	24.6	6.4	0.8	216	3650	793
2	44.3849738	-96.9442170	3.0	21.9	6.2	0.6	206	2780	672
3	44.3863216	-96.9443015	3.3	36.2	7.6	0.9	269	4980	839
4	44.3877266	-96.9442422	3.3	20.9	6.4	0.6	191	2510	596
5	44.3880766	-96.9462404	3.2	21.6	6.0	0.6	509	2360	549
6	44.3894226	-96.9462689	3.2	21.1	7.1	0.7	149	2970	777
7	44.3893326	-96.9443454	3.5	22.7	6.8	0.7	174	3110	804
8	44.3905456	-96.9462595	3.6	23.1	6.6	0.8	221	3130	804
9	44.3905477	-96.9442898	3.3	29.6	6.1	0.6	218	2490	807
10	44.3905362	-96.9426315	3.6	28.7	6.6	0.9	180	3270	897
11	44.3892037	-96.9424045	3.2	22.8	6.8	0.7	192	2760	902
12	44.3877270	-96.9423955	3.1	21.2	5.6	0.5	183	2400	593
13	44.3863649	-96.9422821	3.3	22.7	6.0	0.5	157	2470	726
14	44.3849364	-96.9422305	3.6	24.1	6.4	0.7	251	3000	855
15	44.3849395	-96.9404207	3.0	19.5	7.0	0.8	169	3800	560
16	44.3864433	-96.9405058	3.5	23.4	6.3	0.6	168	2830	649
17	44.3877366	-96.9406607	3.4	22.1	5.7	0.6	179	2370	655
18	44.3892959	-96.9407110	3.5	25.1	7.8	0.8	200	4500	1664
19	44.3905324	-96.9407824	3.4	23.1	6.9	0.8	188	3990	871
20	44.3905420	-96.9386300	3.6	24.0	7.6	1.0	245	4850	1090
21	44.3893405	-96.9385052	3.3	29.2	7.6	0.7	172	3690	1180
22	44.3877992	-96.9387336	3.1	32.7	6.8	0.7	160	3370	771
23	44.3864869	-96.9386987	2.4	15.4	7.3	0.7	129	4060	476
24	44.3849026	-96.9387805	3.3	22.8	7.7	0.8	178	4930	1090

EC = Electrical Conductivity, SOC= Soil Organic Carbon. Soils from 0-15cm depth.

Table A.2 Continued

Sample No	Latitude (^{O}N)	Longitude (^{O}W)	Na^{+} (mg kg^{-1})	SOEC ($cmol_c$ kg^{-1})	NH_4^{+}-N (mg kg^{-1})	NO_3^{-}-N (mg kg^{-1})	PO_4^{-3} (mg kg^{-1})	Sand (g kg^{-1})	Clay (g kg^{-1})	Silt (g kg^{-1})
1	44.3849033	-96.9461351	29	26	15	55	46	10.71	40.76	48.54
2	44.3849738	-96.9442170	35	20	16	64	42	12.61	36.64	50.75
3	44.3863216	-96.9443015	33	33	9	89	1	20.31	36.10	43.59
4	44.3877266	-96.9442422	32	18	29	56	43	18.51	34.55	46.95
5	44.3880766	-96.9462404	21	18	27	70	71	14.34	36.66	49.00
6	44.3894226	-96.9462689	39	22	18	58	59	19.34	38.59	42.08
7	44.3893326	-96.9443454	31	23	19	66	40	14.49	38.26	47.25
8	44.3905456	-96.9462595	28	23	39	76	40	15.79	39.16	45.05
9	44.3905477	-96.9442898	34	20	34	58	33	9.97	38.93	51.10
10	44.3905362	-96.9426315	31	24	23	86	53	11.32	41.25	47.43
11	44.3892037	-96.9424045	42	22	22	65	25	14.73	37.45	47.82
12	44.3877270	-96.9423955	34	18	34	53	34	20.70	34.57	44.73
13	44.3863649	-96.9422821	25	19	21	45	27	19.40	37.08	43.52
14	44.3849364	-96.9422305	34	23	16	60	54	11.65	39.14	49.20
15	44.3849395	-96.9404207	21	24	11	70	56	45.12	29.66	25.23
16	44.3864433	-96.9405058	20	20	20	56	64	15.80	36.94	47.26
17	44.3877366	-96.9406607	16	18	38	61	22	16.48	36.51	47.01
18	44.3892959	-96.9407110	27	37	10	59	39	20.36	38.96	40.68
19	44.3905324	-96.9407824	26	28	18	59	23	19.65	40.98	39.37
20	44.3905420	-96.9386300	22	34	12	80	43	14.87	41.85	43.27
21	44.3893405	-96.9385052	24	29	12	61	46	19.36	39.41	41.23
22	44.3877992	-96.9387336	19	24	23	64	30	26.64	34.33	39.03
23	44.3864869	-96.9386987	15	25	17	70	36	43.48	27.35	29.17
24	44.3849026	-96.9387805	26	34	11	71	15	22.36	38.05	39.59

SOEC = Sum of Extractable Cation. Soils from 0-15cm depth.

Table A.3 Field B (Brookings County, SD) soil test data set

Sample No	Latitude (^{O}N)	Longitude (^{O}W)	SOC (g kg^{-1})	Moisture (g kg^{-1})	pH (1:1)	EC (dS m^{-1}) (1:1)	K^{+} (mg kg^{-1})	Ca^{2+} (mg kg^{-1})	Mg^{2+} (mg kg^{-1})
1	44.4629807	-96.8467720	2.0	15.6	6.1	0.6	300	1890	363
2	44.4630070	-96.8448609	2.1	12.4	6.1	0.5	267	2170	405
3	44.4629894	-96.8428560	1.4	10.1	6.4	0.5	259	1270	261
4	44.4628501	-96.8409707	2.2	14.7	7.3	0.7	232	2350	652
5	44.4628333	-96.8389601	2.7	14.9	6.2	0.5	199	2170	402
6	44.4613164	-96.8388696	2.6	15.9	6.1	0.5	208	2360	448
7	44.4614810	-96.8409738	3.5	22.0	7.5	0.7	322	3670	1010
8	44.4615306	-96.8428734	2.2	11.2	6.6	0.5	208	2230	445
9	44.4617706	-96.8447335	2.2	12.6	6.8	0.5	184	1990	398
10	44.4617408	-96.8467150	1.8	11.4	6.4	0.5	230	1660	324
11	44.4603363	-96.8466976	2.4	16.9	7.3	0.6	284	2840	579
12	44.4603057	-96.8444288	2.3	12.9	6.4	0.4	210	2200	441
13	44.4598756	-96.8431769	1.9	11.3	6.8	0.4	197	1850	389
14	44.4597715	-96.8409587	2.0	11.8	6.1	0.6	293	1360	273
15	44.4594313	-96.8393745	2.2	14.3	6.7	0.5	174	2170	558
16	44.4587020	-96.8390945	2.5	16.2	6.2	0.4	238	2270	459
17	44.4587136	-96.8410623	2.6	16.7	6.6	0.5	253	2870	569
18	44.4587878	-96.8430260	2.3	14.2	6.6	0.5	212	2120	436
19	44.4588545	-96.8449193	2.4	15.6	6.7	0.5	272	2110	426
20	44.4588720	-96.8467019	2.6	15.5	6.9	0.7	319	2600	525
21	44.4573421	-96.8391653	3.1	17.7	6.3	0.7	368	2450	431
22	44.4573916	-96.8411028	2.2	16.3	6.1	0.5	285	2580	441
23	44.4574460	-96.8429200	2.9	17.7	7.3	0.7	260	3830	597
24	44.4574153	-96.8448636	2.6	17.1	7.0	0.6	226	2930	553
25	44.4575522	-96.8467046	2.9	17.9	7.0	0.6	383	2640	517

EC = Electrical Conductivity, SOC= Soil Organic Carbon. Soils from 0-15cm depth.

Table A.3 Continued

Sample No	Latitude (^{O}N)	Longitude (^{O}W)	Na^{+} (mg kg^{-1})	SOEC ($cmol_c$ kg^{-1})	NH_4^{+}-N (mg kg^{-1})	NO_3^{-}-N (mg kg^{-1})	PO_4^{-3} (mg kg^{-1})	Sand (g kg^{-1})	Clay (g kg^{-1})	Silt (g kg^{-1})
1	44.4629807	-96.8467720	48	27	46	51	14	62.46	18.70	18.83
2	44.4630070	-96.8448609	50	21	31	42	15	56.32	20.47	23.2
3	44.4629894	-96.8428560	60	34	30	48	9	73.07	12.42	14.52
4	44.4628501	-96.8409707	54	19	41	37	18	59.96	22.82	17.22
5	44.4628333	-96.8389601	44	25	33	40	15	53.75	25.01	21.24
6	44.4613164	-96.8388696	40	11	28	37	16	42.68	19.24	38.07
7	44.4614810	-96.8409738	70	87	0	42	28	41.92	27.63	30.46
8	44.4615306	-96.8428734	75	8	24	35	16	58.61	18.24	23.15
9	44.4617706	-96.8447335	66	16	30	44	14	60.47	20.55	18.98
10	44.4617408	-96.8467150	41	14	35	40	12	60.17	18.70	21.13
11	44.4603363	-96.8466976	87	34	29	31	20	45.55	24.94	29.51
12	44.4603057	-96.8444288	44	25	25	40	15	54.31	22.70	22.98
13	44.4598756	-96.8431769	46	26	17	47	13	63.14	18.18	18.68
14	44.4597715	-96.8409587	65	45	35	50	10	66.53	12.47	21.00
15	44.4594313	-96.8393745	39	14	23	27	16	60.23	18.59	21.18
16	44.4587020	-96.8390945	39	19	21	52	16	43.07	27.31	29.61
17	44.4587136	-96.8410623	70	35	18	39	20	42.09	26.63	31.28
18	44.4587878	-96.8430260	52	28	17	37	15	51.74	24.70	23.56
19	44.4588545	-96.8449193	83	39	20	44	15	56.07	22.79	21.14
20	44.4588720	-96.8467019	113	52	27	41	19	48.38	30.50	21.12
21	44.4573421	-96.8391653	84	58	41	60	17	49.11	27.19	23.70
22	44.4573916	-96.8411028	59	25	30	41	18	46.8	27.44	25.76
23	44.4574460	-96.8429200	57	20	41	36	25	40.84	31.57	27.58
24	44.4574153	-96.8448636	54	12	29	32	20	40.53	31.85	27.61
25	44.4575522	-96.8467046	70	37	27	50	19	41.13	31.42	27.45

SOEC = Sum of Extractable Cation. Soils from 0-15cm depth.

Table A.4 Field C (Brookings County, SD) soil test data set

Sample No	Latitude (^{O}N)	Longitude (^{O}W)	SOC (g kg^{-1})	Moisture (g kg^{-1})	pH (1:1)	EC (dS m^{-1}) (1:1)	K^{+} (mg kg^{-1})	Ca^{2+} (mg kg^{-1})	Mg^{2+} (mg kg^{-1})
1	44.4286008	-96.8672630	2.0	13.0	5.4	0.3	209	1450	264
2	44.4299830	-96.8671877	2.4	14.9	5.8	0.4	253	1690	327
3	44.4314178	-96.8671488	2.3	14.8	5.7	0.6	268	1630	336
4	44.4328201	-96.8670861	2.4	15.5	5.5	0.5	239	1690	348
5	44.4342010	-96.8670197	1.9	13.2	5.7	0.3	185	1370	281
6	44.4341373	-96.8651006	2.4	16.6	5.8	0.4	180	1780	334
7	44.4327896	-96.8651324	1.3	9.5	5.5	0.2	239	944	189
8	44.4315933	-96.8649219	1.3	8.6	5.6	0.1	252	851	171
9	44.4299906	-96.8651800	2.3	15.0	5.7	0.3	218	1430	271
10	44.4285866	-96.8652243	2.4	15.8	5.7	0.5	264	1800	329
11	44.4285134	-96.8636093	2.3	15.5	5.6	0.5	299	1860	322
12	44.4299351	-96.8635234	1.6	17.7	5.6	0.3	282	1140	221
13	44.4314315	-96.8634919	1.1	8.8	5.6	0.3	237	800	173
14	44.4327920	-96.8634859	1.3	9.0	5.6	0.3	237	893	191
15	44.4341988	-96.8635278	2.4	16.2	5.3	0.4	189	1620	283
16	44.4341861	-96.8616905	1.3	14.8	5.2	0.2	155	819	152
17	44.4342965	-96.8589566	1.5	11.7	5.2	0.2	164	960	173
18	44.4330571	-96.8594005	2.3	22.2	5.2	0.3	167	1400	234
19	44.4312102	-96.8589493	2.3	18.1	5.0	0.4	176	1360	233
20	44.4312967	-96.8612596	2.0	12.4	5.1	0.3	219	1140	200
21	44.4321796	-96.8621143	1.1	7.3	4.9	0.2	160	607	122
22	44.4305035	-96.8624173	2.8	22.2	6.6	0.4	167	2660	451
23	44.4298767	-96.8611440	2.2	16.8	5.1	0.4	242	1230	206
24	44.4293013	-96.8592668	2.7	21.1	6.9	0.4	497	2320	514
25	44.4287346	-96.8625206	2.0	16.4	5.9	0.3	133	1670	233

EC = Electrical Conductivity, SOC= Soil Organic Carbon. Soils from 0-15cm depth.

Table A.4 Continued

Sample No	Latitude (^{O}N)	Longitude (^{O}W)	Na^{+} (mg kg^{-1})	SOEC ($cmol_c$ kg^{-1})	NH_4^{+}-N (mg kg^{-1})	NO_3^{-}-N (mg kg^{-1})	PO_4^{-3} (mg kg^{-1})	Sand (g kg^{-1})	Clay (g kg^{-1})	Silt (g kg^{-1})
1	44.4286008	-96.8672630	28	6	28	79	10	59.66	17.17	23.17
2	44.4299830	-96.8671877	25	7	33	77	12	51.72	18.71	29.57
3	44.4314178	-96.8671488	28	8	52	89	12	51.51	19.23	29.26
4	44.4328201	-96.8670861	56	11	51	94	12	52.11	18.59	29.30
5	44.4342010	-96.8670197	28	7	25	72	10	65.79	19.22	14.99
6	44.4341373	-96.8651006	32	7	33	66	12	57.20	15.30	27.50
7	44.4327896	-96.8651324	31	7	22	129	7	71.40	11.93	16.67
8	44.4315933	-96.8649219	24	6	18	111	6	74.68	10.71	14.61
9	44.4299906	-96.8651800	23	7	28	93	10	53.22	17.25	29.53
10	44.4285866	-96.8652243	26	5	38	106	13	55.28	17.14	27.58
11	44.4285134	-96.8636093	24	8	45	59	13	57.99	16.60	25.41
12	44.4299351	-96.8635234	30	6	20	137	8	70.95	12.29	16.76
13	44.4314315	-96.8634919	23	5	12	107	6	75.53	10.07	14.40
14	44.4327920	-96.8634859	29	7	15	111	7	75.40	12.05	12.55
15	44.4341988	-96.8635278	35	8	36	87	11	57.20	17.24	25.57
16	44.4341861	-96.8616905	16	6	17	90	6	75.30	8.10	16.60
17	44.4342965	-96.8589566	32	9	17	106	7	62.97	16.13	20.90
18	44.4330571	-96.8594005	31	7	29	62	10	52.06	16.80	31.14
19	44.4312102	-96.8589493	27	11	35	73	9	47.41	18.93	33.66
20	44.4312967	-96.8612596	20	8	26	106	8	63.62	11.00	25.38
21	44.4321796	-96.8621143	19	7	12	104	5	75.59	11.88	12.53
22	44.4305035	-96.8624173	26	8	23	57	18	40.09	23.57	36.35
23	44.4298767	-96.8611440	23	8	32	96	9	55.16	17.37	27.48
24	44.4293013	-96.8592668	32	9	28	78	17	43.44	18.59	37.97
25	44.4287346	-96.8625206	32	5	23	60	11	66.08	16.66	17.25

SOEC = Sum of Extractable Cation. Soils from 0-15cm depth.

Table A.5 Field D (Lac qui Parle County, MN) soil test data set

Sample No	Latitude (^{O}N)	Longitude (^{O}W)	SOC (g kg^{-1})	Moisture (g kg^{-1})	pH (1:1)	EC (dS m^{-1}) (1:1)	K^{+} (mg kg^{-1})	Ca^{2+} (mg kg^{-1})	Mg^{2+} (mg kg^{-1})
1	45.0768865	-96.4362314	3.2	23.5	0.9	5.4	335	2440	499
2	45.0758906	-96.4364095	2.6	15.6	0.4	5.3	216	1680	370
3	45.0758857	-96.4383055	2.3	15.9	0.7	7.5	213	4280	347
4	45.0759825	-96.4402876	2.4	16.0	0.9	6.9	366	4170	391
5	45.0774180	-96.4402832	2.5	16.2	0.9	7.4	241	3260	441
6	45.0771265	-96.4422473	2.2	12.0	0.4	5.1	230	1800	389
7	45.0771957	-96.4439341	2.6	13.6	0.4	5.3	185	1950	448
8	45.0770702	-96.4455203	3.1	16.3	1.0	6.3	998	2530	446
9	45.0774757	-96.4487111	2.9	16.9	0.9	5.8	239	2610	435
10	45.0764312	-96.4482571	2.6	15.0	0.5	5.5	184	2100	392
11	45.0760938	-96.4461640	2.4	15.8	0.8	7.2	280	3520	433
12	45.0760722	-96.4442455	2.0	13.2	0.4	5.4	166	1700	366
13	45.0760254	-96.4422684	2.5	13.6	0.4	5.1	257	1820	383
14	45.0745309	-96.4403463	2.1	12.5	0.8	7.2	189	3180	417
15	45.0745025	-96.4383209	2.8	16.1	0.5	5.8	336	2620	595
16	45.0745160	-96.4364722	2.5	15.4	0.8	7.0	874	2720	409
17	45.0732658	-96.4365536	2.8	15.0	0.7	7.1	553	3870	370
18	45.0731716	-96.4384935	1.4	8.7	0.9	7.5	211	2690	295
19	45.0731979	-96.4404375	2.7	16.2	0.4	5.6	208	2100	389
20	45.0731901	-96.4424481	2.2	13.9	0.7	6.8	197	3250	501
21	45.0746446	-96.4423459	2.3	13.2	0.5	6.1	165	2470	419
22	45.0746846	-96.4442935	1.7	12.3	1.0	7.5	182	4230	304
23	45.0733040	-96.4443572	2.5	15.1	0.4	5.2	351	1890	409
24	45.0747104	-96.4462512	2.5	15.0	0.4	5.4	233	2160	472
25	45.0733217	-96.4463004	2.7	16.2	0.3	5.4	237	2100	468

EC = Electrical Conductivity, SOC= Soil Organic Carbon. Soils from 0-15cm depth.

Table A.5 Continued

Sample No	Latitude (^{O}N)	Longitude (^{O}W)	SOC (g kg^{-1})	Moisture (g kg^{-1})	pH (1:1)	EC (dS m^{-1}) (1:1)	K^{+} (mg kg^{-1})	Ca^{2+} (mg kg^{-1})	Mg^{2+} (mg kg^{-1})
26	45.0719406	-96.4463698	2.5	14.8	5.5	0.4	336	1940	490
27	45.0719065	-96.4444189	2.0	13.4	7.3	0.8	165	3940	403
28	45.0718627	-96.4424870	2.8	15.3	6.4	0.9	211	2550	373
29	45.0717867	-96.4405900	1.9	12.8	7.3	0.9	148	4080	383
30	45.0717768	-96.4385603	1.8	12.7	7.0	0.8	172	2710	392
31	45.0706961	-96.4369017	1.9	11.5	5.8	0.9	192	1720	358
32	45.0703982	-96.4386233	2.1	11.8	5.2	0.4	218	1660	390
33	45.0704304	-96.4405649	2.0	13.0	6.0	0.5	167	1920	441
34	45.0704920	-96.4425195	2.2	13.7	5.5	0.5	201	1740	487
35	45.0705178	-96.4444782	2.5	15.0	5.2	0.4	214	1970	453
36	45.0705538	-96.4464279	2.7	16.0	5.5	0.9	252	2080	554
37	45.0691506	-96.4464765	2.1	15.3	6.7	0.8	389	2520	615
38	45.0692235	-96.4484432	2.7	15.5	6.6	0.9	247	3290	578
39	45.0692628	-96.4504036	2.3	12.2	5.9	0.9	219	2100	432
40	45.0678721	-96.4502198	2.9	16.5	7.0	0.9	208	4430	646
41	45.0678494	-96.4485233	2.7	17.4	6.5	0.9	247	2640	809
42	45.0681561	-96.4466793	2.7	18.4	7.0	0.9	291	3240	631

EC = Electrical Conductivity, SOC= Soil Organic Carbon. Soils from 0-15cm depth.

Table A.5 Continued

Sample No	Latitude (^{O}N)	Longitude (^{O}W)	Na^{+} (mg kg^{-1})	SOEC ($cmol_c$ kg^{-1})	NH_4^{+}-N (mg kg^{-1})	NO_3^{-}-N (mg kg^{-1})	PO_4^{-3} (mg kg^{-1})	Sand (g kg^{-1})	Clay (g kg^{-1})	Silt (g kg^{-1})
1	45.0768865	-96.4362314	35	45	34	99	17	34.70	36.89	28.42
2	45.0758906	-96.4364095	32	60	21	92	12	44.65	31.77	23.58
3	45.0758857	-96.4383055	27	33	53	37	25	47.04	35.80	17.16
4	45.0759825	-96.4402876	25	36	41	67	25	44.55	31.82	23.63
5	45.0774180	-96.4402832	15	44	84	76	21	53.20	25.25	21.54
6	45.0771265	-96.4422473	21	54	19	96	13	52.91	27.38	19.71
7	45.0771957	-96.4439341	14	59	25	78	14	45.02	29.05	25.94
8	45.0770702	-96.4455203	16	54	50	358	19	43.30	32.56	24.14
9	45.0774757	-96.4487111	17	44	31	81	17	41.56	30.14	28.31
10	45.0764312	-96.4482571	22	43	31	58	14	54.97	27.46	17.58
11	45.0760938	-96.4461640	16	36	41	32	22	46.95	33.85	19.21
12	45.0760722	-96.4442455	22	43	20	69	12	54.50	27.93	17.57
13	45.0760254	-96.4422684	45	61	22	84	13	44.73	27.42	27.85
14	45.0745309	-96.4403463	21	45	45	66	20	60.07	24.60	15.33
15	45.0745025	-96.4383209	20	62	25	61	19	39.71	34.14	26.15
16	45.0745160	-96.4364722	17	26	35	180	19	46.51	31.97	21.53
17	45.0732658	-96.4365536	16	31	42	92	24	42.38	31.50	26.12
18	45.0731716	-96.4384935	14	31	28	35	17	68.04	21.07	10.89
19	45.0731979	-96.4404375	16	52	28	81	14	46.40	29.53	24.07
20	45.0731901	-96.4424481	16	43	18	43	21	42.94	33.34	23.72
21	45.0746446	-96.4423459	25	38	22	54	16	53.16	29.27	17.56
22	45.0746846	-96.4442935	23	34	28	31	24	59.89	26.96	13.15
23	45.0733040	-96.4443572	20	58	20	116	14	39.90	31.97	28.13
24	45.0747104	-96.4462512	28	50	23	46	16	40.06	34.21	25.72
25	45.0733217	-96.4463004	29	26	19	37	15	33.26	33.94	32.80

SOEC = Sum of Extractable Cation, Soils from 0-15cm depth.

Table A.5 Continued

Sample No	Latitude (^{O}N)	Longitude (^{O}W)	Na^{+} (mg kg^{-1})	SOEC ($cmol_c$ kg^{-1})	NH_4^{+}-N (mg kg^{-1})	NO_3^{-}-N (mg kg^{-1})	PO_4^{-3} (mg kg^{-1})	Sand (g kg^{-1})	Clay (g kg^{-1})	Silt (g kg^{-1})
26	45.0719406	-96.4463698	22	59	21	47	15	41.97	32.09	25.93
27	45.0719065	-96.4444189	20	40	27	28	24	40.22	30.23	29.56
28	45.0718627	-96.4424870	22	41	27	55	17	41.49	34.95	23.57
29	45.0717867	-96.4405900	33	28	31	34	24	45.12	29.90	24.98
30	45.0717768	-96.4385603	19	51	34	51	17	55.37	27.87	16.76
31	45.0706961	-96.4369017	20	70	31	73	12	58.59	24.38	17.03
32	45.0703982	-96.4386233	26	63	14	87	12	51.75	28.79	19.46
33	45.0704304	-96.4405649	21	43	26	47	14	54.58	25.03	20.39
34	45.0704920	-96.4425195	26	65	25	41	13	41.28	33.17	25.56
35	45.0705178	-96.4444782	29	42	23	62	14	32.94	33.09	33.97
36	45.0705538	-96.4464279	23	69	24	57	16	35.02	37.21	27.77
37	45.0691506	-96.4464765	30	48	21	30	19	41.98	38.73	19.29
38	45.0692235	-96.4484432	28	44	23	33	22	34.90	35.21	29.88
39	45.0692628	-96.4504036	37	53	25	62	15	51.81	28.65	19.54
40	45.0678721	-96.4502198	23	51	44	1	28	34.51	38.20	27.29
41	45.0678494	-96.4485233	27	57	32	68	21	33.86	40.76	25.38
42	45.0681561	-96.4466793	24	35	47	79	22	30.26	42.46	27.28

SOEC = Sum of Extractable Cation, Soils from 0-15cm depth.

Table A.6 Field E (Lac qui Parle County, MN) soil test data set

Sample No	Latitude (^{O}N)	Longitude (^{O}W)	SOC (g kg^{-1})	Moisture (g kg^{-1})	pH (1:1)	EC (dS m^{-1}) (1:1)	K^{+} (mg kg^{-1})	Ca^{2+} (mg kg^{-1})	Mg^{2+} (mg kg^{-1})
1	45.0943806	-96.4513185	3.1	27.8	8.0	1.0	198	4900	845
2	45.0929747	-96.4513923	3.4	27.8	7.8	0.9	263	6120	565
3	45.0915799	-96.4514550	2.6	23.0	6.0	0.3	188	2440	473
4	45.0901786	-96.4515281	2.4	20.2	6.8	1.0	185	3260	421
5	45.0887707	-96.4515790	3.3	30.9	7.7	0.9	258	5360	1188
6	45.0889359	-96.4495657	3.6	30.6	7.8	1.0	336	5540	1010
7	45.0901325	-96.4495335	2.9	22.5	7.0	0.9	279	4140	686
8	45.0915302	-96.4494752	3.3	26.8	7.8	0.9	259	5550	459
9	45.0929397	-96.4494075	4.4	35.0	7.7	1.0	269	5780	854
10	45.0943300	-96.4493448	2.8	26.5	7.8	0.9	197	5390	650
11	45.0942824	-96.4473747	2.2	18.1	7.6	0.5	222	3560	423
12	45.0928912	-96.4474360	3.1	27.5	7.0	1.0	397	4020	895
13	45.0914956	-96.4474954	3.4	18.1	7.3	1.0	200	4810	598
14	45.0900797	-96.4475597	2.8	23.2	5.2	0.9	527	2090	405
15	45.0887645	-96.4475490	2.4	16.0	5.0	0.4	270	1800	405
16	45.0888396	-96.4456319	2.2	21.6	7.6	0.4	134	4490	478
17	45.0900333	-96.4455679	3.2	28.3	7.8	0.9	278	5730	723

EC = Electrical Conductivity, SOC= Soil Organic Carbon, Soils from 0-15cm depth.

Table A.6 Continued

Sample No	Latitude (^{O}N)	Longitude (^{O}W)	SOC (g kg^{-1})	Moisture (g kg^{-1})	pH (1:1)	EC (dS m^{-1}) (1:1)	K^{+} (mg kg^{-1})	Ca^{2+} (mg kg^{-1})	Mg^{2+} (mg kg^{-1})
18	45.0914428	-96.4455129	3.4	29.1	7.8	0.9	463	5710	821
19	45.0928519	-96.4454535	3.2	27.3	7.4	1.0	308	4560	665
20	45.0945058	-96.4453727	1.9	17.0	6.1	0.4	283	2450	446
21	45.0944088	-96.4434982	2.5	22.5	5.9	0.3	158	2180	428
22	45.0930105	-96.4434506	2.2	18.4	6.0	0.4	217	2320	443
23	45.0914038	-96.4435331	2.1	16.7	6.8	1.0	328	2560	395
24	45.0899940	-96.4435857	2.7	22.1	6.3	0.4	348	2800	514
25	45.0889262	-96.4437037	2.1	17.5	7.0	0.4	205	2790	516
26	45.0886864	-96.4412690	1.8	16.3	5.2	0.4	319	1440	332
27	45.0899627	-96.4414004	2.4	16.1	5.2	0.4	309	1590	319
28	45.0929605	-96.4416428	1.8	14.2	6.9	0.5	207	2590	433
29	45.0903772	-96.4357051	2.9	18.9	5.7	0.5	334	2730	531
30	45.0889570	-96.4357631	2.6	20.3	7.7	0.7	171	4920	714
31	45.0889662	-96.4376383	2.5	22.2	7.0	0.7	180	2970	764
32	45.0887612	-96.4394635	1.8	17.2	6.6	0.5	194	2160	440
33	45.0899445	-96.4393686	2.6	21.0	5.7	0.3	417	2140	414
34	45.0902827	-96.4377227	3.0	22.8	6.3	0.4	327	2970	724

EC = Electrical Conductivity, SOC= Soil Organic Carbon. Soils from 0-15cm depth.

Table A.6 Continued

Sample No	Latitude (^{O}N)	Longitude (^{O}W)	Na+ (mg kg^{-1})	SOEC (cmolc kg^{-1})	NH_4^+-N (mg kg^{-1})	NO_3^--N (mg kg^{-1})	PO_4^{3-} (mg kg^{-1})	Sand (g kg^{-1})	Clay (g kg^{-1})	Silt (g kg^{-1})
1	45.0943806	-96.4513185	28	32	7	11	0.5	39.43	35.19	25.38
2	45.0929747	-96.4513923	31	36	7	13	0.5	34.09	48.61	17.30
3	45.0915799	-96.4514550	33	17	8	10	35.3	41.88	28.36	29.76
4	45.0901786	-96.4515281	29	20	9	11	30.5	42.69	29.29	28.02
5	45.0887707	-96.4515790	37	38	10	9	33.2	24.37	41.26	34.37
6	45.0889359	-96.4495657	40	37	9	14	1.2	25.87	42.28	31.85
7	45.0901325	-96.4495335	30	27	11	15	46.0	40.48	31.90	27.63
8	45.0915302	-96.4494752	18	32	9	18	0.6	39.98	31.07	28.95
9	45.0929397	-96.4494075	48	37	11	14	0.7	26.87	40.92	32.21
10	45.0943300	-96.4493448	28	33	9	11	0.4	39.67	34.59	25.74
11	45.0942824	-96.4473747	31	22	7	15	37.5	53.99	24.84	21.17
12	45.0928912	-96.4474360	21	29	10	10	45.5	47.19	41.36	11.45
13	45.0914956	-96.4474954	19	30	11	17	33.0	42.11	32.42	25.47
14	45.0900797	-96.4475597	25	15	11	30	101.2	43.37	26.55	30.08
15	45.0887645	-96.4475490	27	13	9	22	58.2	48.54	25.81	25.65
16	45.0888396	-96.4456319	28	27	8	10	29.5	45.56	27.12	27.32
17	45.0900333	-96.4455679	79	36	9	13	0.5	33.18	36.79	30.03

SOEC = Sum of Extractable Cation, Soils from 0-15cm depth.

Table A.6 Continued

Sample No	Latitude (^{O}N)	Longitude (^{O}W)	Na^{+} (mg kg^{-1})	SOEC ($cmol_c$ kg^{-1})	NH_4^{+}-N (mg kg^{-1})	NO_3^{-}-N (mg kg^{-1})	PO_4^{-3} (mg kg^{-1})	Sand (g kg^{-1})	Clay (g kg^{-1})	Silt (g kg^{-1})
18	45.0914428	-96.4455129	31	37	9	12	1	32.91	36.85	30.24
19	45.0928519	-96.4454535	40	29	10	14	26	41.98	32.26	25.76
20	45.0945058	-96.4453727	28	17	11	15	72	50.77	25.93	23.30
21	45.0944088	-96.4434982	37	15	23	19	25	50.75	23.44	25.81
22	45.0930105	-96.4434506	25	16	25	19	8	57.42	21.52	21.06
23	45.0914038	-96.4435331	22	17	28	31	60	56.06	22.92	21.02
24	45.0899940	-96.4435857	24	19	12	8	41	35.15	32.70	32.15
25	45.0889262	-96.4437037	21	19	8	13	55	55.33	23.42	21.25
26	45.0886864	-96.4412690	27	11	40	15	72	55.25	23.64	21.11
27	45.0899627	-96.4414004	24	12	43	21	57	52.63	23.92	23.45
28	45.0929605	-96.4416428	22	17	23	26	42	63.84	19.19	16.97
29	45.0903772	-96.4357051	28	19	30	21	76	41.98	29.81	28.21
30	45.0889570	-96.4357631	38	31	5	36	24	51.19	27.41	21.40
31	45.0889662	-96.4376383	38	22	22	26	25	50.75	27.40	21.85
32	45.0887612	-96.4394635	39	15	23	23	24	63.71	19.15	17.14
33	45.0899445	-96.4393686	25	15	26	26	82	53.64	23.11	23.25
34	45.0902827	-96.4377227	38	22	24	26	43	46.40	28.12	25.48

SOEC = Sum of Extractable Cation, Soils from 0-15cm depth.

Appendix B

Table B.1 The complete Pearson correlation matrix for Landsat 8 data (n= 150)

Parameters	BSI	Band 4	Band 5	MSAVI2	NDVI	Band 7	Band 6	Band 2	Band 3	BI
BSI	1									
Band 4	**0.95**	1								
Band 5	**0.95**	**0.93**	1							
MSAVI2	**0.72**	**0.61**	**0.86**	1						
NDVI	0.18	0.00	**0.36**	**0.78**	1					
Band 7	**0.68**	**0.73**	**0.76**	**0.61**	0.19	1				
Band 6	**0.79**	**0.79**	**0.89**	**0.82**	**0.42**	**0.94**	1			
Band 2	**0.80**	**0.92**	**0.75**	**0.33**	**-0.29**	**0.63**	**0.62**	1		
Band 3	**0.92**	**0.98**	**0.87**	**0.50**	-0.12	**0.67**	**0.71**	**0.97**	1	
BI	**0.94**	1.00	**0.91**	**0.57**	-0.05	**0.71**	**0.76**	**0.94**	**0.99**	1

See Tables 2.8 and 2.10 for Landsat 8 bands and indices descriptions. All values in **bold print** are significant ($P<0.05$).

Table B.2 Field A (Brookings County, SD) Landsat 8 single bands and remote sensing indices data set

Sample No	Latitude (^{O}N)	Longitude (^{O}W)	Band 2 µm	Band 3 µm	Band 4 µm	Band 5 µm	Band 6 µm	Band 7 µm	BSI	MSAVI2	NDVI	BI
1	44.3849033	-96.9461351	0.10445	0.09320	0.10571	0.16984	0.28971	0.25253	97.62	0.10378	0.23	0.07047
2	44.3849738	-96.9442170	0.10251	0.08647	0.09304	0.14838	0.27666	0.24632	96.27	0.09186	0.23	0.06351
3	44.3863216	-96.9443015	0.10935	0.09459	0.10272	0.15713	0.28223	0.25122	96.82	0.08879	0.21	0.06982
4	44.3877266	-96.9442422	0.10149	0.08844	0.09877	0.16190	0.29519	0.26284	97.10	0.10347	0.24	0.06629
5	44.3880766	-96.9462404	0.09975	0.08626	0.09447	0.16456	0.26111	0.21928	96.97	0.11551	0.27	0.06396
6	44.3894226	-96.9462689	0.10258	0.08732	0.09326	0.14617	0.26502	0.23491	96.45	0.08785	0.22	0.06388
7	44.3893326	-96.9443454	0.10156	0.08738	0.09730	0.15735	0.28730	0.25253	96.81	0.09878	0.24	0.06539
8	44.3905456	-96.9462595	0.10278	0.08774	0.09497	0.14779	0.26610	0.23414	96.53	0.08745	0.22	0.06465
9	44.3905477	-96.9442898	0.10347	0.09017	0.10054	0.16296	0.29108	0.25386	97.09	0.10201	0.24	0.06752
10	44.3905362	-96.9426315	0.10388	0.08732	0.09270	0.14079	0.26049	0.23254	96.10	0.08004	0.21	0.06368
11	44.3892037	-96.9424045	0.10089	0.08481	0.09162	0.14472	0.27184	0.24033	96.19	0.08842	0.22	0.06242
12	44.3877270	-96.9423955	0.10220	0.09088	0.10405	0.17026	0.29854	0.26126	97.58	0.10738	0.24	0.06907
13	44.3863649	-96.9422821	0.10083	0.08501	0.09073	0.14254	0.26463	0.23549	96.23	0.08644	0.22	0.06217
14	44.3849364	-96.9422305	0.10445	0.08952	0.09686	0.15072	0.27655	0.24580	96.62	0.08884	0.22	0.06595
15	44.3849395	-96.9404207	0.10490	0.09435	0.10848	0.17446	0.30137	0.26448	97.81	0.10619	0.23	0.07188
16	44.3864433	-96.9405058	0.10336	0.08836	0.09667	0.15694	0.29154	0.25737	96.63	0.09923	0.24	0.06549
17	44.3877366	-96.9406607	0.10349	0.09067	0.10147	0.16452	0.29341	0.25721	97.21	0.10284	0.24	0.06804
18	44.3892959	-96.9407110	0.10657	0.09098	0.09730	0.14894	0.26334	0.23235	96.49	0.08517	0.21	0.06660
19	44.3905324	-96.9407824	0.10170	0.08670	0.09414	0.14902	0.27527	0.24162	96.52	0.09093	0.23	0.06399
20	44.3905420	-96.9386300	0.10370	0.08684	0.09256	0.13998	0.25837	0.23042	96.02	0.07897	0.20	0.06346
21	44.3893405	-96.9385052	0.10285	0.08643	0.09112	0.13871	0.25721	0.23063	96.08	0.07945	0.21	0.06280
22	44.3877992	-96.9387336	0.10480	0.09270	0.10613	0.17924	0.31789	0.27587	97.50	0.11786	0.26	0.07046
23	44.3864869	-96.9386987	0.10299	0.08695	0.09418	0.14977	0.28113	0.25072	96.30	0.09208	0.23	0.06409
24	44.3849026	-96.9387805	0.10312	0.08797	0.09570	0.15004	0.27828	0.24601	96.53	0.08980	0.22	0.06499

See Tables 2.8 and 2.10 for Landsat 8 bands and indices descriptions.

Table B.3 Field B (Brookings County, SD) Landsat 8 single bands and remote sensing indices data set

Sample No	Latitude (^{O}N)	Longitude (^{O}W)	Band 2 µm	Band 3 µm	Band 4 µm	Band 5 µm	Band 6 µm	Band 7 µm	BSI	MSAVI2	NDVI	BI
1	44.4629807	-96.8467720	0.09979	0.08486	0.09370	0.15528	0.27626	0.24025	96.57	0.10189	0.25	0.06321
2	44.4630070	-96.8448609	0.09793	0.08220	0.08747	0.14220	0.27176	0.23880	96.02	0.09179	0.24	0.06002
3	44.4629894	-96.8428560	0.09861	0.08415	0.08851	0.15447	0.30666	0.24389	96.12	0.11003	0.29	0.06106
4	44.4628501	-96.8409707	0.09411	0.07554	0.07647	0.12267	0.24177	0.21311	94.80	0.07923	0.23	0.05375
5	44.4628333	-96.8389601	0.09634	0.07898	0.08562	0.14023	0.26116	0.22942	95.66	0.09190	0.24	0.05824
6	44.4613164	-96.8388696	0.09395	0.07532	0.08109	0.13414	0.26399	0.23163	95.22	0.09006	0.25	0.05534
7	44.4614810	-96.8409738	0.09323	0.07339	0.07427	0.11600	0.22668	0.20423	94.34	0.07194	0.22	0.05221
8	44.4615306	-96.8428734	0.09813	0.08288	0.09011	0.15303	0.29117	0.23885	96.17	0.10476	0.27	0.06121
9	44.4617706	-96.8447335	0.09821	0.08279	0.09472	0.16141	0.28775	0.25359	96.72	0.10997	0.25	0.06290
10	44.4617408	-96.8467150	0.09976	0.08514	0.09214	0.15386	0.29242	0.25556	96.40	0.10241	0.26	0.06273
11	44.4603363	-96.8466976	0.09598	0.07941	0.08952	0.15176	0.26058	0.21769	96.31	0.10375	0.26	0.05983
12	44.4603057	-96.8444288	0.09790	0.08223	0.09185	0.16573	0.28907	0.23866	96.53	0.12218	0.27	0.06164
13	44.4598756	-96.8431769	0.09623	0.07869	0.08682	0.16712	0.29127	0.21929	95.91	0.13378	0.31	0.05859
14	44.4597715	-96.8409587	0.09604	0.07974	0.08703	0.15999	0.29467	0.24879	96.32	0.12179	0.28	0.05902
15	44.4594313	-96.8393745	0.09516	0.07717	0.08113	0.13206	0.25947	0.22749	95.23	0.08650	0.24	0.05599
16	44.4587020	-96.8390945	0.09503	0.07827	0.08589	0.14561	0.26122	0.21973	96.01	0.10030	0.26	0.05810
17	44.4587136	-96.8410623	0.09591	0.07824	0.08333	0.13767	0.26063	0.22739	95.55	0.09183	0.24	0.05715
18	44.4587878	-96.8430260	0.09334	0.07587	0.08075	0.14659	0.27485	0.21161	95.49	0.11142	0.30	0.05540
19	44.4588545	-96.8449193	0.09546	0.07886	0.08371	0.14861	0.26986	0.22544	95.80	0.10926	0.27	0.05750
20	44.4588720	-96.8467019	0.09634	0.07965	0.08551	0.13732	0.24878	0.21471	95.83	0.08726	0.23	0.05843
21	44.4573421	-96.8391653	0.09653	0.07957	0.08749	0.14489	0.26097	0.22669	95.95	0.09618	0.24	0.05913
22	44.4573916	-96.8411028	0.09731	0.08081	0.08979	0.14869	0.26161	0.22758	96.21	0.09822	0.24	0.06040
23	44.4574460	-96.8429200	0.09537	0.07940	0.08585	0.14626	0.26633	0.21948	96.12	0.10144	0.26	0.05847
24	44.4574153	-96.8448636	0.09678	0.08107	0.08815	0.14574	0.26314	0.22161	96.21	0.09637	0.25	0.05988
25	44.4575522	-96.8467046	0.09727	0.08064	0.08632	0.13751	0.25169	0.22019	95.86	0.08610	0.23	0.05907

See Tables 2.8 and 2.10 for Landsat 8 bands and indices descriptions.

Table B.4 Field C (Brookings County, SD) Landsat 8 single bands and remote sensing indices data set

Sample No	Latitude (^{O}N)	Longitude (^{O}W)	Band 2 µm	Band 3 µm	Band 4 µm	Band 5 µm	Band 6 µm	Band 7 µm	BSI	MSAVI2	NDVI	BI
1	44.4286008	-96.8672630	0.10623	0.09312	0.10457	0.17275	0.31560	0.29322	97.25	0.110408	0.25	0.07001
2	44.4299830	-96.8671877	0.10850	0.09730	0.10972	0.18237	0.32462	0.29382	97.75	0.116394	0.25	0.07332
3	44.4314178	-96.8671488	0.10711	0.09721	0.10868	0.18177	0.31036	0.27356	98.00	0.117290	0.25	0.07291
4	44.4328201	-96.8670861	0.10659	0.09584	0.10725	0.18219	0.30820	0.26739	97.82	0.120487	0.26	0.07192
5	44.4342010	-96.8670197	0.10937	0.09883	0.11074	0.18483	0.31294	0.27248	97.91	0.118418	0.25	0.07422
6	44.4341373	-96.8651006	0.11008	0.09981	0.11232	0.18657	0.32905	0.29630	97.98	0.118347	0.25	0.07513
7	44.4327896	-96.8651324	0.11072	0.10027	0.11409	0.19189	0.33439	0.29829	97.98	0.123467	0.25	0.07594
8	44.4315933	-96.8649219	0.11403	0.10376	0.12213	0.20667	0.35579	0.32414	98.12	0.131946	0.26	0.08013
9	44.4299906	-96.8651800	0.11465	0.10769	0.12575	0.21041	0.35727	0.32335	98.75	0.131309	0.25	0.08278
10	44.4285866	-96.8652243	0.11016	0.09736	0.10910	0.18225	0.32718	0.29962	97.43	0.117301	0.25	0.07311
11	44.4285134	-96.8636093	0.10176	0.08797	0.09466	0.15767	0.28077	0.24299	96.88	0.104034	0.25	0.06461
12	44.4299351	-96.8635234	0.11122	0.09890	0.11415	0.19347	0.34883	0.32115	97.62	0.125791	0.26	0.07552
13	44.4314315	-96.8634919	0.11544	0.10985	0.12909	0.21238	0.36346	0.32998	99.01	0.128509	0.24	0.08475
14	44.4327920	-96.8634859	0.10960	0.10152	0.11854	0.19767	0.34638	0.30671	98.47	0.124542	0.25	0.07803
15	44.4341988	-96.8635278	0.10224	0.09025	0.09798	0.16581	0.30342	0.26284	97.37	0.111152	0.26	0.06661
16	44.4341861	-96.8616905	0.11600	0.10883	0.12959	0.21639	0.35276	0.31703	98.74	0.133628	0.25	0.08461
17	44.4342965	-96.8589566	0.12045	0.11340	0.13452	0.21032	0.32747	0.26564	98.78	0.116235	0.22	0.08797
18	44.4330571	-96.8594005	0.11031	0.10029	0.11644	0.19958	0.34465	0.30509	98.10	0.131141	0.26	0.07684
19	44.4312102	-96.8589493	0.10731	0.09879	0.11309	0.19628	0.32574	0.27807	98.35	0.131982	0.27	0.07508
20	44.4312967	-96.8612596	0.10981	0.09844	0.11427	0.19274	0.32946	0.29091	97.79	0.124452	0.26	0.07541
21	44.4321796	-96.8621143	0.12038	0.11378	0.13616	0.21531	0.33765	0.27645	98.87	0.120870	0.23	0.08872
22	44.4305035	-96.8624173	0.10586	0.09466	0.10596	0.17693	0.30162	0.25841	97.68	0.114524	0.25	0.07104
23	44.4298767	-96.8611440	0.10987	0.10143	0.11764	0.19840	0.33831	0.30141	98.40	0.127215	0.26	0.07767
24	44.4293013	-96.8592668	0.09472	0.07992	0.08123	0.13327	0.21936	0.17365	96.20	0.088330	0.24	0.05698
25	44.4287346	-96.8625206	0.09189	0.07500	0.07406	0.11671	0.22315	0.18331	95.28	0.073529	0.22	0.05270

See Tables 2.8 and 2.10 for Landsat 8 bands and indices descriptions.

Table B.5 Field D (Lac qui Parle County, MN) Landsat 8 single bands and remote sensing indices data set

Sample No	Latitude (^{O}N)	Longitude (^{O}W)	Band 2 µm	Band 3 µm	Band 4 µm	Band 5 µm	Band 6 µm	Band 7 µm	BSI	MSAVI2	NDVI	BI
1	45.0768865	-96.4362314	0.10035	0.08263	0.08834	0.13734	0.26970	0.24403	95.66	0.08218	0.22	0.06048
2	45.0758906	-96.4364095	0.10266	0.08676	0.09630	0.15544	0.29652	0.26581	96.40	0.09748	0.23	0.06481
3	45.0758857	-96.4383055	0.11145	0.09813	0.10677	0.15995	0.27842	0.24815	97.20	0.08621	0.20	0.07251
4	45.0759825	-96.4402876	0.10031	0.08373	0.08547	0.14609	0.24864	0.20812	96.01	0.10185	0.26	0.05982
5	45.0774180	-96.4402832	0.10584	0.09011	0.09601	0.14283	0.26961	0.24869	96.38	0.07751	0.20	0.06583
6	45.0771265	-96.4422473	0.10594	0.09299	0.10426	0.16461	0.29945	0.26525	97.23	0.09803	0.22	0.06985
7	45.0771957	-96.4439341	0.10519	0.09148	0.10154	0.16109	0.29465	0.26375	97.01	0.09724	0.23	0.06833
8	45.0770702	-96.4455203	0.10968	0.09971	0.11178	0.17868	0.19499	0.13751	98.00	0.10700	0.23	0.07489
9	45.0774757	-96.4487111	0.10058	0.08198	0.08564	0.13179	0.27094	0.25033	95.35	0.07785	0.21	0.05928
10	45.0764312	-96.4482571	0.10162	0.08312	0.08759	0.13576	0.27321	0.25280	95.47	0.08092	0.22	0.06038
11	45.0760938	-96.4461640	0.10509	0.08975	0.09717	0.14418	0.25829	0.23570	96.48	0.07765	0.19	0.06614
12	45.0760722	-96.4442455	0.10571	0.09368	0.10646	0.16980	0.30334	0.26963	97.47	0.10239	0.23	0.07090
13	45.0760254	-96.4422684	0.10721	0.09432	0.10754	0.17300	0.30344	0.26862	97.33	0.10554	0.23	0.07152
14	45.0745309	-96.4403463	0.10330	0.08955	0.09530	0.14459	0.27452	0.24902	96.82	0.08164	0.21	0.06538
15	45.0745025	-96.4383209	0.10349	0.08948	0.09755	0.15029	0.28054	0.25074	96.82	0.08691	0.21	0.06619
16	45.0745160	-96.4364722	0.10704	0.09304	0.10368	0.16012	0.28522	0.25791	96.98	0.09190	0.21	0.06965
17	45.0732658	-96.4365536	0.10355	0.08944	0.09836	0.15228	0.27508	0.24715	96.82	0.08871	0.22	0.06647
18	45.0731716	-96.4384935	0.11290	0.10482	0.11754	0.17379	0.29195	0.26280	98.41	0.08942	0.19	0.07874
19	45.0731979	-96.4404375	0.10580	0.09187	0.10278	0.16407	0.29526	0.26400	97.00	0.09978	0.23	0.06893
20	45.0731901	-96.4424481	0.11018	0.09958	0.11263	0.17435	0.29893	0.26093	97.87	0.09876	0.22	0.07517
21	45.0746446	-96.4423459	0.10711	0.09345	0.10509	0.16242	0.29014	0.25899	97.08	0.09309	0.21	0.07032
22	45.0746846	-96.4442935	0.11804	0.10825	0.12375	0.18427	0.29536	0.26153	98.17	0.09504	0.20	0.08221
23	45.0733040	-96.4443572	0.10455	0.09150	0.10347	0.16824	0.31117	0.27479	97.21	0.10522	0.24	0.06906
24	45.0747104	-96.4462512	0.10432	0.09046	0.10087	0.15868	0.29494	0.26190	96.95	0.09456	0.22	0.06775
25	45.0733217	-96.4463004	0.10280	0.08859	0.09798	0.15754	0.28865	0.25396	96.82	0.09786	0.23	0.06605

See Tables 2.8 and 2.10 for Landsat 8 bands and indices descriptions.

Table B.5 Continued

Sample No	Latitude (^{O}N)	Longitude (^{O}W)	Band 2 µm	Band 3 µm	Band 4 µm	Band 5 µm	Band 6 µm	Band 7 µm	BSI	MSAVI2	NDVI	BI
26	45.0719406	-96.4463698	0.10746	0.09599	0.10856	0.16860	0.29172	0.25708	97.61	0.09680	0.22	0.07245
27	45.0719065	-96.4444189	0.11299	0.10287	0.11664	0.17853	0.29501	0.25947	98.02	0.09833	0.21	0.07776
28	45.0718627	-96.4424870	0.10565	0.09289	0.10451	0.16425	0.29711	0.26244	97.27	0.09703	0.22	0.06991
29	45.0717867	-96.4405900	0.11631	0.11178	0.12776	0.18892	0.29530	0.25762	99.17	0.09538	0.19	0.08488
30	45.0717768	-96.4385603	0.11020	0.09908	0.11228	0.17444	0.29856	0.26431	97.76	0.09950	0.22	0.07487
31	45.0706961	-96.4369017	0.10908	0.09734	0.11218	0.18061	0.30835	0.27159	97.65	0.10933	0.23	0.07426
32	45.0703982	-96.4386233	0.10702	0.09661	0.11105	0.17635	0.30037	0.26327	97.88	0.10463	0.23	0.07360
33	45.0704304	-96.4405649	0.10819	0.09682	0.11020	0.17838	0.30928	0.27167	97.70	0.10931	0.24	0.07335
34	45.0704920	-96.4425195	0.10569	0.09237	0.10469	0.16579	0.28746	0.25008	97.16	0.09915	0.23	0.06981
35	45.0705178	-96.4444782	0.10634	0.09410	0.10733	0.17753	0.31136	0.27236	97.48	0.11304	0.25	0.07137
36	45.0705538	-96.4464279	0.10499	0.09227	0.10278	0.16001	0.28954	0.25392	97.24	0.09331	0.22	0.06906
37	45.0691506	-96.4464765	0.10754	0.09628	0.10640	0.16101	0.27425	0.24154	97.61	0.08855	0.20	0.07175
38	45.0692235	-96.4484432	0.10607	0.09146	0.10127	0.15465	0.27793	0.24655	96.78	0.08738	0.21	0.06823
39	45.0692628	-96.4504036	0.10659	0.09262	0.10393	0.16332	0.29326	0.26024	97.01	0.09657	0.22	0.06960
40	45.0678721	-96.4502198	0.11317	0.10497	0.11330	0.17061	0.27057	0.22988	98.37	0.09174	0.20	0.07722
41	45.0678494	-96.4485233	0.10235	0.08537	0.09019	0.13759	0.25581	0.22601	95.91	0.07927	0.21	0.06209
42	45.0681561	-96.4466793	0.10499	0.08603	0.08998	0.13391	0.25076	0.22907	95.43	0.07357	0.20	0.06225

See Tables 2.8 and 2.10 for Landsat 8 bands and indices descriptions.

Table B.6 Field E (Lac qui Parle County, MN) Landsat 8 single bands and remote sensing indices data set

Sample No	Latitude (^{O}N)	Longitude (^{O}W)	Band 2 µm	Band 3 µm	Band 4 µm	Band 5 µm	Band 6 µm	Band 7 µm	NDVI	BSI	MSAVI2	BI
1	45.0943806	-96.4513185	0.10945	0.08801	0.0926	0.13211	0.24831	0.23248	0.18	94.92	0.06594	0.06387
2	45.0929747	-96.4513923	0.10565	0.08876	0.09466	0.14262	0.26598	0.24397	0.20	96.09	0.07956	0.06488
3	45.0915799	-96.4514550	0.10802	0.09620	0.10966	0.17414	0.31070	0.28034	0.23	97.58	0.10362	0.07294
4	45.0901786	-96.4515281	0.10804	0.09717	0.10979	0.17502	0.30627	0.27759	0.23	97.78	0.10477	0.07331
5	45.0887707	-96.4515790	0.10393	0.08491	0.08849	0.13092	0.25079	0.23167	0.19	95.34	0.07129	0.06132
6	45.0889359	-96.4495657	0.10602	0.08765	0.09131	0.13287	0.25401	0.24096	0.19	95.60	0.06949	0.06329
7	45.0901325	-96.4495335	0.10316	0.08757	0.09547	0.14902	0.29154	0.26995	0.22	96.42	0.08855	0.06477
8	45.0915302	-96.4494752	0.11222	0.09663	0.10359	0.15444	0.28455	0.26101	0.20	96.66	0.08296	0.07083
9	45.0929397	-96.4494075	0.10526	0.08610	0.08871	0.12277	0.22317	0.21650	0.16	95.24	0.05733	0.06181
10	45.0943300	-96.4493448	0.10974	0.09221	0.09780	0.14262	0.26523	0.24758	0.19	96.04	0.07402	0.06720
11	45.0942824	-96.4473747	0.10480	0.08817	0.09399	0.14104	0.27398	0.25893	0.20	96.12	0.07816	0.06444
12	45.0928912	-96.4474360	0.10517	0.08676	0.09052	0.12965	0.24145	0.23142	0.18	95.53	0.06556	0.06269
13	45.0914956	-96.4474954	0.10551	0.08869	0.09324	0.13715	0.25725	0.24002	0.19	96.04	0.07311	0.06434
14	45.0900797	-96.4475597	0.11459	0.10573	0.12342	0.19376	0.31631	0.26508	0.22	98.35	0.11014	0.08126
15	45.0887645	-96.4475490	0.11461	0.10578	0.12386	0.19439	0.31861	0.26862	0.22	98.36	0.11034	0.08144
16	45.0888396	-96.4456319	0.11540	0.10702	0.12055	0.18017	0.29542	0.25773	0.20	98.40	0.09417	0.08060
17	45.0900333	-96.4455679	0.10430	0.08593	0.08998	0.13319	0.26431	0.24779	0.19	95.56	0.07237	0.06221

See Tables 2.8 and 2.10 for Landsat 8 bands and indices descriptions.

Table B.6 Continued

Sample No	Latitude (^{O}N)	Longitude (^{O}W)	Band 2 µm	Band 3 µm	Band 4 µm	Band 5 µm	Band 6 µm	Band 7 µm	NDVI	BSI	MSAVI2	BI
18	45.0914428	-96.4455129	0.10804	0.08894	0.09291	0.13371	0.24798	0.23888	0.18	95.49	0.06802	0.06431
19	45.0928519	-96.4454535	0.10424	0.08541	0.08788	0.1262	0.24218	0.23534	0.18	95.34	0.06452	0.06127
20	45.0945058	-96.4453727	0.10841	0.09713	0.11062	0.17323	0.30762	0.2772	0.22	97.69	0.10051	0.07360
21	45.0944088	-96.4434982	0.09399	0.07629	0.08009	0.12859	0.25365	0.22722	0.23	95.33	0.08259	0.05530
22	45.0930105	-96.4434506	0.09969	0.08479	0.09395	0.14881	0.27595	0.24557	0.23	96.51	0.09093	0.06328
23	45.0914038	-96.4435331	0.09713	0.08186	0.08965	0.14489	0.28096	0.25899	0.24	96.31	0.09225	0.06070
24	45.0899940	-96.4435857	0.10790	0.09052	0.09804	0.15262	0.28782	0.26995	0.22	96.13	0.08980	0.06672
25	45.0889262	-96.4437037	0.10602	0.09160	0.10231	0.16234	0.30226	0.27518	0.23	96.88	0.09787	0.06866
26	45.0886864	-96.4412690	0.10301	0.09194	0.10896	0.18416	0.31828	0.27909	0.26	97.73	0.12054	0.07128
27	45.0899627	-96.4414004	0.09592	0.07938	0.08844	0.14939	0.2885	0.26174	0.26	96.00	0.10184	0.05942
28	45.0929605	-96.4416428	0.09420	0.07618	0.08071	0.12942	0.26271	0.23628	0.23	95.27	0.08284	0.05549
29	45.0903772	-96.4357051	0.09243	0.07128	0.07398	0.11723	0.23988	0.21903	0.23	94.04	0.07457	0.05137
30	45.0889570	-96.4357631	0.09241	0.07292	0.07516	0.11216	0.22365	0.20633	0.20	94.47	0.06375	0.05236
31	45.0889662	-96.4376383	0.09262	0.07155	0.07259	0.11097	0.22414	0.20621	0.21	93.94	0.06643	0.05096
32	45.0887612	-96.4394635	0.09580	0.07959	0.08564	0.13427	0.25667	0.23302	0.22	95.90	0.08196	0.05846
33	45.0899445	-96.4393686	0.09698	0.08092	0.08959	0.15191	0.29715	0.26768	0.26	96.17	0.10388	0.06036
34	45.0902827	-96.4377227	0.09223	0.07169	0.07365	0.11581	0.23568	0.21523	0.22	94.19	0.07277	0.05139

See Tables 2.8 and 2.10 for Landsat 8 bands and indices descriptions.

Appendix C

Table C.1 The complete Pearson correlation matrix for PlanetScope data (n= 150)

Parameters	MSAVI2	Band 4	Band 3	NDVI	BSI	Band 2	Band 1	BI
MSAVI2	1							
Band 4	**0.63**	1						
Band 3	**0.58**	**0.94**	1					
NDVI	**0.38**	**0.57**	**0.27**	1				
BSI	**0.30**	**0.69**	**0.63**	**0.46**	1			
Band 2	**0.58**	**0.91**	**0.96**	**0.27**	**0.66**	1		
Band 1	**0.57**	**0.86**	**0.95**	**0.19**	**0.60**	**0.98**	1	
BI	**0.59**	**0.93**	**0.99**	**0.27**	**0.65**	**0.99**	**0.97**	1

See Table 2.9 and 2.10 for PlanetScope bands and indices descriptions. All values in **bold print** are significant ($P<0.05$).

Table C.2 Field A (Brookings County, SD) PlanetScope single bands and remote sensing indices data set

Sample No	Latitude (^{O}N)	Longitude (^{O}W)	Band 1 µm	Band 2 µm	Band 3 µm	Band 4 µm	MSAVI2	NDVI	BSI	BI
1	44.3849033	-96.9461351	0.001135	0.001060	0.001071	0.001536	0.103778	0.18	98.86	0.000753
2	44.3849738	-96.9442170	0.001041	0.000933	0.000934	0.001239	0.091858	0.14	97.95	0.000660
3	44.3863216	-96.9443015	0.001140	0.001063	0.001026	0.001322	0.088790	0.13	98.26	0.000739
4	44.3877266	-96.9442422	0.001114	0.001054	0.001053	0.001481	0.103467	0.17	98.91	0.000745
5	44.3880766	-96.9462404	0.001068	0.000949	0.000939	0.001480	0.115513	0.22	98.37	0.000668
6	44.3894226	-96.9462689	0.001082	0.000983	0.000997	0.001357	0.087851	0.15	98.52	0.000700
7	44.3893326	-96.9443454	0.001088	0.000985	0.000963	0.001320	0.098784	0.16	98.52	0.000689
8	44.3905456	-96.9462595	0.001109	0.001020	0.001015	0.001342	0.087449	0.14	98.16	0.000720
9	44.3905477	-96.9442898	0.001131	0.001083	0.001077	0.001490	0.102010	0.16	98.79	0.000764
10	44.3905362	-96.9426315	0.001052	0.000937	0.000937	0.001203	0.080043	0.12	97.84	0.000663
11	44.3892037	-96.9424045	0.001097	0.001012	0.001013	0.001360	0.088417	0.15	98.89	0.000716
12	44.3877270	-96.9423955	0.001166	0.001135	0.001121	0.001567	0.107382	0.17	98.86	0.000797
13	44.3863649	-96.9422821	0.001086	0.001009	0.001009	0.001369	0.086444	0.15	98.18	0.000713
14	44.3849364	-96.9422305	0.001047	0.000947	0.000913	0.001266	0.088840	0.16	97.94	0.000658
15	44.3849395	-96.9404207	0.001138	0.001055	0.001026	0.001444	0.106185	0.17	98.74	0.000736
16	44.3864433	-96.9405058	0.001091	0.001007	0.001007	0.001340	0.099230	0.14	98.18	0.000712
17	44.3877366	-96.9406607	0.001120	0.001065	0.001066	0.001470	0.102836	0.16	98.97	0.000753
18	44.3892959	-96.9407110	0.001053	0.000939	0.000953	0.001245	0.085166	0.13	98.23	0.000669
19	44.3905324	-96.9407824	0.001116	0.001029	0.001028	0.001344	0.090932	0.13	98.69	0.000727
20	44.3905420	-96.9386300	0.001065	0.000974	0.000974	0.001194	0.078972	0.10	98.01	0.000689
21	44.3893405	-96.9385052	0.001061	0.000938	0.000939	0.001156	0.079448	0.10	98.07	0.000664
22	44.3877992	-96.9387336	0.001131	0.001089	0.001094	0.001509	0.117857	0.16	98.99	0.000772
23	44.3864869	-96.9386987	0.001165	0.001120	0.001120	0.001468	0.092076	0.13	99.20	0.000792
24	44.3849026	-96.9387805	0.001050	0.000930	0.000953	0.001227	0.089801	0.13	98.37	0.000666

See Table 2.9 and 2.10 for PlanetScope bands and indices descriptions.

Table C.3 Field B (Brookings County, SD) PlanetScope single bands and remote sensing indices data set

Sample No	Latitude (^{O}N)	Longitude (^{O}W)	Band 1 µm	Band 2 µm	Band 3 µm	Band 4 µm	MSAVI2	NDVI	BSI	BI
1	44.4629807	-96.8467720	0.001224	0.001181	0.001181	0.001649	0.101888	0.17	98.46	0.000835
2	44.4630070	-96.8448609	0.001157	0.001117	0.001107	0.001587	0.091793	0.18	98.53	0.000786
3	44.4629894	-96.8428560	0.001219	0.001197	0.001197	0.001864	0.110032	0.22	98.67	0.000847
4	44.4628501	-96.8409707	0.001216	0.001153	0.001153	0.001611	0.079231	0.17	98.78	0.000816
5	44.4628333	-96.8389601	0.001180	0.001143	0.001143	0.001575	0.091896	0.16	98.35	0.000808
6	44.4613164	-96.8388696	0.001174	0.001087	0.001097	0.001479	0.090057	0.15	98.18	0.000772
7	44.4614810	-96.8409738	0.001093	0.000993	0.001004	0.001288	0.071942	0.12	97.58	0.000706
8	44.4615306	-96.8428734	0.001216	0.001186	0.001186	0.001753	0.104761	0.19	98.72	0.000839
9	44.4617706	-96.8447335	0.001216	0.001178	0.001178	0.001638	0.109966	0.16	98.51	0.000833
10	44.4617408	-96.8467150	0.001191	0.001152	0.001152	0.001602	0.102412	0.16	98.51	0.000815
11	44.4603363	-96.8466976	0.001173	0.001124	0.001124	0.001550	0.103751	0.16	98.16	0.000795
12	44.4603057	-96.8444288	0.001187	0.001170	0.001170	0.001700	0.122183	0.18	98.30	0.000827
13	44.4598756	-96.8431769	0.001179	0.001113	0.001113	0.001597	0.133778	0.18	98.76	0.000787
14	44.4597715	-96.8409587	0.001174	0.001106	0.001105	0.001569	0.121786	0.17	98.70	0.000782
15	44.4594313	-96.8393745	0.001161	0.001093	0.001093	0.001479	0.086503	0.15	98.14	0.000773
16	44.4587020	-96.8390945	0.001099	0.001020	0.001020	0.001460	0.100299	0.18	98.42	0.000721
17	44.4587136	-96.8410623	0.001112	0.001029	0.001029	0.001425	0.091832	0.16	98.40	0.000727
18	44.4587878	-96.8430260	0.001146	0.001092	0.001063	0.001572	0.111417	0.19	98.77	0.000762
19	44.4588545	-96.8449193	0.001160	0.001113	0.001119	0.001539	0.109262	0.16	98.58	0.000789
20	44.4588720	-96.8467019	0.001115	0.001045	0.001045	0.001438	0.087263	0.16	98.14	0.000739
21	44.4573421	-96.8391653	0.001133	0.001056	0.001054	0.001436	0.096175	0.15	98.43	0.000746
22	44.4573916	-96.8411028	0.001151	0.001095	0.001095	0.001466	0.098225	0.14	97.91	0.000774
23	44.4574460	-96.8429200	0.001141	0.001065	0.001065	0.001417	0.101438	0.14	98.00	0.000753
24	44.4574153	-96.8448636	0.001150	0.001087	0.001087	0.001480	0.096366	0.15	98.36	0.000769
25	44.4575522	-96.8467046	0.001156	0.001095	0.001096	0.001485	0.086101	0.15	98.08	0.000774

See Table 2.9 and 2.10 for PlanetScope bands and indices descriptions.

Table C.4 Field C (Brookings County, SD) PlanetScope single bands and remote sensing indices data set

Sample No	Latitude (^{O}N)	Longitude (^{O}W)	Band 1 µm	Band 2 µm	Band 3 µm	Band 4 µm	MSAVI2	NDVI	BSI	BI
1	44.4286008	-96.8672630	0.001179	0.001179	0.001192	0.001596	0.110408	0.14	97.98	0.000838
2	44.4299830	-96.8671877	0.001209	0.001170	0.001171	0.001657	0.116394	0.17	98.81	0.000828
3	44.4314178	-96.8671488	0.001243	0.001206	0.001207	0.001810	0.117290	0.20	98.91	0.000853
4	44.4328201	-96.8670861	0.001342	0.001368	0.001368	0.001931	0.120487	0.17	98.97	0.000967
5	44.4342010	-96.8670197	0.001400	0.001426	0.001421	0.002058	0.118418	0.18	99.23	0.001007
6	44.4341373	-96.8651006	0.001257	0.001238	0.001248	0.001708	0.118347	0.16	98.67	0.000879
7	44.4327896	-96.8651324	0.001362	0.001375	0.001376	0.002040	0.123467	0.19	98.97	0.000972
8	44.4315933	-96.8649219	0.001371	0.001402	0.001402	0.002039	0.131946	0.18	99.19	0.000991
9	44.4299906	-96.8651800	0.001171	0.001148	0.001159	0.001591	0.131309	0.16	98.72	0.000816
10	44.4285866	-96.8652243	0.001124	0.001044	0.001059	0.001454	0.117301	0.16	97.66	0.000744
11	44.4285134	-96.8636093	0.001262	0.001245	0.001244	0.001689	0.104034	0.15	98.62	0.000880
12	44.4299351	-96.8635234	0.001308	0.001294	0.001304	0.001876	0.125791	0.18	98.96	0.000918
13	44.4314315	-96.8634919	0.001459	0.001555	0.001556	0.002159	0.128509	0.16	99.49	0.001100
14	44.4327920	-96.8634859	0.001394	0.001428	0.001431	0.002094	0.124542	0.19	99.70	0.001011
15	44.4341988	-96.8635278	0.001207	0.001178	0.001178	0.001604	0.111152	0.15	98.48	0.000833
16	44.4341861	-96.8616905	0.001356	0.001357	0.001357	0.002075	0.133628	0.21	99.33	0.000960
17	44.4342965	-96.8589566	0.001414	0.001470	0.001482	0.002007	0.116235	0.15	99.46	0.001044
18	44.4330571	-96.8594005	0.001162	0.001113	0.001113	0.001607	0.131141	0.18	98.21	0.000787
19	44.4312102	-96.8589493	0.001142	0.001101	0.001101	0.001493	0.131982	0.15	98.47	0.000778
20	44.4312967	-96.8612596	0.001221	0.001217	0.001218	0.001717	0.124452	0.17	98.89	0.000861
21	44.4321796	-96.8621143	0.001474	0.001515	0.001532	0.002095	0.120870	0.16	99.59	0.001077
22	44.4305035	-96.8624173	0.001088	0.000990	0.000991	0.001294	0.114524	0.13	97.69	0.000700
23	44.4298767	-96.8611440	0.001152	0.001083	0.001072	0.001458	0.127215	0.15	98.16	0.000762
24	44.4293013	-96.8592668	0.001125	0.001017	0.001017	0.001413	0.088330	0.16	97.93	0.000719
25	44.4287346	-96.8625206	0.001091	0.001005	0.001006	0.001316	0.073529	0.13	97.68	0.000711

See Table 2.9 and 2.10 for PlanetScope bands and indices descriptions.

Table C.5 Field D (Lac qui Parle County) PlanetScope single bands and remote sensing indices data set

Sample No	Latitude (^{O}N)	Longitude (^{O}W)	Band 1 µm	Band 2 µm	Band 3 µm	Band 4 µm	MSAVI2	NDVI	BSI	BI
1	45.0768865	-96.4362314	0.001034	0.000959	0.000963	0.001335	0.082183	0.16	97.80	0.000680
2	45.0758906	-96.4364095	0.001083	0.001023	0.001035	0.001592	0.097482	0.20	98.43	0.000728
3	45.0758857	-96.4383055	0.001143	0.001100	0.001095	0.001506	0.086210	0.15	98.53	0.000776
4	45.0759825	-96.4402876	0.001048	0.000971	0.000966	0.001364	0.101851	0.18	97.79	0.000685
5	45.0774180	-96.4402832	0.001049	0.000989	0.000991	0.001335	0.077506	0.14	98.13	0.000700
6	45.0771265	-96.4422473	0.001116	0.001104	0.001106	0.001560	0.098033	0.17	98.56	0.000782
7	45.0771957	-96.4439341	0.001108	0.001084	0.001079	0.001572	0.097242	0.19	98.64	0.000765
8	45.0770702	-96.4455203	0.001356	0.001414	0.001039	0.001412	0.107000	0.16	99.53	0.000877
9	45.0774757	-96.4487111	0.001020	0.000947	0.000972	0.001360	0.077850	0.17	97.94	0.000679
10	45.0764312	-96.4482571	0.001074	0.001021	0.001028	0.001391	0.080917	0.15	98.46	0.000725
11	45.0760938	-96.4461640	0.001072	0.001013	0.001014	0.001430	0.077652	0.18	98.19	0.000717
12	45.0760722	-96.4442455	0.001133	0.001116	0.001116	0.001624	0.102392	0.19	98.82	0.000789
13	45.0760254	-96.4422684	0.001130	0.001108	0.001085	0.001701	0.105541	0.20	98.74	0.000775
14	45.0745309	-96.4403463	0.001152	0.001119	0.001125	0.001545	0.081641	0.15	98.91	0.000793
15	45.0745025	-96.4383209	0.001079	0.001048	0.001047	0.001442	0.086914	0.16	98.31	0.000741
16	45.0745160	-96.4364722	0.001144	0.001123	0.001117	0.001570	0.091898	0.17	98.66	0.000792
17	45.0732658	-96.4365536	0.001071	0.001018	0.001021	0.001410	0.088705	0.16	98.30	0.000721
18	45.0731716	-96.4384935	0.001215	0.001214	0.001182	0.001667	0.089423	0.17	99.25	0.000847
19	45.0731979	-96.4404375	0.001099	0.001065	0.001070	0.001523	0.099781	0.17	98.51	0.000755
20	45.0731901	-96.4424481	0.001188	0.001162	0.001170	0.001698	0.098755	0.18	99.24	0.000824
21	45.0746446	-96.4423459	0.001123	0.001091	0.001093	0.001544	0.093094	0.17	98.78	0.000772
22	45.0746846	-96.4442935	0.001268	0.001231	0.001198	0.001718	0.095037	0.18	99.76	0.000859
23	45.0733040	-96.4443572	0.001138	0.001118	0.001109	0.001635	0.105215	0.19	99.12	0.000787
24	45.0747104	-96.4462512	0.001087	0.001058	0.001071	0.001513	0.094557	0.18	98.42	0.000753
25	45.0733217	-96.4463004	0.001110	0.001086	0.001077	0.001541	0.097859	0.18	99.06	0.000765

See Table 2.9 and 2.10 for PlanetScope bands and indices descriptions.

Table C.5 Continued

Sample No	Latitude (^{O}N)	Longitude (^{O}W)	Band 1 µm	Band 2 µm	Band 3 µm	Band 4 µm	MSAVI2	NDVI	BSI	BI
26	45.0719406	-96.4463698	0.001134	0.001105	0.001104	0.001583	0.096802	0.18	98.74	0.000781
27	45.0719065	-96.4444189	0.001179	0.001168	0.001165	0.001650	0.098331	0.17	99.04	0.000825
28	45.0718627	-96.4424870	0.001122	0.001124	0.001120	0.001604	0.097030	0.17	98.76	0.000793
29	45.0717867	-96.4405900	0.001287	0.001286	0.001299	0.001770	0.095376	0.15	99.67	0.000914
30	45.0717768	-96.4385603	0.001205	0.001216	0.001197	0.001604	0.099499	0.15	98.36	0.000853
31	45.0706961	-96.4369017	0.001115	0.001098	0.001095	0.001647	0.109326	0.20	98.51	0.000775
32	45.0703982	-96.4386233	0.001170	0.001209	0.001185	0.001653	0.104632	0.17	98.59	0.000846
33	45.0704304	-96.4405649	0.001138	0.001138	0.001130	0.001666	0.109314	0.19	99.20	0.000802
34	45.0704920	-96.4425195	0.001147	0.001122	0.001131	0.001679	0.099147	0.20	98.96	0.000797
35	45.0705178	-96.4444782	0.001104	0.001068	0.001082	0.001581	0.113038	0.19	98.63	0.000760
36	45.0705538	-96.4464279	0.001092	0.001058	0.001060	0.001531	0.093307	0.18	98.69	0.000749
37	45.0691506	-96.4464765	0.001123	0.001082	0.001061	0.001530	0.088551	0.18	98.62	0.000758
38	45.0692235	-96.4484432	0.001094	0.001051	0.001016	0.001467	0.087381	0.17	98.43	0.000731
39	45.0692628	-96.4504036	0.001120	0.001071	0.001062	0.001530	0.096567	0.18	98.76	0.000754
40	45.0678721	-96.4502198	0.001046	0.000998	0.000974	0.001393	0.091740	0.15	98.34	0.000697
41	45.0678494	-96.4485233	0.001045	0.000990	0.000993	0.001283	0.079273	0.14	97.68	0.000701
42	45.0681561	-96.4466793	0.001044	0.000965	0.000959	0.001291	0.073571	0.15	97.50	0.000680

See Table 2.9 and 2.10 for PlanetScope bands and indices descriptions.

Table C.6 Field E (Lac qui Parle County) PlanetScope single bands and remote sensing indices data set

Sample No	Latitude (^{O}N)	Longitude (^{O}W)	Band 1 µm	Band 2 µm	Band 3 µm	Band 4 µm	MSAVI2	NDVI	BSI	BI
1	45.0943806	-96.4513185	0.001154	0.001091	0.001081	0.001469	0.065936	0.15	98.68	0.000768
2	45.0929747	-96.4513923	0.001162	0.001124	0.001113	0.001560	0.079561	0.17	99.23	0.000791
3	45.0915799	-96.4514550	0.001201	0.001203	0.001200	0.001767	0.103615	0.19	100.03	0.000850
4	45.0901786	-96.4515281	0.001222	0.001201	0.001204	0.001725	0.104767	0.18	99.62	0.000850
5	45.0887707	-96.4515790	0.001089	0.001025	0.001024	0.001435	0.071286	0.17	98.60	0.000725
6	45.0889359	-96.4495657	0.001143	0.001068	0.001095	0.001468	0.069486	0.15	98.43	0.000765
7	45.0901325	-96.4495335	0.001118	0.001067	0.001086	0.001547	0.088554	0.18	98.94	0.000761
8	45.0915302	-96.4494752	0.001167	0.001129	0.001140	0.001580	0.082959	0.16	99.24	0.000802
9	45.0929397	-96.4494075	0.001123	0.001081	0.001038	0.001399	0.057330	0.15	99.09	0.000749
10	45.0943300	-96.4493448	0.001189	0.001135	0.001107	0.001522	0.074015	0.16	98.90	0.000793
11	45.0942824	-96.4473747	0.001164	0.001112	0.001114	0.001492	0.078158	0.15	98.94	0.000787
12	45.0928912	-96.4474360	0.001107	0.001047	0.001049	0.001444	0.065559	0.16	98.70	0.000741
13	45.0914956	-96.4474954	0.001151	0.001105	0.001097	0.001550	0.073111	0.17	99.06	0.000779
14	45.0900797	-96.4475597	0.001251	0.001269	0.001270	0.001854	0.110137	0.19	100.32	0.000898
15	45.0887645	-96.4475490	0.001249	0.001255	0.001244	0.001781	0.110339	0.18	100.10	0.000884
16	45.0888396	-96.4456319	0.001339	0.001364	0.001340	0.001801	0.094175	0.15	100.42	0.000956
17	45.0900333	-96.4455679	0.001116	0.001044	0.001046	0.001420	0.072368	0.15	98.44	0.000739

See Table 2.9 and 2.10 for PlanetScope bands and indices descriptions.

Table C.6 Continued

Sample No	Latitude (^{O}N)	Longitude (^{O}W)	Band 1 µm	Band 2 µm	Band 3 µm	Band 4 µm	MSAVI2	NDVI	BSI	BI
18	45.0914428	-96.4455129	0.001129	0.001053	0.001079	0.001409	0.068023	0.13	98.37	0.000754
19	45.0928519	-96.4454535	0.001126	0.001047	0.001016	0.001411	0.064518	0.16	98.29	0.000729
20	45.0945058	-96.4453727	0.001233	0.001215	0.001229	0.001751	0.100506	0.18	99.68	0.000864
21	45.0944088	-96.4434982	0.001067	0.001019	0.001028	0.001467	0.082586	0.18	98.94	0.000724
22	45.0930105	-96.4434506	0.001141	0.001110	0.001121	0.001608	0.090929	0.18	99.38	0.000789
23	45.0914038	-96.4435331	0.001101	0.001059	0.001055	0.001579	0.092250	0.20	99.11	0.000747
24	45.0899940	-96.4435857	0.001161	0.001130	0.001130	0.001587	0.089796	0.17	99.39	0.000799
25	45.0889262	-96.4437037	0.001201	0.001170	0.001176	0.001696	0.097874	0.18	99.41	0.000829
26	45.0886864	-96.4412690	0.001180	0.001216	0.001224	0.001899	0.120544	0.22	100.65	0.000863
27	45.0899627	-96.4414004	0.001096	0.001084	0.001084	0.001655	0.101844	0.21	99.75	0.000766
28	45.0929605	-96.4416428	0.001084	0.001031	0.001017	0.001527	0.082841	0.20	98.85	0.000724
29	45.0903772	-96.4357051	0.001050	0.000985	0.000985	0.001424	0.074568	0.18	98.53	0.000697
30	45.0889570	-96.4357631	0.001071	0.001013	0.001012	0.001445	0.063745	0.18	98.71	0.000716
31	45.0889662	-96.4376383	0.001053	0.000962	0.000964	0.001355	0.066434	0.17	97.90	0.000681
32	45.0887612	-96.4394635	0.001129	0.001075	0.001074	0.001558	0.081963	0.18	98.88	0.00076
33	45.0899445	-96.4393686	0.001109	0.001071	0.001079	0.001592	0.103875	0.19	99.22	0.00076
34	45.0902827	-96.4377227	0.001024	0.000957	0.000957	0.001373	0.072769	0.18	98.43	0.000677

See Table 2.9 and 2.10 for PlanetScope bands and indices descriptions.

Appendix D

Table D.1 The complete Pearson correlation matrix for WSS data (n= 150)

Parameters	SOC_WSS	Clay_WSS	Sand_WSS	Silt_WSS	pH_WSS	CEC_WSS
SOC_WSS	1					
Clay_WSS	**0.47**	1				
Sand_WSS	**-0.25**	**-0.80**	1			
Silt_WSS	0.14	**0.63**	**-0.97**	1		
pH_WSS	0.15	0.12	**-0.27**	**0.30**	1	
CEC_WSS	**0.46**	**0.92**	**-0.67**	**0.49**	0.12	1

WSS = Web Soil Survey. All values in **bold print** are significant (P<0.05)

Table D.2 The complete Pearson correlation matrix for Web Soil Survey (WSS) and Soil Test Data (STD) (n= 150)

Parameters	SOC_STD	$pH_{1:1}$_STD	Sand_STD	Clay_STD	Silt_STD	SOEC_STD	SOC_WSS	Clay_WSS	Sand_WSS	Silt_WSS	$pH_{1:1}$_WSS	CEC_WSS
SOC_STD	1.00											
$pH_{1:1}$_STD	**0.39**	1.00										
Sand_STD	**-0.87**	**-0.31**	1.00									
Clay_STD	**0.80**	**0.45**	**-0.87**	1.00								
Silt_STD	**0.74**	0.10	**-0.89**	**0.54**	1.00							
SOEC_STD	**0.72**	0.**84**	**-0.63**	**0.75**	**0.37**	1.00						
SOC_WSS	0.07	0.00	-0.07	**0.27**	-0.12	0.09	1.00					
Clay_WSS	**0.58**	**0.28**	**-0.57**	**0.61**	**0.39**	**0.48**	**0.47**	1.00				
Sand_WSS	**-0.70**	**-0.41**	**0.75**	**-0.76**	**-0.56**	**-0.61**	**-0.25**	**-0.80**	1.00			
Silt_WSS	**0.67**	**0.41**	**-0.74**	**0.74**	**0.56**	**0.60**	0.14	**0.63**	**-0.97**	1.00		
$pH_{1:1}$_WSS	**0.25**	**0.41**	-0.11	**0.33**	-0.12	**0.49**	0.15	0.12	**-0.27**	**0.30**	1.00	
CEC_WSS	**0.49**	0.21	**-0.40**	**0.43**	**0.27**	**0.39**	**0.46**	**0.92**	**-0.67**	**0.49**	0.12	1.00

SOEC = Sum of Extractable Cation. All values in **bold print** are significant (P<0.05)

Table D.3 Field A (Brookings County, SD) Web Soil Survey (WSS) data set

Sample No	Latitude (^{O}N)	Longitude (^{O}W)	OM (g kg^{-1})	SOC (g kg^{-1})	Clay (g kg^{-1})	Sand (g kg^{-1})	Silt (g kg^{-1})	pH (1:1)	CEC ($cmol_c$ kg^{-1})
1	44.3849033	-96.9461351	2.99	1.74	24.92	9.47	65.61	6.48	21.06
2	44.3849738	-96.9442170	3.32	1.93	27.78	15.85	56.37	6.93	22.66
3	44.3863216	-96.9443015	3.65	2.12	29.00	7.00	64.00	7.21	23.29
4	44.3877266	-96.9442422	2.99	1.74	24.92	9.47	65.61	6.48	21.06
5	44.3880766	-96.9462404	3.08	1.79	20.72	42.12	37.16	6.90	17.93
6	44.3894226	-96.9462689	2.99	1.74	24.92	9.47	65.61	6.48	21.06
7	44.3893326	-96.9443454	2.99	1.74	24.92	9.47	65.61	6.48	21.06
8	44.3905456	-96.9462595	3.71	2.16	29.20	7.42	63.38	6.65	24.43
9	44.3905477	-96.9442898	3.71	2.16	29.20	7.42	63.38	6.65	24.43
10	44.3905362	-96.9426315	3.65	2.12	29.00	7.00	64.00	7.21	23.29
11	44.3892037	-96.9424045	2.99	1.74	24.92	9.47	65.61	6.48	21.06
12	44.3877270	-96.9423955	2.99	1.74	24.92	9.47	65.61	6.48	21.06
13	44.3863649	-96.9422821	3.65	2.12	29.00	7.00	64.00	7.21	23.29
14	44.3849364	-96.9422305	3.65	2.12	29.00	7.00	64.00	7.21	23.29
15	44.3849395	-96.9404207	3.32	1.93	27.78	15.85	56.37	6.93	22.66
16	44.3864433	-96.9405058	3.65	2.12	29.00	7.00	64.00	7.21	23.29
17	44.3877366	-96.9406607	2.99	1.74	24.92	9.47	65.61	6.48	21.06
18	44.3892959	-96.9407110	3.65	2.12	29.00	7.00	64.00	7.21	23.29
19	44.3905324	-96.9407824	3.59	2.09	29.07	6.92	64.01	6.70	24.21
20	44.3905420	-96.9386300	3.65	2.12	29.00	7.00	64.00	7.21	23.29
21	44.3893405	-96.9385052	3.65	2.12	29.00	7.00	64.00	7.21	23.29
22	44.3877992	-96.9387336	2.99	1.74	24.92	9.47	65.61	6.48	21.06
23	44.3864869	-96.9386987	3.65	2.12	29.00	7.00	64.00	7.21	23.29
24	44.3849026	-96.9387805	5.68	3.30	21.56	40.99	37.46	7.85	22.23

CEC = Cation Exchange Capacity, OM= Organic Matter, SOC= Soil Organic Carbon.

Table D.4 Field B (Brookings County, SD) Web Soil Survey (WSS) data set

Sample No	Latitude (^{O}N)	Longitude (^{O}W)	OM (g kg^{-1})	SOC (g kg^{-1})	Clay (g kg^{-1})	Sand (g kg^{-1})	Silt (g kg^{-1})	pH (1:1)	CEC ($cmol_c$ kg^{-1})
1	44.4629807	-96.8467720	3.45	2.01	15.26	62.99	21.75	6.65	14.78
2	44.4630070	-96.8448609	3.45	2.01	15.26	62.99	21.75	6.65	14.78
3	44.4629894	-96.8428560	3.84	2.23	15.14	64.64	20.22	6.65	15.31
4	44.4628501	-96.8409707	5.73	3.33	25.32	31.90	42.78	7.13	26.08
5	44.4628333	-96.8389601	5.04	2.93	29.42	35.98	34.60	6.83	24.83
6	44.4613164	-96.8388696	5.04	2.93	29.42	35.98	34.60	6.83	24.83
7	44.4614810	-96.8409738	5.73	3.33	25.32	31.90	42.78	7.13	26.08
8	44.4615306	-96.8428734	3.45	2.01	15.26	62.99	21.75	6.65	14.78
9	44.4617706	-96.8447335	5.80	3.37	24.44	30.25	45.31	6.84	24.98
10	44.4617408	-96.8467150	3.45	2.01	15.26	62.99	21.75	6.65	14.78
11	44.4603363	-96.8466976	5.04	2.93	29.42	35.98	34.60	6.83	24.83
12	44.4603057	-96.8444288	3.45	2.01	15.26	62.99	21.75	6.65	14.78
13	44.4598756	-96.8431769	5.80	3.37	24.44	30.25	45.31	6.84	24.98
14	44.4597715	-96.8409587	3.45	2.01	15.26	62.99	21.75	6.65	14.78
15	44.4594313	-96.8393745	3.45	2.01	15.26	62.99	21.75	6.65	14.78
16	44.4587020	-96.8390945	3.35	1.95	20.88	40.14	38.99	7.35	16.77
17	44.4587136	-96.8410623	5.04	2.93	29.42	35.98	34.60	6.83	24.83
18	44.4587878	-96.8430260	3.45	2.01	15.26	62.99	21.75	6.65	14.78
19	44.4588545	-96.8449193	3.45	2.01	15.26	62.99	21.75	6.65	14.78
20	44.4588720	-96.8467019	5.04	2.93	29.42	35.98	34.60	6.83	24.83
21	44.4573421	-96.8391653	5.04	2.93	29.42	35.98	34.60	6.83	24.83
22	44.4573916	-96.8411028	5.04	2.93	29.42	35.98	34.60	6.83	24.83
23	44.4574460	-96.8429200	5.04	2.93	29.42	35.98	34.60	6.83	24.83
24	44.4574153	-96.8448636	5.04	2.93	29.42	35.98	34.60	6.83	24.83
25	44.4575522	-96.8467046	5.04	2.93	29.42	35.98	34.60	6.83	24.83

CEC = Cation Exchange Capacity, OM= Organic Matter, SOC= Soil Organic Carbon.

Table D.5 Field C (Brookings County, SD) Web Soil Survey (WSS) data set

Sample No	Latitude (^{O}N)	Longitude (^{O}W)	OM (g kg^{-1})	SOC (g kg^{-1})	Clay (g kg^{-1})	Sand (g kg^{-1})	Silt (g kg^{-1})	pH (1:1)	CEC ($cmol_c$ kg^{-1})
1	44.4286008	-96.8672630	5.77	3.35	24.86	55.25	19.89	6.47	24.60
2	44.4299830	-96.8671877	5.77	3.35	24.86	55.25	19.89	6.47	24.60
3	44.4314178	-96.8671488	5.77	3.35	24.86	55.25	19.89	6.47	24.60
4	44.4328201	-96.8670861	5.77	3.35	24.86	55.25	19.89	6.47	24.60
5	44.4342010	-96.8670197	5.77	3.35	24.86	55.25	19.89	6.47	24.60
6	44.4341373	-96.8651006	3.08	1.79	13.89	67.11	19.00	6.64	16.98
7	44.4327896	-96.8651324	5.77	3.35	24.86	55.25	19.89	6.47	24.60
8	44.4315933	-96.8649219	3.08	1.79	13.89	67.11	19.00	6.64	16.98
9	44.4299906	-96.8651800	4.39	2.55	20.00	71.35	8.66	6.73	14.95
10	44.4285866	-96.8652243	4.39	2.55	20.00	71.35	8.66	6.73	14.95
11	44.4285134	-96.8636093	3.08	1.79	13.89	67.11	19.00	6.64	16.98
12	44.4299351	-96.8635234	3.08	1.79	13.89	67.11	19.00	6.64	16.98
13	44.4314315	-96.8634919	3.08	1.79	13.89	67.11	19.00	6.64	16.98
14	44.4327920	-96.8634859	3.08	1.79	13.89	67.11	19.00	6.64	16.98
15	44.4341988	-96.8635278	2.32	1.35	11.67	66.26	22.08	6.97	12.73
16	44.4341861	-96.8616905	5.77	3.35	24.86	55.25	19.90	6.47	24.60
17	44.4342965	-96.8589566	3.08	1.79	13.89	67.11	19.00	6.64	16.98
18	44.4330571	-96.8594005	3.08	1.79	13.89	67.11	19.00	6.64	16.98
19	44.4312102	-96.8589493	3.08	1.79	13.89	67.11	19.00	6.64	16.98
20	44.4312967	-96.8612596	5.77	3.35	24.86	55.25	19.89	6.47	24.60
21	44.4321796	-96.8621143	3.70	2.15	21.36	37.85	40.79	6.47	24.60
22	44.4305035	-96.8624173	5.77	3.35	24.86	55.25	19.89	6.47	24.60
23	44.4298767	-96.8611440	5.77	3.35	24.86	55.25	19.89	6.47	24.60
24	44.4293013	-96.8592668	5.77	3.35	24.86	55.25	19.89	6.47	24.60
25	44.4287346	-96.8625206	5.77	3.35	24.86	55.25	19.89	6.47	24.60

CEC = Cation Exchange Capacity, OM= Organic Matter, SOC= Soil Organic Carbon.

Table D.6 Field D (Lac qui Parle County, MN) Web Soil Survey (WSS) data set

Sample No	Latitude (^{O}N)	Longitude (^{O}W)	OM (g kg^{-1})	SOC (g kg^{-1})	Clay (g kg^{-1})	Sand (g kg^{-1})	Silt (g kg^{-1})	pH (1:1)	CEC ($cmol_c$ kg^{-1})
1	45.0768865	-96.4362314	7.17	4.17	27.70	9.22	63.09	7.58	23.56
2	45.0758906	-96.4364095	5.94	3.45	23.03	39.71	37.26	7.02	20.09
3	45.0758857	-96.4383055	7.37	4.28	12.52	44.30	43.18	7.55	10.42
4	45.0759825	-96.4402876	7.17	4.17	27.70	9.22	63.09	7.58	23.56
5	45.0774180	-96.4402832	7.53	4.38	23.73	29.66	46.62	8.07	22.54
6	45.0771265	-96.4422473	8.53	4.96	23.72	38.62	37.67	7.00	19.21
7	45.0771957	-96.4439341	5.94	3.45	23.03	39.71	37.26	7.02	20.09
8	45.0770702	-96.4455203	8.53	4.96	23.72	38.62	37.67	7.00	19.21
9	45.0774757	-96.4487111	7.53	4.38	23.73	29.66	46.62	8.07	22.54
10	45.0764312	-96.4482571	7.17	4.17	27.70	9.22	63.09	7.58	23.56
11	45.0760938	-96.4461640	8.53	4.96	23.72	38.62	37.67	7.00	19.21
12	45.0760722	-96.4442455	5.94	3.45	23.03	39.71	37.26	7.02	20.09
13	45.0760254	-96.4422684	5.94	3.45	23.03	39.71	37.26	7.02	20.09
14	45.0745309	-96.4403463	3.02	1.75	24.66	38.91	36.43	7.29	19.92
15	45.0745025	-96.4383209	5.94	3.45	23.03	39.71	37.26	7.02	20.09
16	45.0745160	-96.4364722	4.27	2.48	12.52	44.30	43.18	7.50	10.75
17	45.0732658	-96.4365536	5.94	3.45	23.03	39.71	37.26	7.02	20.09
18	45.0731716	-96.4384935	4.27	2.48	12.52	44.30	43.18	7.50	10.75
19	45.0731979	-96.4404375	16.88	9.81	30.85	25.49	43.67	6.78	27.40
20	45.0731901	-96.4424481	5.94	3.45	23.03	39.71	37.26	7.02	20.09
21	45.0746446	-96.4423459	3.02	1.75	24.66	38.91	36.43	7.29	19.92
22	45.0746846	-96.4442935	3.02	1.75	24.66	38.91	36.43	7.29	19.92
23	45.0733040	-96.4443572	8.53	4.96	23.72	38.62	37.67	7.00	19.21
24	45.0747104	-96.4462512	16.88	9.81	30.85	25.49	43.67	6.78	27.40
25	45.0733217	-96.4463004	7.66	4.45	30.73	33.95	35.32	6.82	27.27

CEC = Cation Exchange Capacity, OM= Organic Matter, SOC= Soil Organic Carbon.

Table D.6 Continued

Sample No	Latitude (^{O}N)	Longitude (^{O}W)	OM (g kg^{-1})	SOC (g kg^{-1})	Clay (g kg^{-1})	Sand (g kg^{-1})	Silt (g kg^{-1})	pH (1:1)	CEC ($cmol_c$ kg^{-1})
26	45.0719406	-96.4463698	3.12	1.81	15.72	56.42	27.87	7.19	14.76
27	45.0719065	-96.4444189	8.53	4.96	23.72	38.62	37.67	7.00	19.21
28	45.0718627	-96.4424870	8.53	4.96	23.72	38.62	37.67	7.00	19.21
29	45.0717867	-96.4405900	7.37	4.28	12.52	44.30	43.18	7.55	10.42
30	45.0717768	-96.4385603	4.27	2.48	12.52	44.30	43.18	7.50	10.75
31	45.0706961	-96.4369017	3.22	1.87	13.93	65.00	21.07	6.91	13.72
32	45.0703982	-96.4386233	3.22	1.87	13.93	65.00	21.07	6.91	13.72
33	45.0704304	-96.4405649	16.88	9.81	30.85	25.49	43.67	6.78	27.40
34	45.0704920	-96.4425195	7.66	4.45	30.73	33.95	35.32	6.82	27.27
35	45.0705178	-96.4444782	7.66	4.45	30.73	33.95	35.32	6.82	27.27
36	45.0705538	-96.4464279	7.66	4.45	30.73	33.95	35.32	6.82	27.27
37	45.0691506	-96.4464765	7.66	4.45	30.73	33.95	35.32	6.82	27.27
38	45.0692235	-96.4484432	8.53	4.96	23.72	38.62	37.67	7.00	19.21
39	45.0692628	-96.4504036	8.53	4.96	23.72	38.62	37.67	7.00	19.21
40	45.0678721	-96.4502198	8.53	4.96	23.72	38.62	37.67	7.00	19.21
41	45.0678494	-96.4485233	7.66	4.45	30.73	33.95	35.32	6.82	27.27
42	45.0681561	-96.4466793	16.88	9.81	30.85	25.49	43.67	6.78	27.40

CEC = Cation Exchange Capacity, OM= Organic Matter, SOC= Soil Organic Carbon.

Table D.7 Field E (Lac qui Parle County, MN) Web Soil Survey (WSS) data set

Sample No	Latitude (^{O}N)	Longitude (^{O}W)	OM (g kg^{-1})	SOC (g kg^{-1})	Clay (g kg^{-1})	Sand (g kg^{-1})	Silt (g kg^{-1})	pH (1:1)	CEC ($cmol_c$ kg^{-1})
1	45.0943806	-96.4513185	5.93	3.45	30.30	32.27	37.43	7.82	24.55
2	45.0929747	-96.4513923	5.26	3.06	30.73	33.95	35.32	6.82	27.27
3	45.0915799	-96.4514550	4.32	2.51	23.56	39.57	36.87	7.15	19.94
4	45.0901786	-96.4515281	4.32	2.51	23.56	39.57	36.87	7.15	19.94
5	45.0887707	-96.4515790	7.45	4.33	33.35	20.98	45.67	7.14	27.77
6	45.0889359	-96.4495657	4.90	2.85	29.14	7.43	63.43	6.45	24.64
7	45.0901325	-96.4495335	5.93	3.45	30.30	32.27	37.43	7.82	24.55
8	45.0915302	-96.4494752	2.82	1.64	13.93	65.00	21.07	6.91	13.72
9	45.0929397	-96.4494075	5.76	3.35	31.57	9.55	58.89	7.85	31.32
10	45.0943300	-96.4493448	5.76	3.35	31.57	9.55	58.89	7.85	31.32
11	45.0942824	-96.4473747	2.76	1.60	15.72	56.42	27.87	7.19	14.76
12	45.0928912	-96.4474360	5.76	3.35	31.57	9.55	58.89	7.85	31.32
13	45.0914956	-96.4474954	5.76	3.35	31.57	9.55	58.89	7.85	31.32
14	45.0900797	-96.4475597	2.29	1.33	14.35	65.97	19.68	6.58	16.12
15	45.0887645	-96.4475490	2.82	1.64	13.93	65.00	21.07	6.91	13.72
16	45.0888396	-96.4456319	2.63	1.53	13.66	64.58	21.76	6.82	13.30
17	45.0900333	-96.4455679	6.95	4.04	31.60	25.20	43.20	6.77	26.69

CEC = Cation Exchange Capacity, OM= Organic Matter, SOC= Soil Organic Carbon.

Table D.7 Continued

Sample No	Latitude (^{O}N)	Longitude (^{O}W)	OM (g kg^{-1})	SOC (g kg^{-1})	Clay (g kg^{-1})	Sand (g kg^{-1})	Silt (g kg^{-1})	pH (1:1)	CEC ($cmol_c$ kg^{-1})
18	45.0914428	-96.4455129	5.76	3.35	31.57	9.55	58.89	7.85	31.32
19	45.0928519	-96.4454535	6.26	3.64	22.43	41.59	35.99	7.90	23.38
20	45.0945058	-96.4453727	2.82	1.64	13.93	65.00	21.07	6.91	13.72
21	45.0944088	-96.4434982	3.34	1.94	14.86	66.40	18.74	6.81	15.75
22	45.0930105	-96.4434506	3.34	1.94	14.86	66.40	18.74	6.81	15.75
23	45.0914038	-96.4435331	2.82	1.64	13.93	65.00	21.07	6.91	13.72
24	45.0899940	-96.4435857	7.45	4.33	33.35	20.98	45.67	7.14	27.77
25	45.0889262	-96.4437037	5.10	2.96	23.03	39.80	37.18	7.02	26.63
26	45.0886864	-96.4412690	2.82	1.64	13.93	65.00	21.07	6.91	13.72
27	45.0899627	-96.4414004	2.82	1.64	13.93	65.00	21.07	6.91	13.72
28	45.0929605	-96.4416428	2.76	1.60	15.72	56.42	27.87	7.19	14.76
29	45.0903772	-96.4357051	4.57	2.65	13.39	61.87	24.75	7.71	16.58
30	45.0889570	-96.4357631	6.26	3.64	22.43	41.59	35.99	7.90	23.38
31	45.0889662	-96.4376383	4.57	2.65	13.39	61.87	24.75	7.71	16.58
32	45.0887612	-96.4394635	2.82	1.64	13.93	65.00	21.07	6.91	13.72
33	45.0899445	-96.4393686	4.57	2.65	13.39	61.87	24.75	7.71	16.58
34	45.0902827	-96.4377227	6.26	3.64	22.43	41.59	35.99	7.90	23.38

CEC = Cation Exchange Capacity, OM= Organic Matter, SOC= Soil Organic Carbon.

Appendix E

Table E.1 The complete Pearson correlation matrix for Landsat 8 and Soil Test Data (n= 150).

Parameters	SOC (g kg^{-1})	Moisture (g kg^{-1})	$EC_{1:1}$(dS m^{-1})	$pH_{1:1}$	Sand (g kg^{-1})	Clay (g kg^{-1})	Silt (g kg^{-1})	K^+ (mg kg^{-1})	Ca^{2+} (mg kg^{-1})	Mg^{2+} (mg kg^{-1})	Na^+ (mg kg^{-1})	PO_4^{3-} (mg kg^{-1})	NH_4^+-N (mg kg^{-1})	NO_3^--N (mg kg^{-1})	SOEC ($cmol_c$ kg^{-1})
BSI	**-0.44**	**-0.38**	**-0.27**	**-0.42**	0.21	**-0.29**	-0.09	-0.08	**-0.39**	**-0.47**	**-0.39**	**0.43**	-0.04	0.02	**-0.44**
$Band_L$ 4	**-0.42**	**-0.30**	-0.20	**-0.36**	0.22	**-0.25**	-0.15	-0.08	**-0.29**	**-0.42**	**-0.44**	**0.41**	-0.09	-0.08	**-0.35**
$Band_L$ 5	**-0.52**	**-0.42**	**-0.41**	**-0.53**	**0.33**	**-0.45**	-0.15	-0.09	**-0.52**	**-0.55**	**-0.31**	**0.51**	-0.11	-0.06	**-0.57**
MSAVI2	**-0.54**	**-0.50**	**-0.60**	**-0.63**	**0.40**	**-0.61**	-0.11	-0.08	**-0.71**	**-0.61**	-0.06	**0.53**	-0.10	-0.02	**-0.73**
NDVI	**-0.39**	**-0.44**	**-0.61**	**-0.51**	**0.34**	**-0.59**	-0.03	-0.04	**-0.68**	**-0.46**	**0.27**	**0.35**	-0.04	0.03	**-0.67**
$Band_L$ 7	**-0.44**	**-0.27**	**-0.40**	**-0.48**	**0.31**	**-0.40**	-0.16	**-0.31**	**-0.40**	**-0.45**	**-0.36**	**0.32**	-0.20	-0.16	**-0.46**
$Band_L$ 6	**-0.54**	**-0.41**	**-0.51**	**-0.58**	**0.37**	**-0.51**	-0.16	**-0.29**	**-0.56**	**-0.56**	**-0.29**	**0.42**	-0.16	-0.12	**-0.61**
$Band_L$ 2	-0.24	-0.10	0.03	-0.14	0.10	-0.05	-0.12	-0.06	-0.01	-0.23	-0.50	**0.27**	-0.15	-0.09	-0.08
$Band_L$ 3	**-0.35**	-0.23	-0.10	**-0.26**	0.17	-0.17	-0.13	-0.07	-0.17	**-0.35**	**-0.48**	**0.35**	-0.12	-0.06	-0.23
BI	**-0.39**	**-0.27**	-0.16	**-0.32**	0.20	-0.22	-0.14	-0.08	-0.24	**-0.39**	**-0.46**	**0.39**	-0.10	-0.07	**-0.31**

SOEC = Sum of Extractable Cation, EC = Electrical Conductivity, SOC = Soil Organic Carbon. All values in **bold print** are significant (P<0.05). $Band_L$ represents Landsat 8 data (See Table 2.8 and 2.10), Soils test data from 0-15cm depth.

Table E.2 The complete Pearson correlation matrix for PlanetScope and Soil Test Data (n= 150).

Parameters	SOC (g kg^{-1})	Moisture (g kg^{-1})	$EC_{1:1}$(dS m^{-1})	$pH_{1:1}$	Sand (g kg^{-1})	Clay (g kg^{-1})	Silt (g kg^{-1})	K^+ (mg kg^{-1})	Ca^{2+} (mg kg^{-1})	Mg^{2+} (mg kg^{-1})	Na^+ (mg kg^{-1})	NH_4^+-N (mg kg^{-1})	NO_3^--N (mg kg^{-1})	SOEC ($cmol_c$ kg^{-1})	PO_4^{3-} (mg kg^{-1})
MSAVI2	**-0.54**	**-0.50**	**-0.60**	**-0.63**	**0.40**	**-0.61**	-0.11	-0.08	**-0.71**	**-0.61**	-0.06	-0.10	-0.02	**-0.73**	**0.53**
$Band_P$ 4	**-0.74**	**-0.56**	**-0.49**	**-0.44**	**0.67**	**-0.65**	**-0.53**	-0.08	**-0.53**	**-0.67**	-0.07	-0.17	**-0.45**	**-0.60**	**0.38**
$Band_P$ 3	**-0.69**	**-0.49**	**-0.45**	**-0.34**	**0.64**	**-0.64**	**-0.49**	-0.12	**-0.44**	**-0.60**	-0.05	**-0.28**	**-0.39**	**-0.52**	**0.35**
NDVI	**-0.45**	**-0.41**	**-0.30**	**-0.45**	**0.39**	**-0.32**	**-0.36**	0.12	**-0.44**	**-0.49**	-0.09	0.20	**-0.39**	**-0.48**	**0.25**
BSI	**-0.35**	-0.16	-0.17	-0.16	**0.28**	-0.22	**-0.27**	0.01	-0.12	**-0.32**	-0.24	-0.16	**-0.33**	-0.18	0.10
$Band_P$ 2	**-0.66**	**-0.48**	**-0.39**	**-0.32**	**0.62**	**-0.60**	**-0.49**	0.02	**-0.42**	**-0.60**	-0.07	-0.24	**-0.35**	**-0.50**	**0.42**
$Band_P$ 1	**-0.61**	**-0.42**	**-0.37**	**-0.25**	**0.58**	**-0.61**	**-0.42**	-0.01	**-0.38**	**-0.53**	0.00	**-0.34**	**-0.29**	**-0.45**	**0.37**
BI	**-0.68**	**-0.49**	**-0.42**	**-0.34**	**0.63**	**-0.62**	**-0.49**	-0.05	**-0.44**	**-0.60**	-0.06	**-0.26**	**-0.37**	**-0.51**	**0.39**

SOEC = Sum of Extractable Cation, EC = Electrical Conductivity, SOC = Soil Organic Carbon. All values in **bold print** are significant (P<0.05). $Band_P$ represents PlanetScope data (See Table 2.8 and 2.10), Soils test data from 0-15cm depth.

Table E.3 The complete Pearson correlation matrix for PlanetScope and Web Soil Survey data (n= 150).

Parameters	SOC_WSS*	Clay_WSS	Sand_WSS	Silt_WSS	$pH_{1:1}$_WSS	CEC_WSS
MSAVI2	-0.20	**-0.39**	**0.47**	**-0.46**	**-0.61**	**-0.33**
$Band_P$ 4	-0.15	**-0.47**	**0.60**	**-0.58**	**-0.33**	**-0.36**
$Band_P$ 3	-0.20	**-0.43**	**0.54**	**-0.52**	**-0.34**	**-0.32**
$NDVI_P$	0.07	**-0.30**	**0.41**	**-0.41**	-0.13	**-0.25**
BSI_P	-0.20	**-0.33**	**0.29**	-0.24	-0.07	**-0.30**
$Band_P$ 2	-0.17	**-0.42**	**0.52**	**-0.50**	**-0.32**	**-0.32**
$Band_P$ 1	-0.24	**-0.39**	**0.48**	**-0.46**	**-0.35**	**-0.28**
BI_P	-0.19	**-0.43**	**0.53**	**-0.51**	**-0.33**	**-0.32**

*WSS = Web Soil Survey, SOC = Soil Organic Carbon, CEC = Cation Exchange Capacity. All values in **bold print** are significant (P<0.05). $Band_P$ represents PlanetScope data (See Table 2.8 and 2.10).

Table E.4 The complete Pearson correlation matrix for Landsat 8, PlanetScope and Web Soil Survey data (n= 150).

Parameters	SOC_WSS*	Clay_WSS	Sand_WSS	Silt_WSS	$pH_{1:1}$_WSS	CEC_WSS	$MSAVI2_P$	$Band_P$ 4	$Band_P$ 3	$NDVI_P$	BSI_P	$Band_P$ 2	$Band_P$ 1	BI_P
BSI_L	-0.09	**-0.31**	**0.30**	**-0.26**	**-0.40**	**-0.33**	**0.72**	**0.60**	**0.62**	0.21	**0.49**	**0.64**	**0.60**	**0.64**
$Band_L$ 4	-0.05	**-0.29**	**0.27**	-0.24	**-0.26**	**-0.29**	**0.61**	**0.63**	**0.66**	0.17	**0.54**	**0.68**	**0.63**	**0.68**
$Band_L$ 5	-0.12	**-0.37**	**0.40**	**-0.37**	**-0.45**	**-0.34**	**0.86**	**0.70**	**0.70**	0.29	**0.49**	**0.71**	**0.68**	**0.71**
$MSAVI2_L$	-0.20	**-0.39**	**0.47**	**-0.46**	**-0.61**	**-0.33**	**1.00**	**0.63**	**0.58**	**0.38**	**0.30**	**0.58**	**0.57**	**0.59**
$NDVI_L$	-0.23	**-0.29**	**0.41**	**-0.41**	**-0.57**	-0.24	**0.78**	**0.33**	0.24	**0.37**	-0.01	0.22	0.24	0.23
$Band_L$ 7	-0.11	**-0.29**	**0.32**	**-0.30**	**-0.26**	-0.23	**0.61**	**0.60**	**0.59**	**0.27**	**0.39**	**0.48**	**0.44**	**0.54**
$Band_L$ 6	-0.15	**-0.38**	**0.41**	**-0.38**	**-0.43**	**-0.32**	**0.82**	**0.69**	**0.67**	**0.33**	**0.42**	**0.59**	**0.55**	**0.63**
$Band_L$ 2	0.05	-0.14	0.11	-0.08	-0.05	-0.15	**0.33**	**0.47**	**0.54**	0.01	**0.45**	**0.56**	**0.53**	**0.56**
$Band_L$ 3	-0.01	-0.24	0.21	-0.18	-0.19	**-0.25**	**0.50**	**0.56**	**0.62**	0.09	**0.50**	**0.64**	**0.60**	**0.63**
BI_L	-0.03	**-0.27**	**0.25**	-0.21	-0.23	**-0.27**	**0.57**	**0.60**	**0.65**	0.14	**0.52**	**0.67**	**0.62**	**0.66**

*WSS = Web Soil Survey. See Table 2.8, 2.9 and 2.10 for PlanetScope, Landsat 8 bands and remote sensing indices description. $Band_L$ and $Indices_L$ represents Landsat 8 data, $Band_P$ and $Indices_p$ shows PlanetScope data. All values in **bold print** are significant (P<0.05), Soils test data from 0-15cm depth.